Selective enhancement of the (6-4) photoproduct formation in dithymine dinucleotides driven by specific sugar puckerings

Jouda Jakhlal, Clément Denhez, Stéphanie Coantic-Castex, Agathe Martinez, Dominique Harakat, Thierry Douki, Dominique Guillaume and Pascale Clivio*

Table of contents

1. Synthesis of dinucleotides 12-17

Materials. Solvents and chemicals used for the reactions were purchased from commercial suppliers and used without further purification unless otherwise stated. Acetonitrile was dried by distillation from calcium hydride and anhydrous THF was obtained using Innovative Technology Pure Solv Solvent Purification Systems. 5'-*O*-dimethoxytrityl-2'-α-fluorothymidine 3′-*N,N*′-diisopropyl(cyanoethyl)phosphoramidite (**18**) was prepared from 2'-α-fluorothymidine following a known procedure.[1,2] 5'-*O*-dimethoxytrityl-2'-*O*-methyl,5-methyluridine 3′-*N,N*′-diisopropyl(cyanoethyl)phosphoramidite (**19**) was prepared from 2'-*O*-methyl,5-methyluridine (purchased from Carbosynth) as reported.[3,4] 5′-*O*-dimethoxytritylthymidine 3′-*N,N*′-diisopropyl(cyanoethyl)phosphoramidite (**20**) was from Eurogentec. 2′-*O*-4′-*C*-methylene-5′-*O*-dimethoxytrityl-5-methyluridine 3′-*N,N*′-diisopropyl(cyanoethyl)phosphoramidite (**24**) was prepared from 2′-*O*-4′-*C*-methylene-5-methyluridine (purchased from Exiquon) as reported.[5] 3′-*O*-acetyl-2′-β-fluorothymidine (**21**) was prepared from 2′-β-fluorothymidine (purchased from Carbosynth) as previously described.[6] 3'-*O*-Acetylthymidine (**22**) was prepared from thymidine (purchased from Aldrich) using standard procedures.[7] 3′-deoxy-3′-α-fluorothymidine (3′-α-FT, **23**) was prepared from thymidine (purchased from Aldrich) as reported.[8] Phosphoramidites and 3′-acetates were dried overnight at room temperature in a desiccator over P_2O_5 prior to use. Chromatography was performed on silica gel 60, particle size 40-63 μm, unless otherwise stated.

All NMR spectra were recorded in D_2O at 298 K. Observed chemical shift (δ) values are given in ppm and coupling constants (J) in Hz. ^{1}H NMR and ^{13}C NMR spectra were recorded on a 600 MHz spectrometer. For the determination of the sugar conformer populations, spectra were analyzed using PERCH NMR software (v 2014.1). Following abbreviations are used: s (singlet), d (doublet), t (triplet), q (quartet), dd (doublet of doublet)..., Tp and pT represents the 5′-end and the 3′-end modified thymidine moieties of dinucleotides, respectively. Prochiral H2'

proton was attributed from its NOE with the H6 proton of the base or from the analysis of the coupling constants with H1' and H3' protons. Prochiral H5', H5" (and H6', H6" for **16**) protons have not been assigned and the most deshielded one has been arbitrarily labeled H5' and H6'. ^{1}H and ^{13}C NMR δ were calibrated in D_2O using residual solvent signal at 4.80 for δ_H and from dioxane at 67.8 ppm for δ_C. ^{31}P NMR and ^{19}F NMR chemical shifts were recorded on a 500 MHz spectrometer and reported from an external capillary standard of 85% phosphoric acid (δ_P 0.00 ppm) and $CFCl_3$ (δ_F -77.00 ppm), respectively.

High Resolution Mass Spectra (HRMS) were recorded on a Q-Tof Micromass spectrometer using electrospray ionization (ESI). HPLC purification of dinucleotides **12-17** was performed on a Sunfire C18 (5 μm, 10 x 250 mm) column using a 67 min, 4 mL/min gradient of 0-20% CH_3CN in 0.05 M aqueous ammonium acetate. The detection was set at 260 nm.

General protocol for the synthesis of dinucleotides 12-17.

Phosphoramidites **18-20**, **24** and nucleosides **21-23** were used to prepare dinucleotides **12-17** as indicated in scheme 1 and 2 of the manuscript.

The alcohol was dried overnight at room temperature in a desiccator over P_2O_5 prior to use. To an anhydrous acetonitrile solution (ca 11 mL/mmol, addition of 2.6 mL/mmol of THF for the synthesis of $T_{2'}\alpha_F pT_{3'}\alpha_F$ **14**) of the phosphoramidite (0.2 to 0.4 mmol scale) and alcohol (1.2 eq) under argon was added a condensing reagent (5-(ethylthio)-1*H*-tetrazole (3.3 eq) for **12**-**15**, imidazolium triflate (1.1 eq) for **16**, 1*H*-tetrazole (3.3 eq) for **17**). The mixture was stirred at room temperature (30 min for **12**, **14**, **15**, **17**; 40 min for **13**; 1 h for **16**). An oxidative reagent (0.2 M iodine solution in THF/H_2O/2,6-lutidine (3 eq) for **12**-**14**, **17** and *tert*-butyl hydroperoxide in nonane solution (5-6 M) (2 to 2.5 eq for **16** and **15**, respectively) was then added. After 50 min of stirring at room temperature (1 h for **16**), when iodine was used (**12**-**14**, **17**), a saturated aqueous $Na_2S_2O_3$ solution was added until discoloration. The reaction mixture, whenever the oxidative conditions, was then diluted with CH_2Cl_2 (50 mL/mmol for **12**-**14**, 24

mL/mmol for **17**) and washed with water (50 mL/mmol for **12**-**14**, 24 mL/mmol for **17**). The organic phase was dried over anhydrous Na_2SO_4, filtered and concentrated. Except for **13** and **16**, the residue for **12**, **14**, **15**, and **17** was transiently purified by silica gel chromatography using a gradient of methanol in dichloromethane (0 to 15% in the presence of 0.5% Et_3N) for **12**, **14**, **17** and a gradient of AcOEt in petroleum ether (10 to 100% in the presence of 0.5% Et_3N) followed by a gradient of methanol in AcOEt (0 to 20% in the presence of 0.5% Et_3N) for **15**. The concentrated crude reaction mixture (for **13**, **16**) or the concentrated fractions of interest (for **12**, **14**, **15**, **17**) were dissolved in conc. aqueous NH_4OH (10 mL/mmol for **12**, **14**, **15**; 14 mL/mmol for **17**; 22 mL/mm for **16**; and 25 mL/mol for **13**) and stirred at room temperature overnight. The solution was concentrated, and the residue dissolved in 80% aqueous acetic acid (10 mL/mmol for **12**, **14**, **15**; 14 mL/mmol for **17** and 25 mL/mol for **13**, **16**). The resulting solution was stirred at room temperature for 4 h and concentrated under reduced pressure. Water (6 mL (25 mL for **16**)) was added, and the aqueous phase was washed with CH_2Cl_2 (2 x 5 mL (2x25 mL for **16**)), concentrated under vacuum then purified by HPLC.

$T_{2'}\alpha_F pT_{2'}\beta_F$ 12.

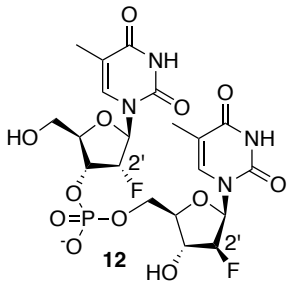

12

Scale: phosphoramidite **18** (160 mg, 0.21 mmol), alcohol **21** (80 mg, 0.26 mmol). Yield: 9 mg, 0.015 mmol, 10%.

^{1}H NMR (D_2O, 600 MHz): δ 7.80 (1H, br s, H6 Tp), 7.74 (1H, br s, H6 pT), 6.31 (1H, dd, $J_{1',2'}$ = 5.1 Hz, $J_{1',F}$ = 11.3 Hz, H1' pT), 5.93 (1H, d, $J_{1',F}$ = 17.5 Hz, H1' Tp), 5.30 (1H, dd, $J_{2',3'}$ = 4.2 Hz, $J_{2',F}$ = 51.5 Hz, H2' Tp), 5.27 (1H, br td, $J_{2',1'}$ = $J_{2',3'}$ = 4.8 Hz, $J_{2',F}$ = 52.3 Hz, H2' pT), 4.63 (1H, dddd, $J_{3',2'}$ = 4.2 Hz, $J_{3',4'}$ = 8.8 Hz, $J_{3',P}$ = 8.4 Hz, $J_{3',F}$ = 21.8 Hz, H3' Tp), 4.56 (1H, ddd, $J_{3',2'}$ = 4.4 Hz, $J_{3',4'}$ = 6.3 Hz, $J_{3',F}$ = 19.6 Hz, H3' pT), 4.31 (1H, ddd, $J_{4',5'}$ = 2.1 Hz, $J_{4',5''}$ = 3.2 Hz, $J_{4',3'}$ = 8.8 Hz, H4' Tp), 4.21(2H, m, H5', H5" pT), 4.17 (1H, m, H4' pT), 4.07 (1H, dd, $J_{5',4'}$ = 2.1 Hz, $J_{5',5''}$ = 13.3 Hz, H5' Tp), 3.89 (1H, dd, $J_{5'',4'}$ =

3.2 Hz, $J_{5",5'}$ = 13.3 Hz, H5" Tp), 1.86 (3H, d, J = 1.2 Hz, CH_3 pT), 1.85 (3H, d, J = 1.2 Hz, CH_3 Tp). $^{13}C\{^1H\}$ NMR (D_2O, 150.9 MHz): δ 167.2 (C4 Tp), 167.0 (C4 pT), 152.4 (C2 pT), 152.1 (C2 Tp), 138.1 (C6 pT), 138.0 (C6 Tp), 112.2 (C5 Tp), 112.1 (C5 pT), 95.8 (d, $J_{C2',F}$ = 193.1 Hz, C2' pT), 93.2 (d, $J_{C2',F}$ = 188.2 Hz, C2' Tp), 89.5 (d, $J_{C1',F}$ = 34.6 Hz, C1' Tp), 84.0 (d, $J_{C1',F}$ = 17.1 Hz, C1' pT), 82.9 (d, $J_{C4',P}$ = 8.8 Hz, C4' Tp), 82.0 (dd, $J_{C4',F}$ = 6.9 Hz, $J_{C4',P}$ = 8.9 Hz, C4' pT), 73.0 (d, $J_{C3',F}$ = 24.8 Hz, C3' pT), 71.1 (dd, $J_{C3',P}$ = 5.4 Hz, $J_{C3',F}$ = 15.9 Hz, C3' Tp), 64.4 (d, $J_{C5',P}$ = 4.6 Hz, C5' pT), 59.7 (C5' Tp), 12.8 (CH_3 pT), 12.7 (CH_3 Tp). $^{19}F\{^1H\}$ NMR (D_2O, 470.6 MHz): δ -200.3, -200.7. $^{31}P\{^1H\}$ NMR (D_2O, 202.5 MHz): δ -0.97. HRMS ($(M-H)^-$, MeOH): calc. for $C_{20}H_{24}F_2N_4O_{12}P$ 581.1096, found 581.1091.

$T_{2'}\alpha_F$pT 13.

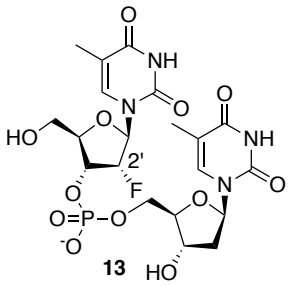

13

Scale: phosphoramidite **18** (169 mg, 0.20 mmol), 3'-acetylthymidine **22** (67 mg, 0.24 mmol). Yield: 27 mg, 0.048 mmol, 37%.

^1H NMR (D_2O, 600 MHz): δ 7.77 (1H, br s, H6 pT), 7.76 (1H, br s, H6 Tp), 6.33 (1H, t, $J_{1',2'}$ = $J_{1',2"}$ = 6.4 Hz, H1' pT), 5.92 (1H, br d, $J_{1',F}$ = 18.1 Hz, H1' Tp), 5.27 (1H, dd, $J_{2',3'}$ = 4.4 Hz, $J_{2',F}$ = 51.6 Hz, H2' Tp), 4.64 (1H, dddd, $J_{3',2'}$ = 4.4 Hz, $J_{3',P}$ = 8.3 Hz, $J_{3',4'}$ = 8.6 Hz, $J_{3',F}$ = 20.9 Hz, H3' Tp), 4.59 (1H, td, $J_{3',2'}$ = $J_{3',4'}$ = 4.7 Hz, $J_{3',2"}$ = 6.4 Hz, H3' pT), 4.28 (1H, ddd, $J_{4',5'}$ = 2.3 Hz, $J_{4',5"}$ = 3.4 Hz, $J_{4',3'}$ = 8.6 Hz, H4' Tp), 4.15 (2H, ddd, $J_{5',4'}$ = 2.5 Hz, $J_{5',P}$ = 4.0 Hz, $J_{5',5"}$ = 11.3 Hz, H5' pT), 4.12 (1H, m, H4' pT), 4.11 (1H, m, H5" pT), 4.03 (1H, dd, $J_{5',4'}$ = 2.3 Hz, $J_{5',5"}$ = 13.3 Hz, H5' Tp), 3.85 (1H, dd, $J_{5",4'}$ = 3.4 Hz, $J_{5",5'}$ = 13.3 Hz, H5" Tp), 2.37 (2H, m, H2', H2" pT), 1.86 (6H, br s, CH_3 Tp, CH_3 pT). $^{13}C\{^1H\}$ NMR (D_2O, 150.9 MHz): δ 167.4 (C4 Tp), 167.1 (C4 pT), 152.7 (C2 pT), 152.2 (C2 Tp), 138.3 (C6 Tp), 138.0 (C6 pT), 112.7 (C5 pT), 112.2 (C5 Tp), 93.1 (d, $J_{C2',F}$ = 188.5 Hz, C2' Tp), 90.1 (d, $J_{C1',F}$ = 34.7 Hz, C1' Tp), 86.1 (d, $J_{C4',P}$ = 9.5 Hz, C4' pT), 86.0 (C1' pT), 83.0 (d, $J_{C4',P}$ = 8.6 Hz, C4' Tp), 71.3 (dd, $J_{C3',P}$ = 5.1 Hz, $J_{C3',F}$ = 15.9 Hz, C3' Tp), 71.0 (C3' pT), 65.6 (d, $J_{C5',P}$ = 4.3

Hz, C5' pT), 59.9 (C5' Tp), 40.2 (C2' pT), 12.8 (CH_3 Tp), 12.7 (CH_3 pT). $^{19}F\{^1H\}$ NMR (D_2O, 470.6 MHz): δ -199.8. $^{31}P\{^1H\}$ NMR (D_2O, 202.5 MHz): δ -1.2. HRMS ($(M-H)^-$, MeOH): calc. for $C_{20}H_{25}FN_4O_{12}P$ 563.1191, found 563.1187.

$T_{2'}\alpha_F pT_{3'}\alpha_F$ 14.

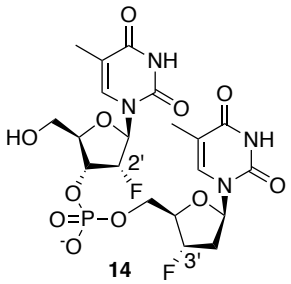

Scale: phosphoramidite **18** (147 mg, 0.19 mmol), alcohol **23** (61 mg, 0.25 mmol). Yield: 26 mg, 0.046 mmol, 24%.

^1H NMR (D_2O, 600 MHz): δ 7.77 (1H, br s, H6 pT), 7.75 (1H, br s, H6 Tp), 6.45 (1H, dd, $J_{1',2''}$ = 5.8 Hz, $J_{1',2'}$ = 9.1 Hz, H1' pT), 5.94 (1H, dd, $J_{1',2'}$ = 1.5 Hz, $J_{1',F}$ = 18.6 Hz, H1' Tp), 5.46 (1H, dd, $J_{3',2'}$ = 5.0 Hz, $J_{3',F}$ = 53.0 Hz, H3' pT), 5.25 (1H, ddd, $J_{2',1'}$ = 1.5 Hz, $J_{2',3'}$ = 4.5 Hz, $J_{2',F}$ = 51.7 Hz, H2' Tp), 4.69 (1H, dddd, $J_{3',2'}$ = 4.5 Hz, $J_{3',P}$ = 8.0 Hz, $J_{3'4'}$ = 8.3 Hz, $J_{3',F}$ = 20.1 Hz, H3' Tp), 4.54 (1H, br dd, $J_{4',5'}$ = 2.1 Hz, $J_{4',F}$ = 27.2 Hz, H4' pT), 4.27 (1H, ddd, $J_{4',5'}$ = 2.3 Hz, $J_{4',5''}$ = 3.4 Hz, $J_{4',3'}$ = 8.3 Hz, H4' Tp), 4.17 (2H, m, H5', H5" pT), 4.04 (1H, dd, $J_{5',4'}$ = 2.3 Hz, $J_{5',5''}$ = 13.2 Hz, H5' Tp), 3.85 (1H, dd, $J_{5'',4'}$ = 3.4 Hz, $J_{5'',5'}$ = 13.2 Hz, H5" Tp), 2.64 (1H, ddd, $J_{2'',1'}$ = 5.8 Hz, $J_{2'',2'}$ = 14.7 Hz, $J_{2'',F}$ = 21.3 Hz, H2" pT), 2.37 (1H, dddd, $J_{2',3'}$ = 5.0 Hz, $J_{2',1'}$ = 9.1 Hz, $J_{2',2''}$ = 14.7 Hz, $J_{2',F}$ = 39.5 Hz, H2' pT), 1.88 (3H, d, J = 1.3 Hz, CH_3 Tp), 1.87 (3H, d, J = 1.3 Hz, CH_3 pT). $^{13}C\{^1H\}$ NMR (D_2O, 150.9 MHz): δ 167.5 (C4 Tp), 167.2 (C4 pT), 152.9 (C2 pT), 152.3 (C2 Tp), 138.6 (C6 Tp), 138.0 (C6 pT), 113.1 (C5 pT), 112.3 (C5 Tp), 96.0 (d, $J_{C3',F}$ = 174.8 Hz, C3' pT), 93.0 (d, $J_{C2',F}$ = 188.5 Hz, C2' Tp), 90.3 (d, $J_{C1',F}$ = 35.2 Hz, C1' Tp), 86.2 (C1' pT), 84.8 (dd, $J_{C4',P}$ = 9.2 Hz, $J_{C4',F}$ = 26.2 Hz, C4' pT), 83.1 (d, $J_{C4',P}$ = 8.6 Hz, C4' Tp), 71.6 (dd, $J_{C3',P}$ = 5.1 Hz, $J_{C3',F}$ = 15.6 Hz, C3' Tp), 66.2 (dd, $J_{C5',P}$ = 3.5 Hz, $J_{C5',F}$ = 11.5 Hz, C5' pT), 60.1 (C5' Tp), 38.6 (d, $J_{C2',F}$ = 20.8 Hz, C2' pT), 12.8 (CH_3 Tp), 12.7 (CH_3 pT). $^{19}F\{^1H\}$ NMR (D_2O, 470.6 MHz): δ -174.4, -199.5. $^{31}P\{^1H\}$ NMR (D_2O, 202.5 MHz): δ -1.35. HRMS ($(M-H)^-$, MeOH): calc. for $C_{20}H_{24}F_2N_4O_{11}P$ 565.1147, found 565.1141.

$T_{2'mo}pT_{3'}\alpha_F$ 15.

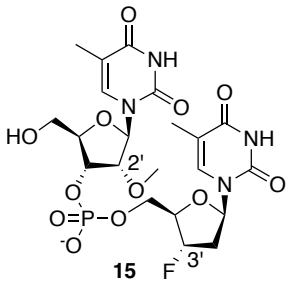

15

Scale: phosphoramidite **19** (195 mg, 0.25 mmol), alcohol **23** (80 mg, 0.33 mmol). Yield: 7 mg, 0.012 mmol, 10%.

^{1}H NMR (D_2O, 600 MH): δ 7.84 (1H, br s, H6 Tp), 7.78 (1H, br s, H6 pT), 6.44 (1H, dd, $J_{1',2''}$ = 5.8 Hz, $J_{1',2'}$ = 9.1 Hz, H1' pT), 5.93 (1H, d, $J_{1',2'}$ = 3.4 Hz, H1' Tp), 5.45 (1H, dd, $J_{3',2'}$ = 5.0 Hz, $J_{3',F}$ = 53 Hz, H3' pT), 4.66 (1H, m, H3' Tp), 4.55 (1H, br d, $J_{4',F}$ = 27.2 Hz, H4' pT), 4.26 (1H, ddd, $J_{4',5'}$ = 2.6 Hz, $J_{4',5''}$ = 3.4 Hz, $J_{4',3'}$ = 6.4 Hz, H4' Tp), 4.16 (2H, m, H5', H5" pT), 4.11 (1H, dd, $J_{2',1'}$ = 3.4 Hz, $J_{2',3'}$ = 5.1 Hz, H2' Tp), 3.96 (1H, dd, $J_{5',4'}$ = 2.6 Hz, $J_{5',5''}$ = 13.1 Hz, H5' Tp), 3.85 (1H, dd, $J_{5'',4'}$ = 3.4 Hz, $J_{5'',5'}$ = 13.1 Hz, H5" Tp), 3.54 (3H, s, OCH_3), 2.64 (1H, ddd, $J_{2'',1'}$ = 5.8 Hz, $J_{2'',2'}$ = 14.9 Hz, $J_{2'',F}$ = 21.8 Hz, H2" pT), 2.38 (1H, dddd, $J_{2',3'}$ = 5.0 Hz, $J_{2',1'}$ = 9.1 Hz, $J_{2',2''}$ = 14.9 Hz, $J_{2',F}$ = 39.3 Hz, H2' pT), 1.88 (3H, d, J = 0.9 Hz, CH_3 Tp), 1.87 (3H, d, J = 1.0 Hz, CH_3 pT). ^{13}C{^{1}H} NMR (D_2O, 150.9 MHz): δ 167.5 (C4 Tp), 167.2 (C4 pT), 152.9 (C2 pT), 152.6 (C2 Tp), 138.1 (C6 Tp and pT), 113.1 (C5 pT), 112.4 (C5 Tp), 96.1 (d, $J_{C3',F}$ = 175 Hz, C3' pT), 88.3 (C1' Tp), 86.3 (C1' pT), 84.8 (dd, $J_{C4',P}$ = 9.1 Hz, $J_{C4',F}$ = 26 Hz, C4' pT), 84.4 (d, $J_{C4',P}$ = 6.2 Hz, C4' Tp), 82.6 (C2' Tp), 72.3 (d, $J_{C3',P}$ = 5.4 Hz, C3' Tp), 66.3 (dd, $J_{C5',P}$ = 5.3 Hz, $J_{C5',F}$ = 11.8 Hz, C5' pT), 60.7 (C5' Tp), 58.9 (OCH_3), 38.5 (d, $J_{C2',F}$ = 21 Hz, C2' pT), 12.9 (CH_3 Tp), 12.6 (CH_3 pT). ^{19}F{^{1}H} NMR (D_2O, 470.6 MHz): δ -174.6. ^{31}P{^{1}H} NMR (D_2O, 202.5 MHz): δ -1.2. HRMS ($(M+H)^+$, MeOH): calc. for $C_{21}H_{29}FN_4O_{12}P$ 579.1504, found 579.1514.

$T_{2'4'L}pT_{3'}\alpha_F$ 16.

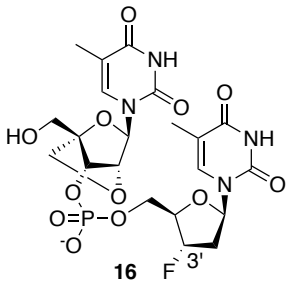

Scale: phosphoramidite **24** (348 mg, 0.45 mmol) and alcohol **23** (121 mg, 0.49 mmol). Yield: 22 mg, 0.038 mmol, 8%.

^{1}H NMR (D_2O, 600 MHz): δ 7.77 (1H, br s, H6 pT), 7.64 (1H, br s, H6 Tp), 6.45 (1H, dd, $J_{1',2'}$ = 5.8 Hz, $J_{1',2''}$ = 9.0 Hz, H1′ pT), 5.62 (1H, br d, $J_{1',2'}$ = 1.3 Hz, H1′ Tp), 5.39 (1H, dd, $J_{3',2'}$ = 5.0 Hz, $J_{3',F}$ = 53.0 Hz, H3′ pT), 4.68 (1H, br s, H2′ Tp), 4.52 (1H, br d, $J_{4',F}$ = 26.9 Hz, H4′ pT), 4.41 (1H, d, $J_{3',P}$ = 5.7 Hz, H3′ Tp), 4.14 (2H, m, H5′, H5″ pT), 4.08 (1H, d, $J_{6',6''}$ = 8.4 Hz, H6′ Tp), 4.03 (2H, m, H5′, H5″ Tp), 3.97 (1H, d, $J_{6'',6'}$ = 8.4 Hz, H6″ Tp), 2.64 (1H, ddd, $J_{2',1'}$ = 5.9 Hz, $J_{2',2''}$ = 14.9 Hz, $J_{2',F}$ = 21.3 Hz, H2′ pT), 2.27 (1H, dddd, $J_{2'',3'}$ = 5.1 Hz, $J_{2'',1'}$ = 9.0 Hz, $J_{2'',2'}$ = 14.9 Hz, $J_{2'',F}$ = 38.7 Hz, H2″ pT), 1.87 (3H, br s, CH_3 Tp), 1.83 (3H, br s, CH_3 pT). $^{13}C\{^1H\}$ NMR (D_2O, 150.9 MHz): δ 166.1 (C4 Tp), 166.0 (C4 pT), 151.5 (C2 pT), 150.8 (C2 Tp), 136.6 (C6 pT), 135.7 (C6 Tp), 111.8 (C5 pT), 110.7 (C5 Tp), 94.5 (d, $J_{C3',F}$ = 175.0 Hz, C3′ pT), 88.5 (d, $J_{C4',P}$ = 8.5 Hz, C4′ Tp), 86.9 (C1′ Tp), 85.1(C1′ pT), 83.5 (dd, $J_{C4',P}$ = 8.8 Hz, $J_{C4',F}$ = 25.9 Hz, C4′ pT), 77.9 (C2′ Tp), 72.0 (d, $J_{C3',P}$ = 5.3 Hz, C3′ Tp), 71.6 (C6′ Tp), 64.8 (dd, $J_{C5',P}$ = 5.3 Hz, $J_{C5',F}$ = 11.6 Hz, C5′ pT), 56.0 (C5′ Tp), 37.5 (d, $J_{C2',F}$ = 21.1 Hz, C2′ pT), 11.7 (CH_3 Tp), 11.3 (CH_3 pT). $^{19}F\{^1H\}$ NMR (D_2O, 470.6 MHz): δ -174.4. $^{31}P\{^1H\}$ NMR (D_2O, 202.5 MHz): δ -1.35. HRMS ($(M+Na)^+$, MeOH): calc. for $C_{21}H_{26}FN_4O_{12}PNa$ 599.1167, found 599.1165.

TpT$_{3'}\alpha_F$ 17.

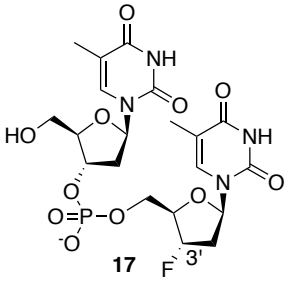

Scale: phosphoramidite **20** (215 mg, 0.29 mmol) and alcohol **23** (84 mg, 0.35 mmol). Yield: 15 mg, 0.027 mmol, 14% yield.

^{1}H NMR (D_2O, 600 MHz): δ 7.74 (1H, br s, H6 pT), 7.67 (1H, br s, H6 Tp), 6.41 (1H, dd, $J_{1',2''}$ = 5.7 Hz, $J_{1',2'}$ = 9.3 Hz, H1' pT), 6.23 (1H, br t, $J_{1',2'} = J_{1',2''}$ = 6.8 Hz, H1' Tp), 5.46 (1H, dd, $J_{3',2'}$ = 5.1 Hz, $J_{3',F}$ = 53.2 Hz, H3' pT), 4.79 (1H, m, H3' Tp), 4.50 (1H, br d, $J_{4',F}$ = 27.4 Hz, H4' pT), 4.20 (1H, m, H4' Tp), 4.15 (2H, m, H5', H5" pT), 3.82 (2H, m, H5', H5" Tp), 2.63 (1H, ddd, $J_{2'',1'}$ = 5.7 Hz, $J_{2'',2'}$ = 14.9 Hz, $J_{2'',F}$ = 22.0 Hz, H2" pT), 2.56 (1H, ddd, $J_{2',3'}$ = 3.4 Hz, $J_{2',1'}$ = 6.1 Hz, $J_{2',2''}$ = 14.2 Hz, H2" Tp), 2.40 (1H, dddd, $J_{2',3'}$ = 5.1 Hz, $J_{2',1'}$ = 9.3 Hz, $J_{2',2''}$ = 14.9 Hz, $J_{2',F}$ = 38.4 Hz, H2' pT), 2.35 (1H, m, H2' Tp), 1.91 (3H, br s, CH_3 pT), 1.89 (3H, br s, CH_3 Tp). ^{13}C{^{1}H} NMR (D_2O, 150.9 MHz): δ 167.6 (C4 Tp), 167.4 (C4 pT), 152.9 (C2 pT), 152.6 (C2 Tp), 138.5 (C6 Tp), 138.3 (C6 pT), 112.9 (C5 pT), 112.7 (C5 Tp), 95.6 (d, $J_{C3',F}$ = 174.0 Hz, C3' pT), 86.8 (d, $J_{C4',P}$ = 7.6 Hz, C4' Tp), 86.4 (C1' Tp), 86.1 (C1' pT), 84.7 (dd, $J_{C4',P}$ = 9.3 Hz, $J_{C4',F}$ = 26.2 Hz, C4' pT), 76.2 (d, $J_{C3',P}$ = 5.2 Hz, C3' Tp), 66.1 (dd, $J_{C5',P}$ = 5.3 Hz, $J_{C5',F}$ = 11.4 Hz, C5' pT), 62.1 (C5' Tp), 38.7 (d, $J_{C2',P}$ = 2.7 Hz, C2' Tp), 38.3 (d, $J_{C2',F}$ = 20.8 Hz, C2' pT), 12.8 (2C, CH_3 Tp, CH_3 pT). ^{19}F{^{1}H} NMR (D_2O, 470.6 MHz): δ -174.8. ^{31}P{^{1}H} NMR (D_2O, 202.5 MHz): δ -1.16. HRMS ($(M-H)^-$, MeOH): calc. for $C_{20}H_{25}FN_4O_{11}P$ 547.1241, found 547.1244.

2. NMR Spectra

Figure S11: ^{1}H NMR spectrum of **12** (600 MHz, D_2O).

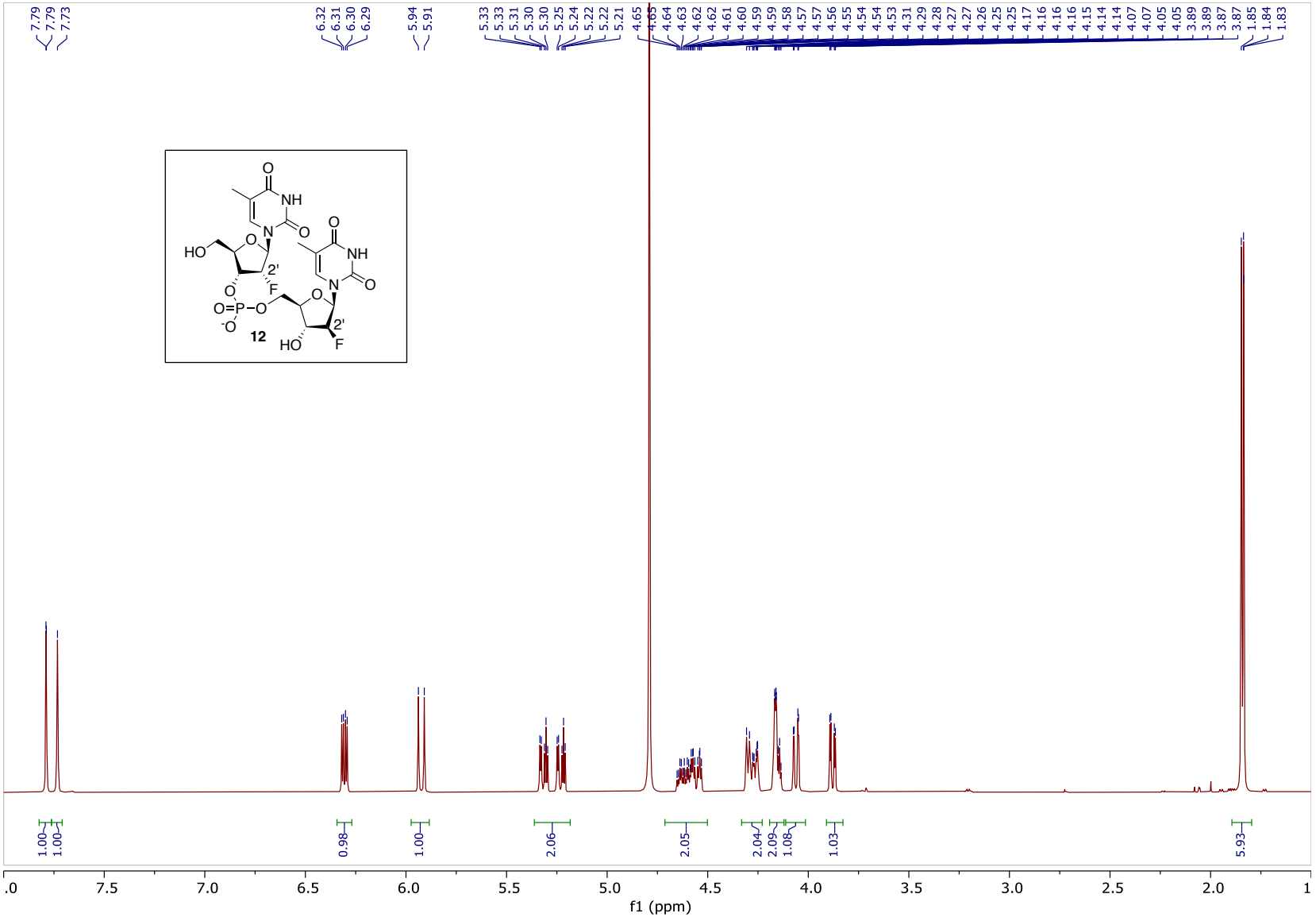

Figure S12: ^{13}C NMR spectrum of **12** (150 MHz, D_2O).

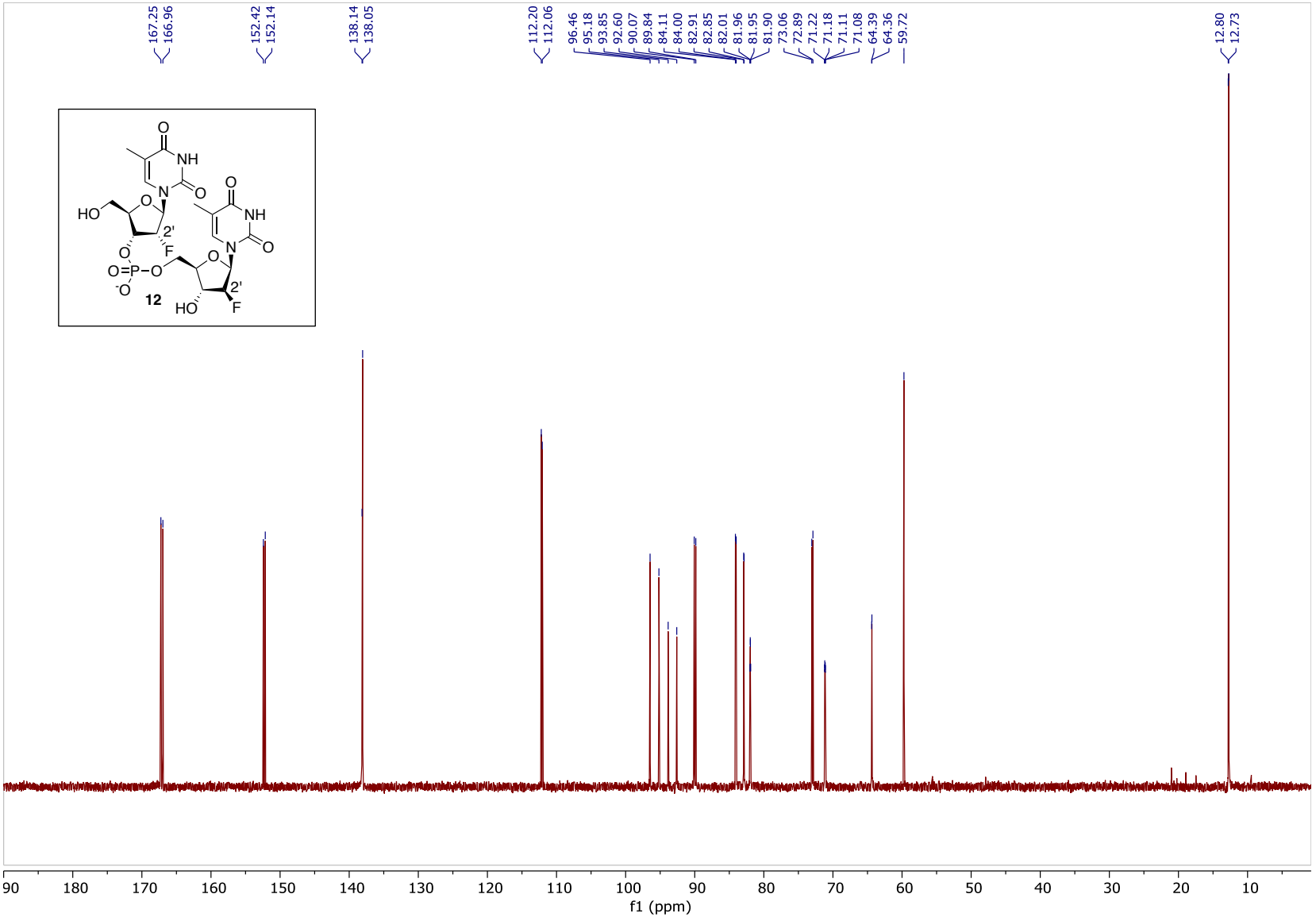

Figure S13: COSY spectrum of **12** (600 MHz, D_2O).

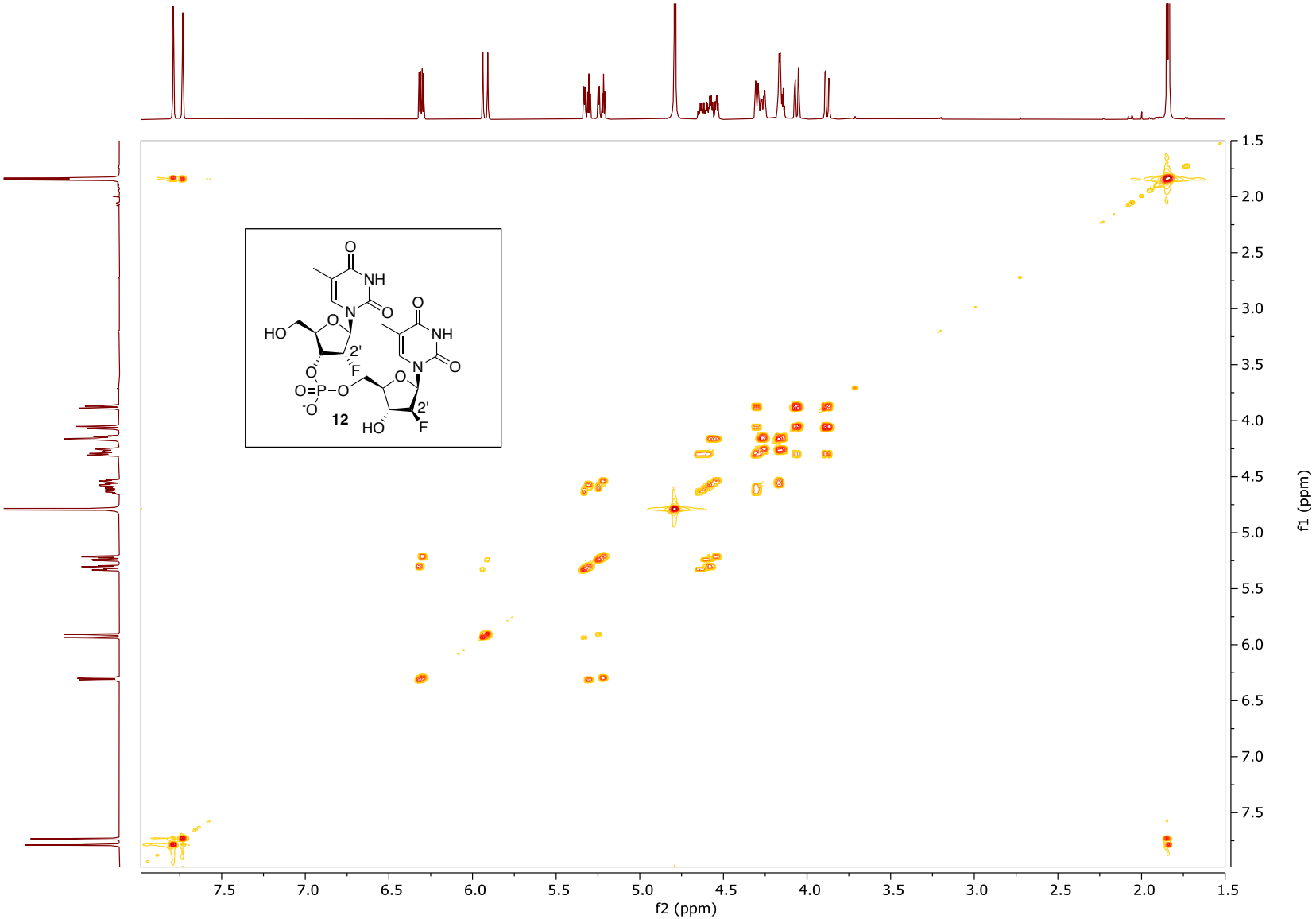

Figure S14: HSQC spectrum of **12** (600 MHz, D_2O).

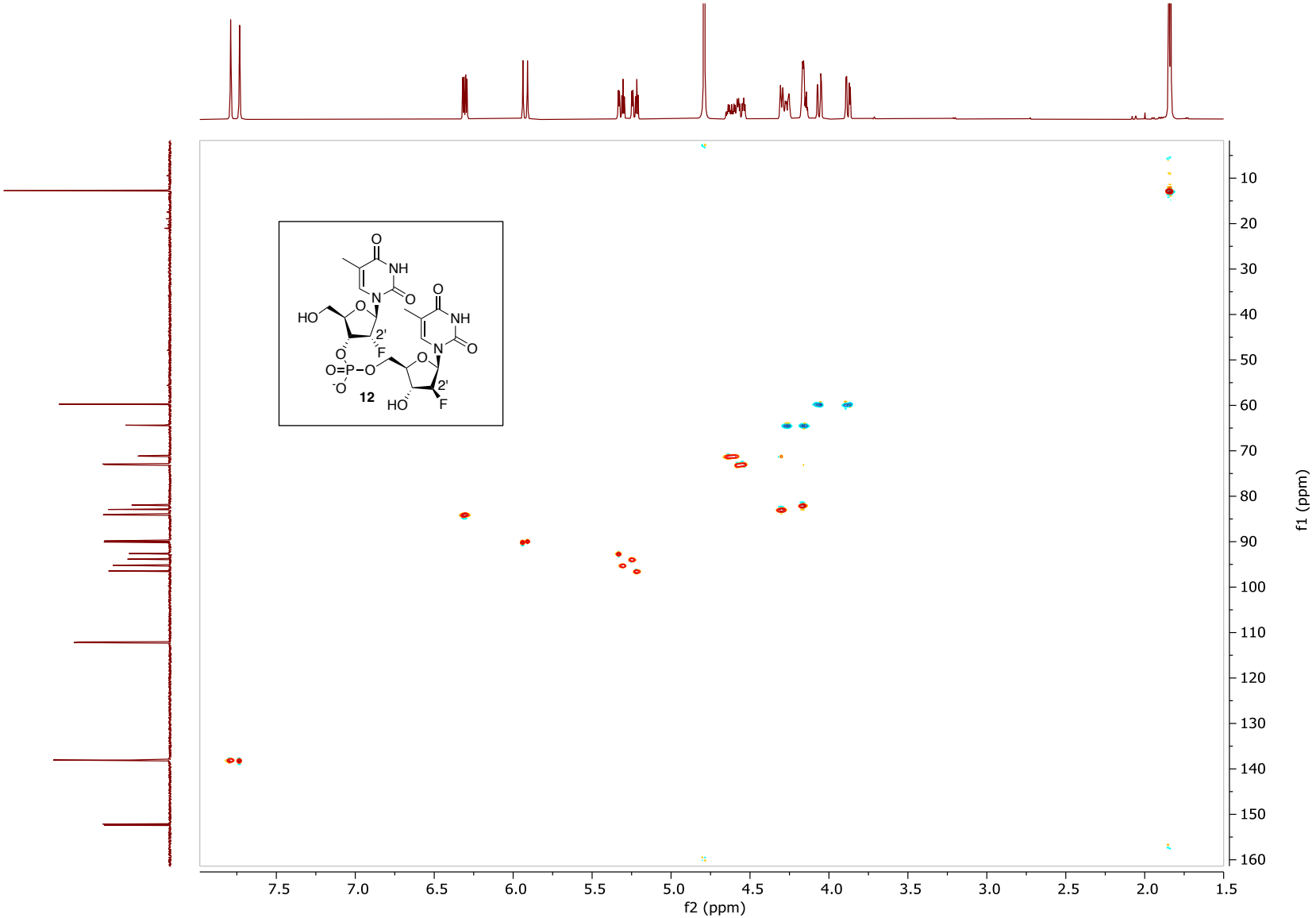

Figure S15: HMBC spectrum of **12** (600 MHz, D_2O).

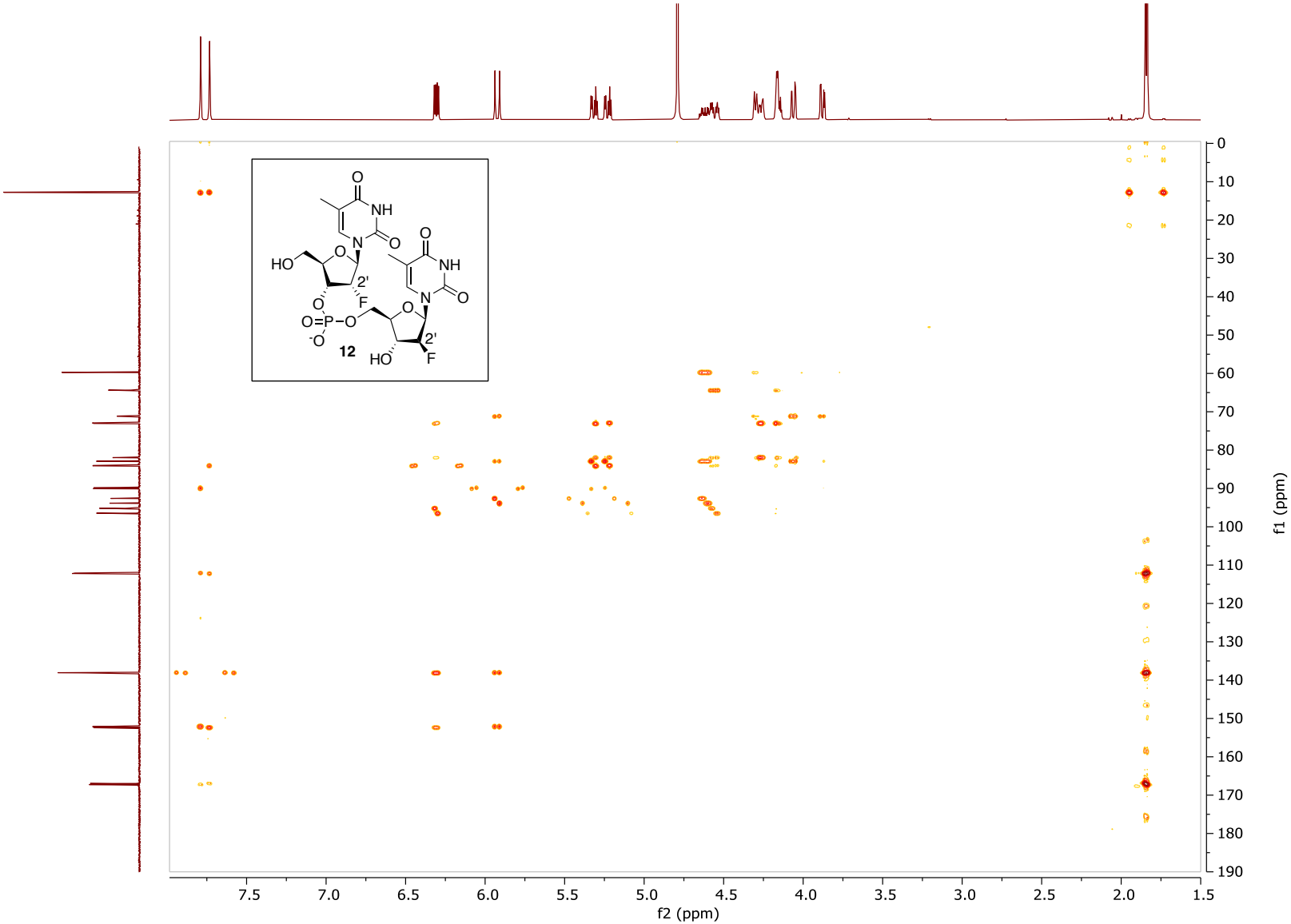

Figure S16: ^{1}H NMR spectrum of **13** (600 MHz, D_2O).

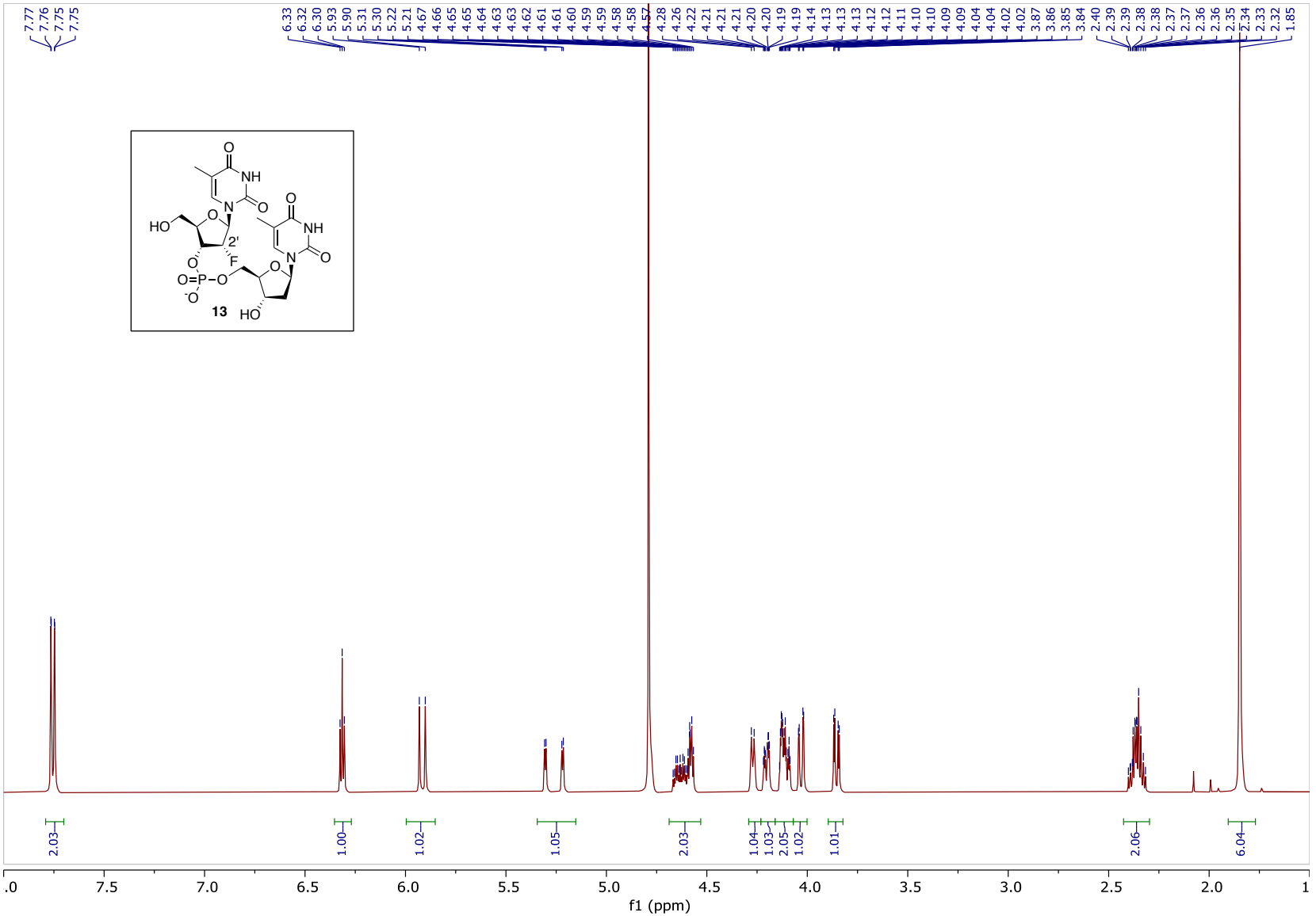

Figure S17: ^{13}C NMR spectrum of **13** (150 MHz, D_2O).

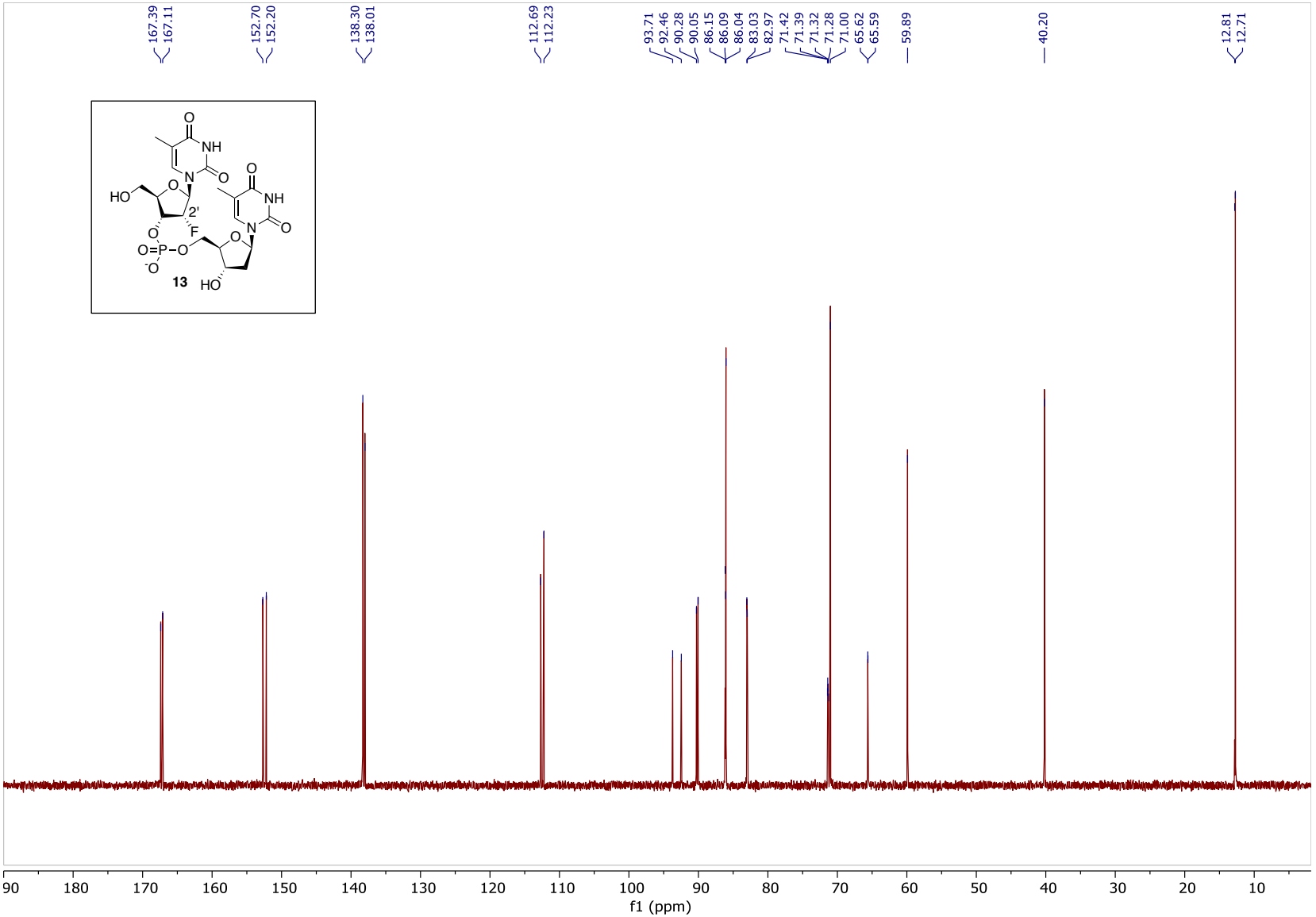

Figure S18: COSY spectrum of **13** (600 MHz, D_2O).

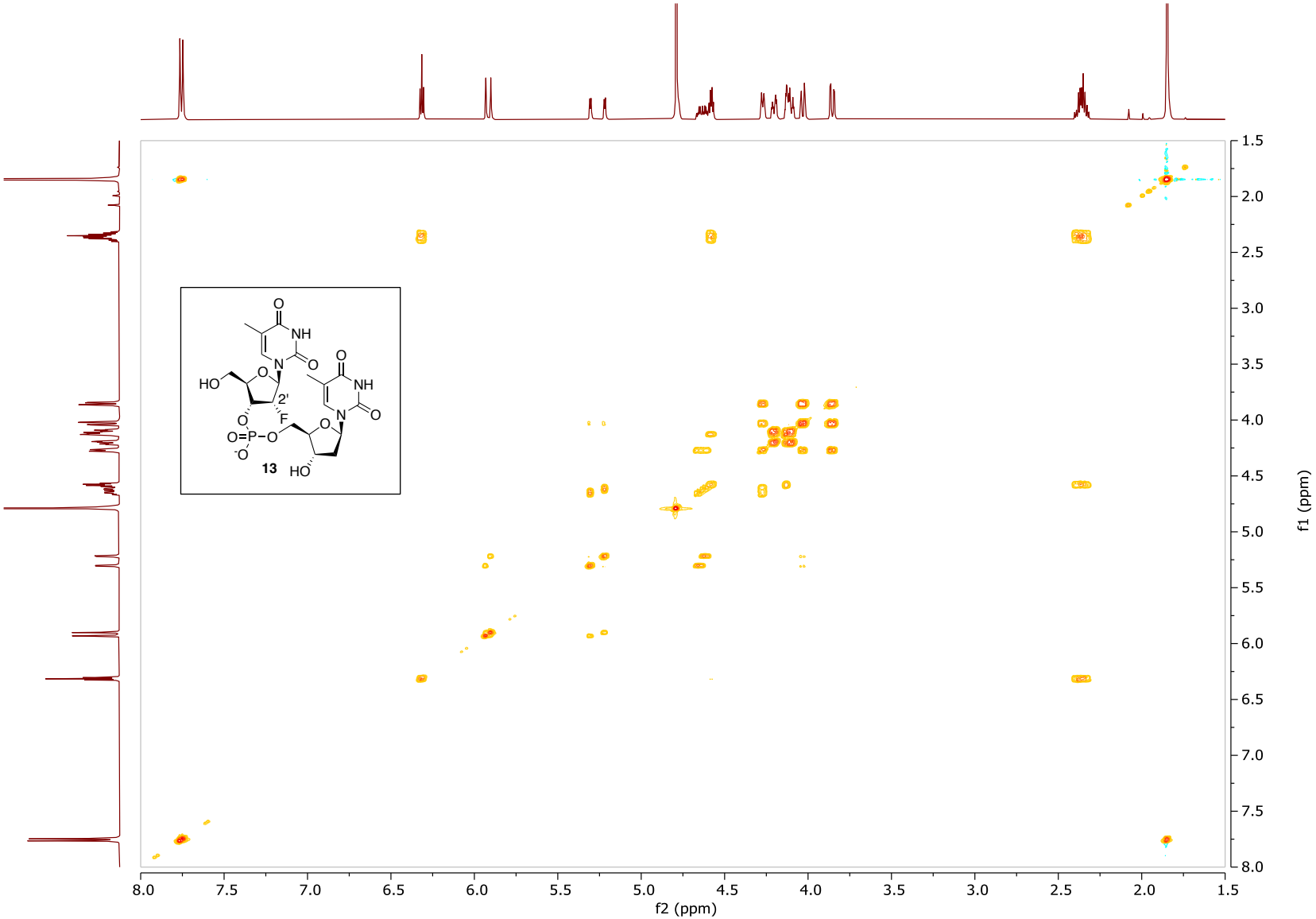

Figure S19: HSQC spectrum of **13** (600 MHz, D_2O).

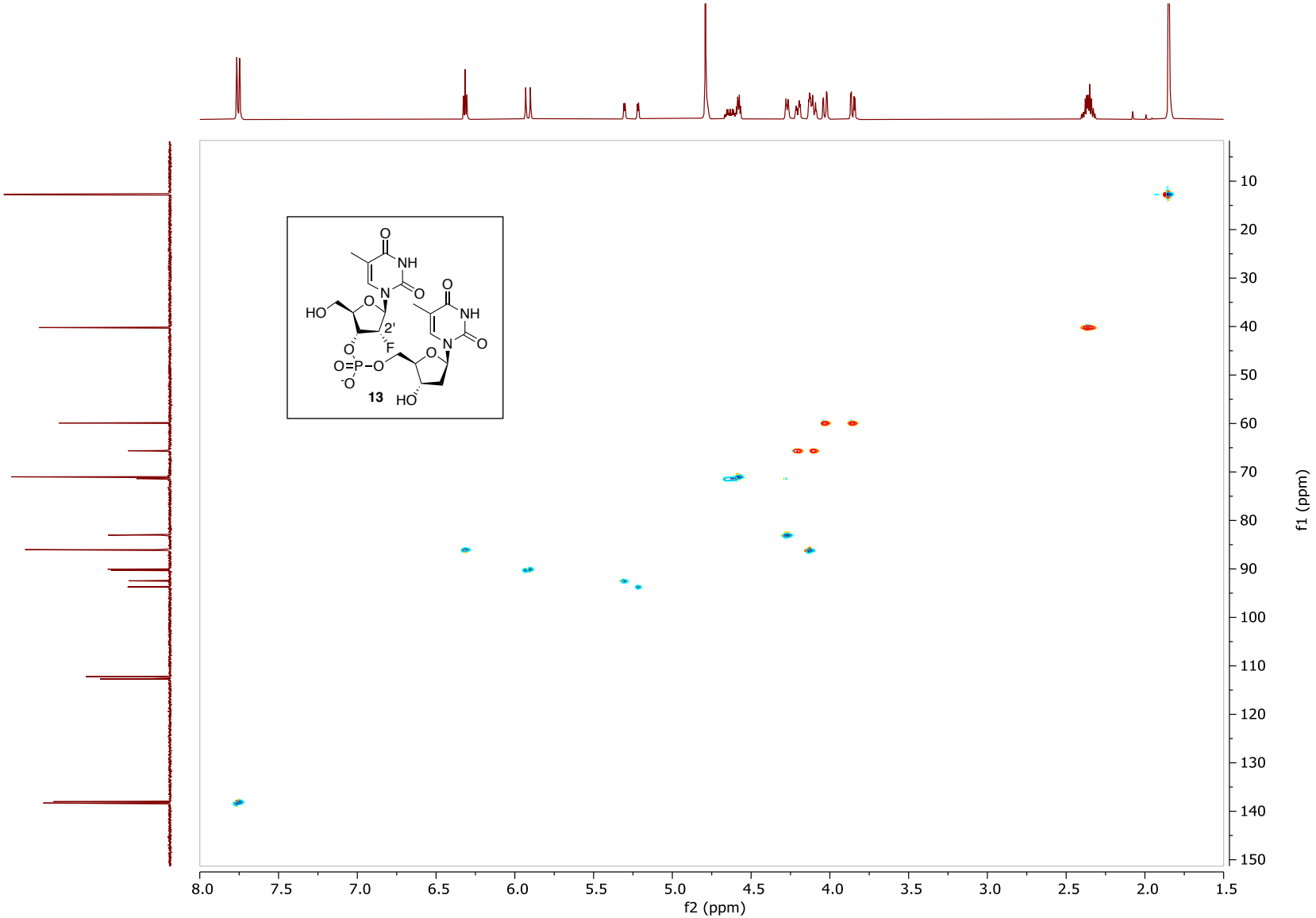

Figure S20: HMBC spectrum of **13** (600 MHz, D_2O).

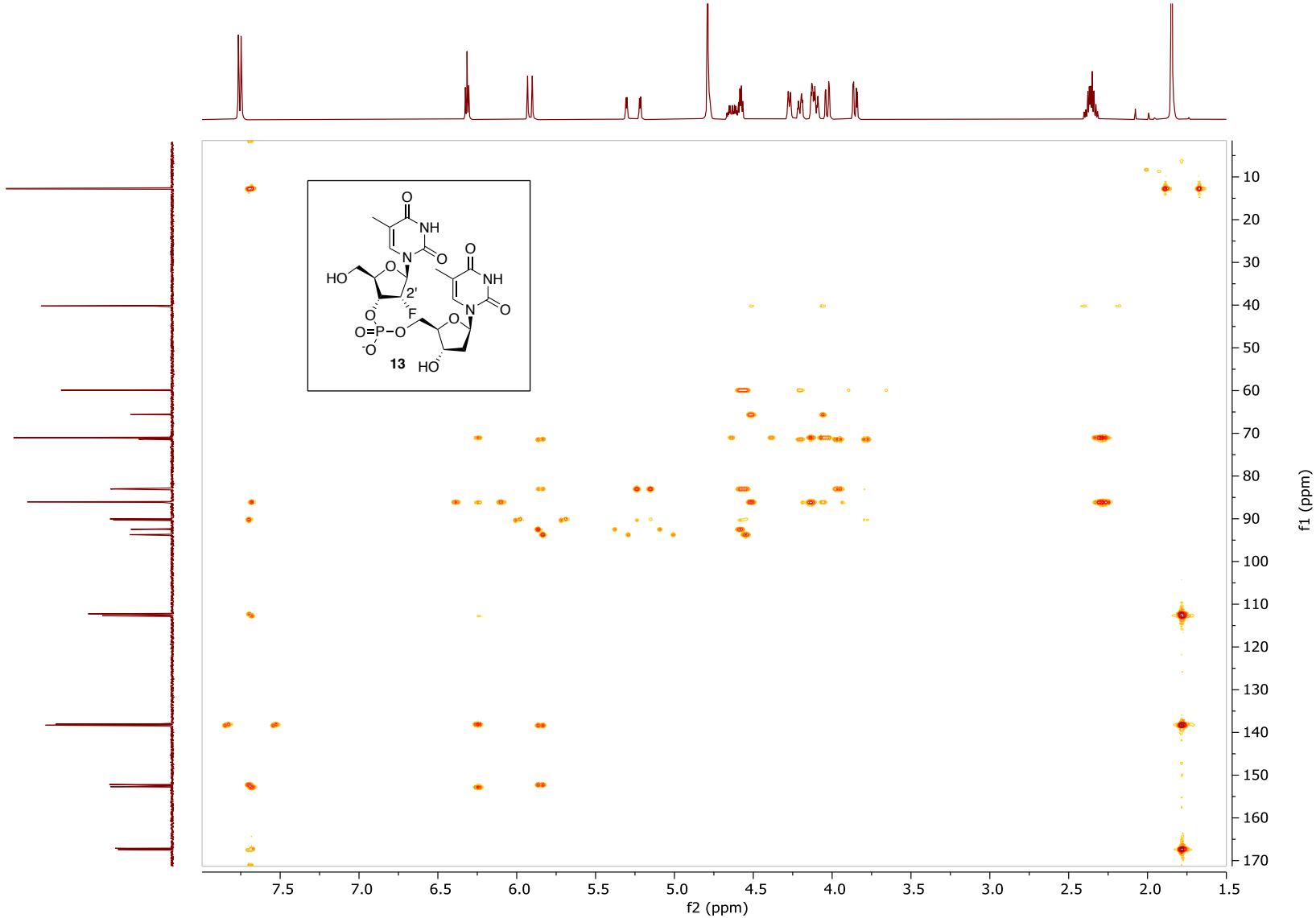

Figure S21: ^{1}H NMR spectrum of **14** (600 MHz, D_2O).

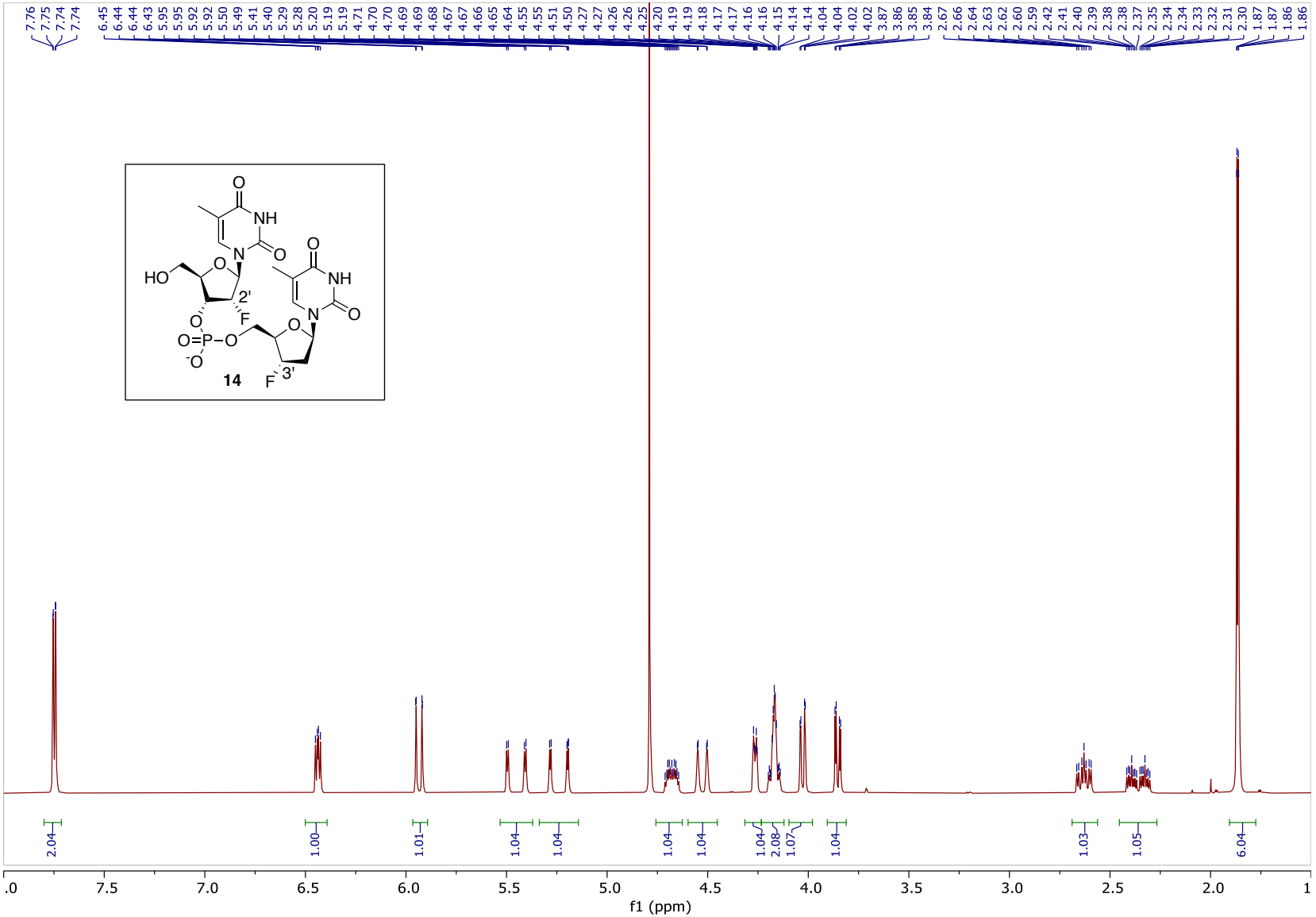

Figure S22: ^{13}C NMR spectrum of **14** (150 MHz, D_2O).

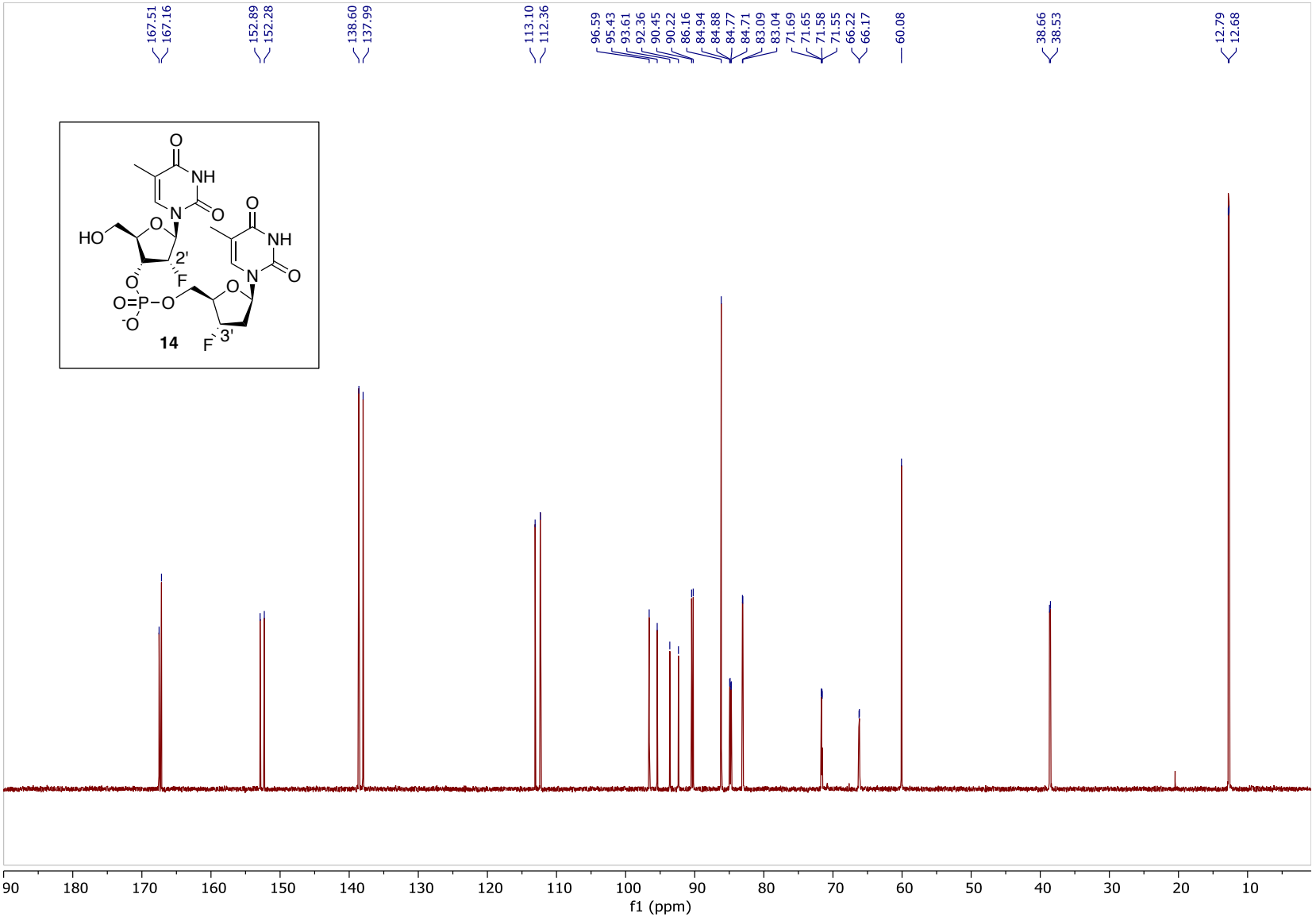

Figure S23: COSY spectrum of **14** (600 MHz, D_2O).

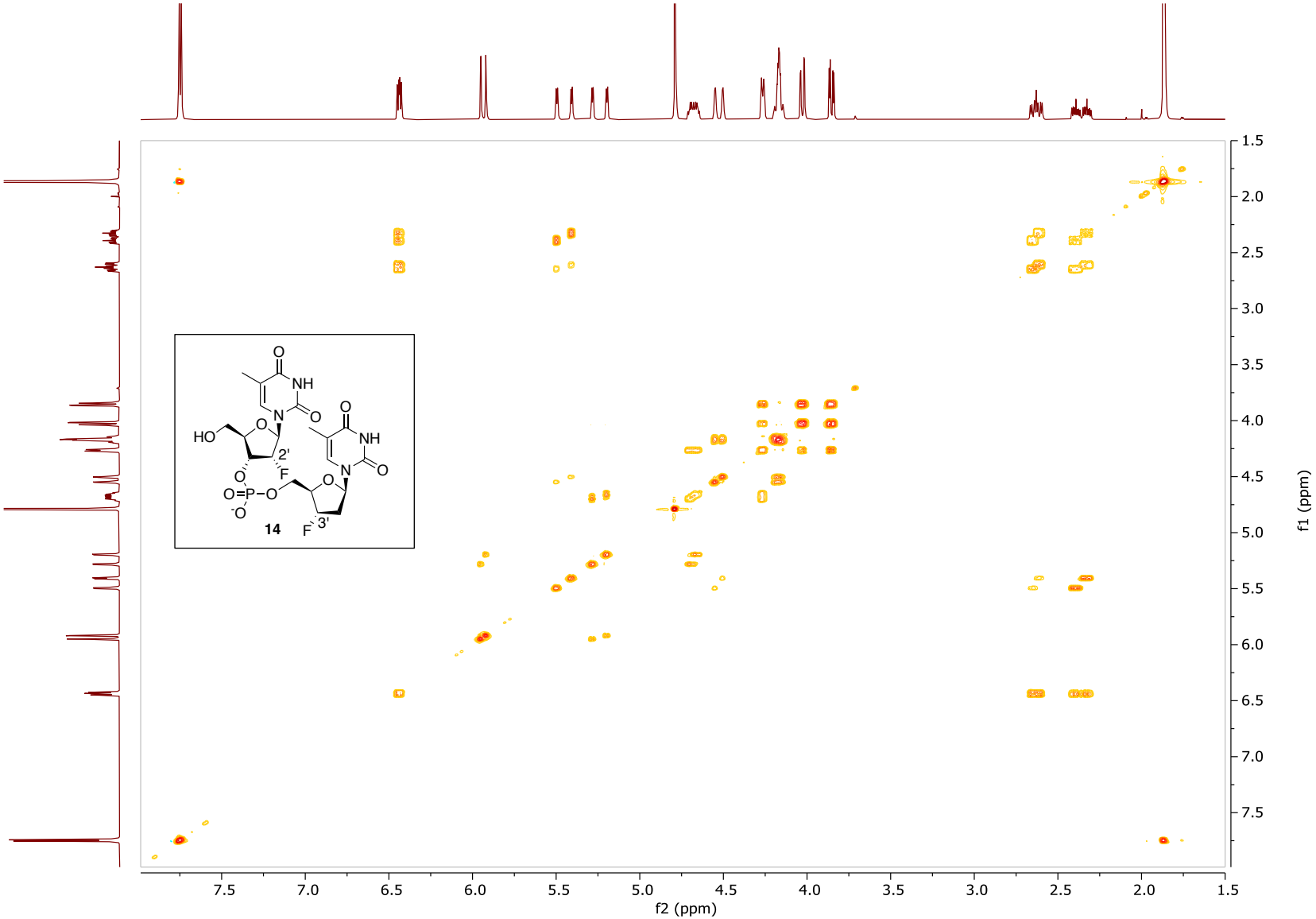

Figure S24: HSQC spectrum of **14** (600 MHz, D_2O).

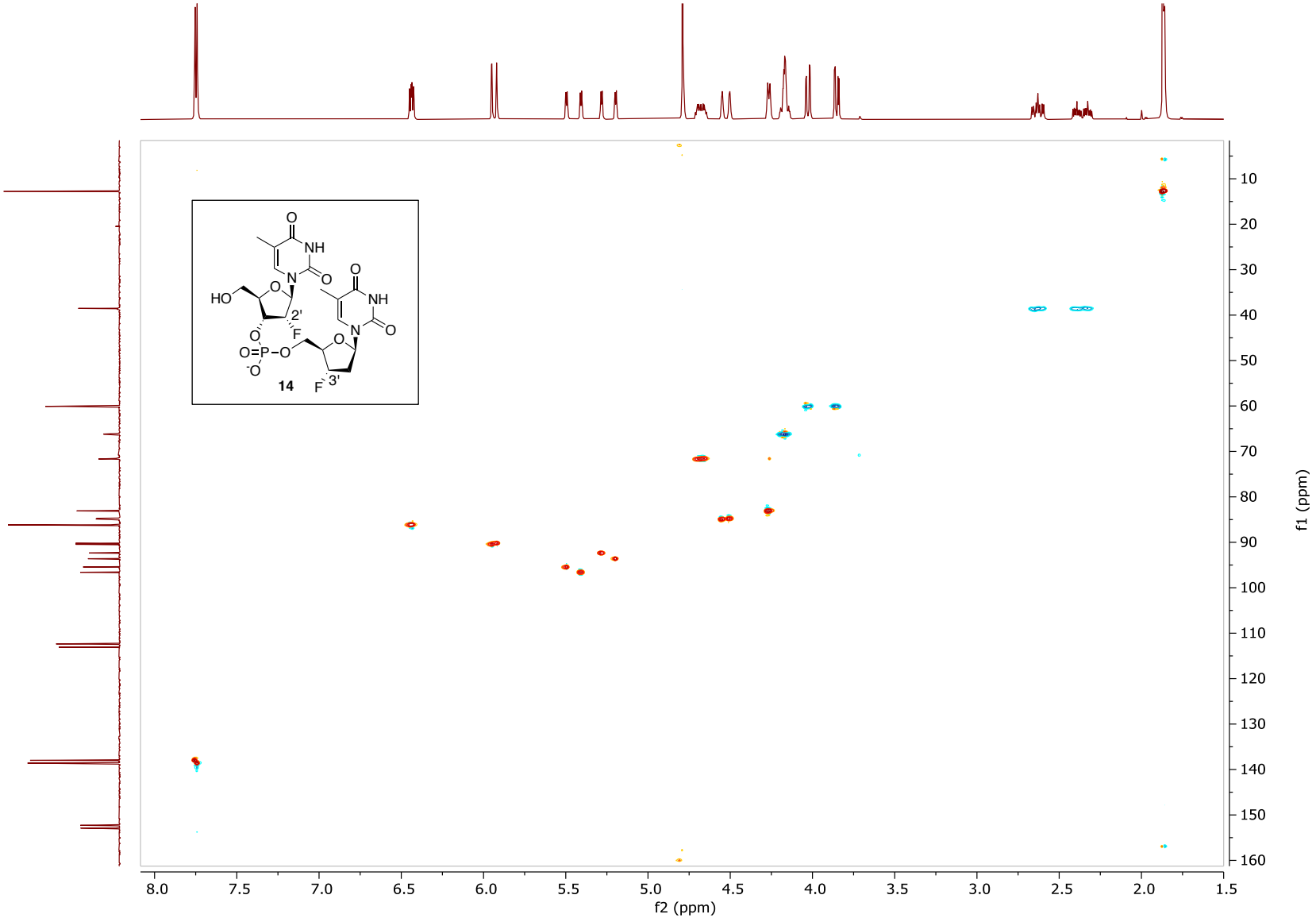

Figure S25: HMBC spectrum of **14** (600 MHz, D_2O).

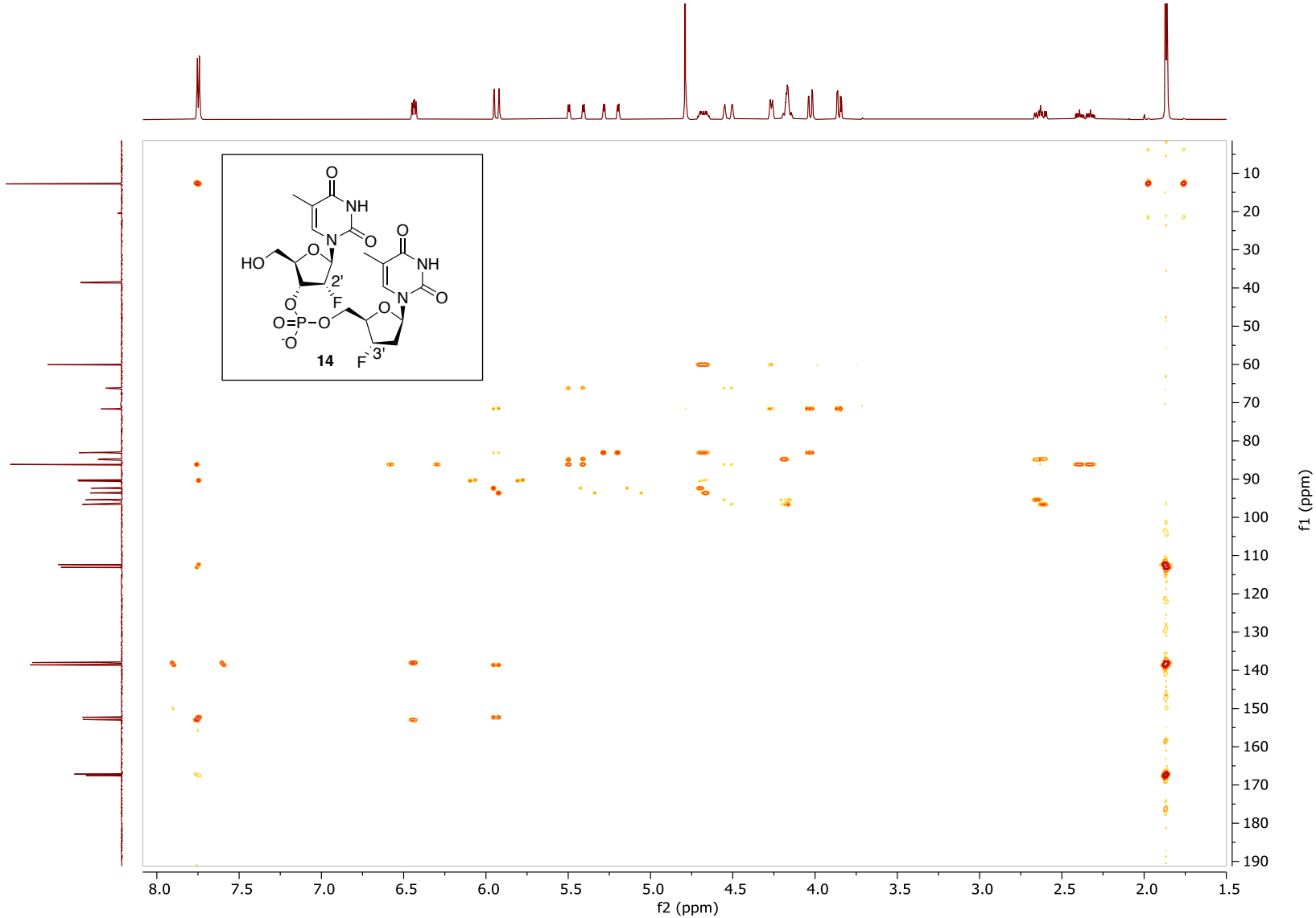

Figure S26: ^{1}H NMR spectrum of **15** (600 MHz, D_2O).

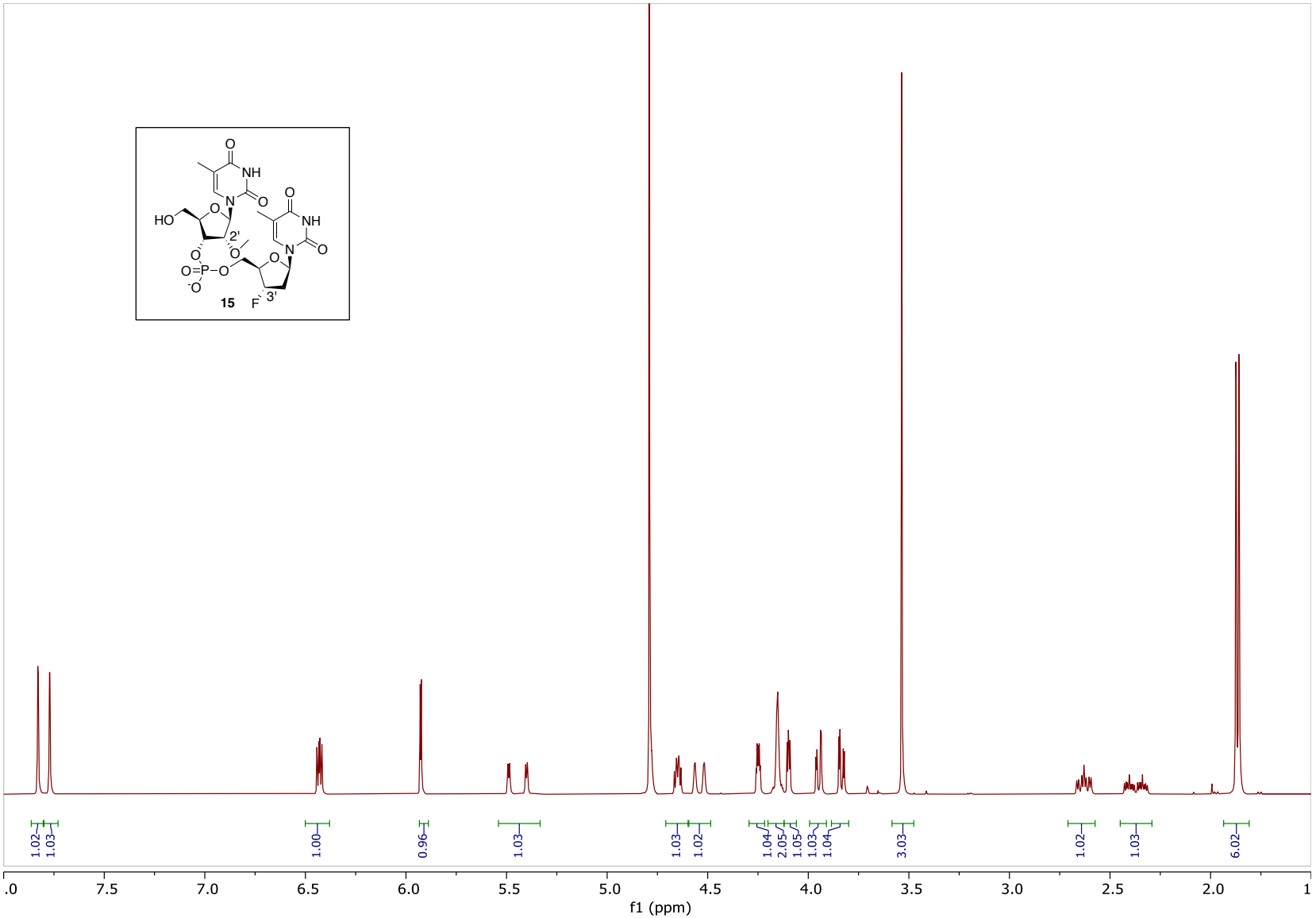

Figure S27: ^{13}C NMR spectrum of **15** (150 MHz, D_2O).

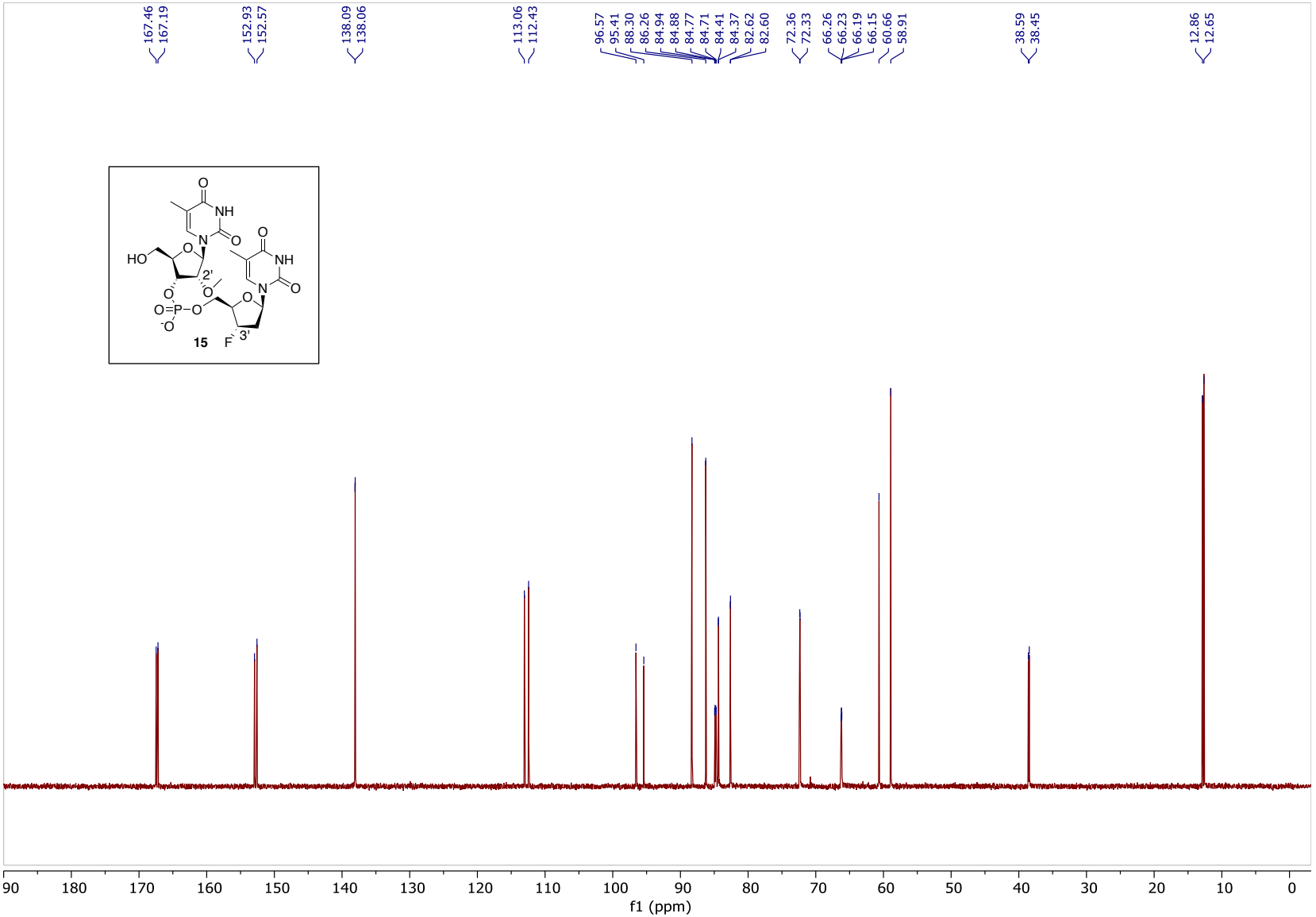

Figure S28: COSY spectrum of **15** (600 MHz, D_2O).

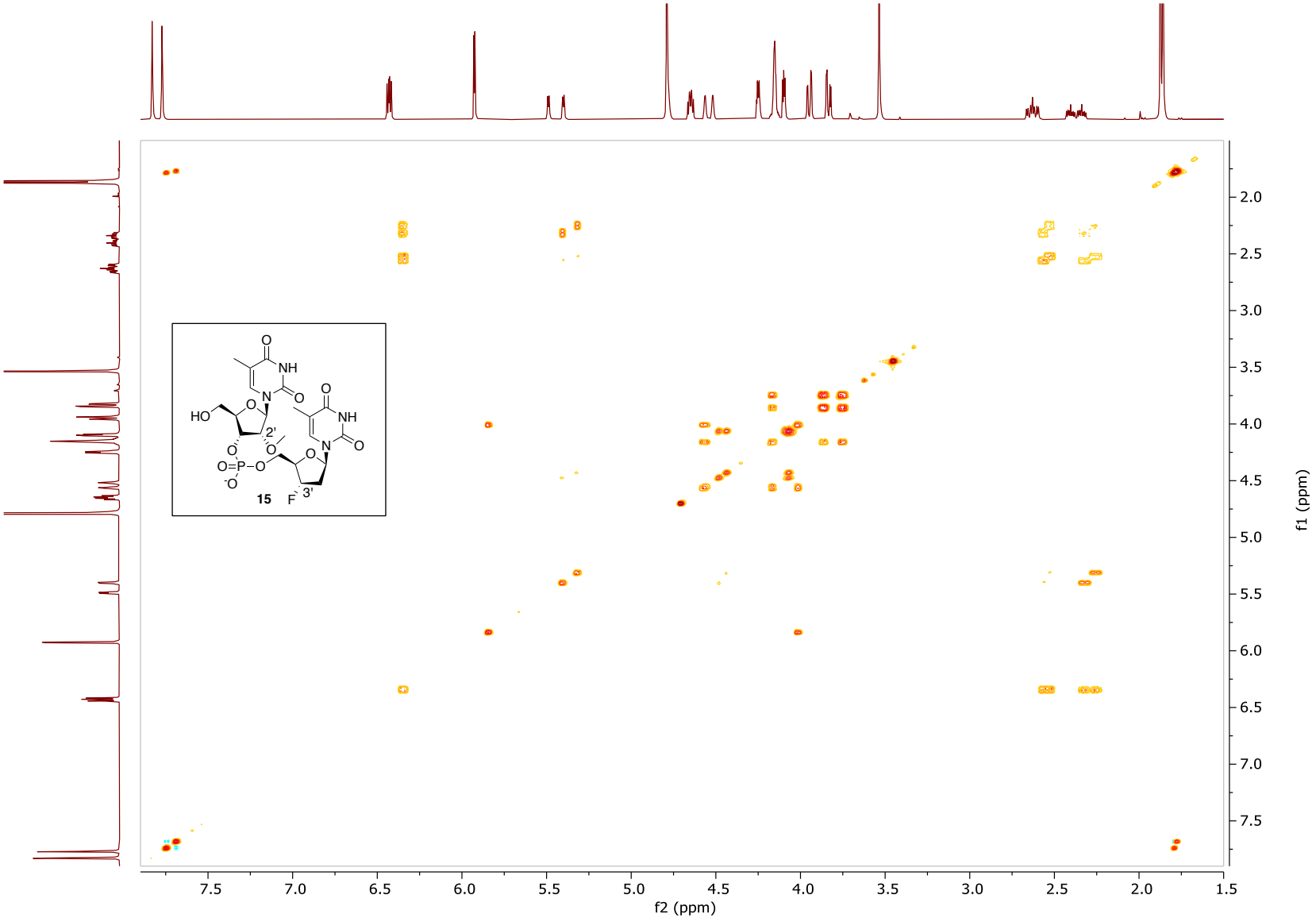

Figure S29: HSQC spectrum of **15** (600 MHz, D_2O).

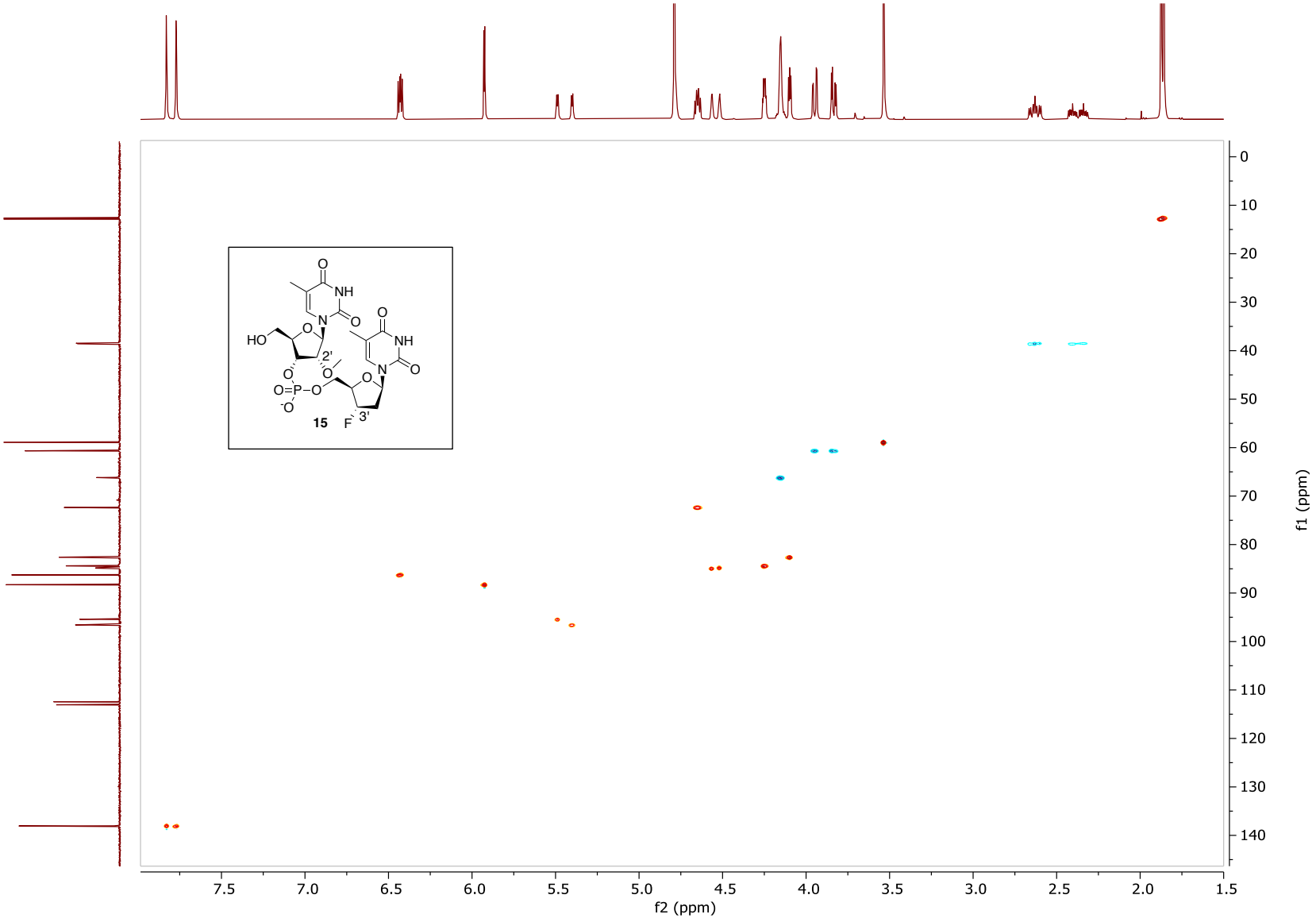

Figure S30: HMBC spectrum of **15** (600 MHz, D_2O).

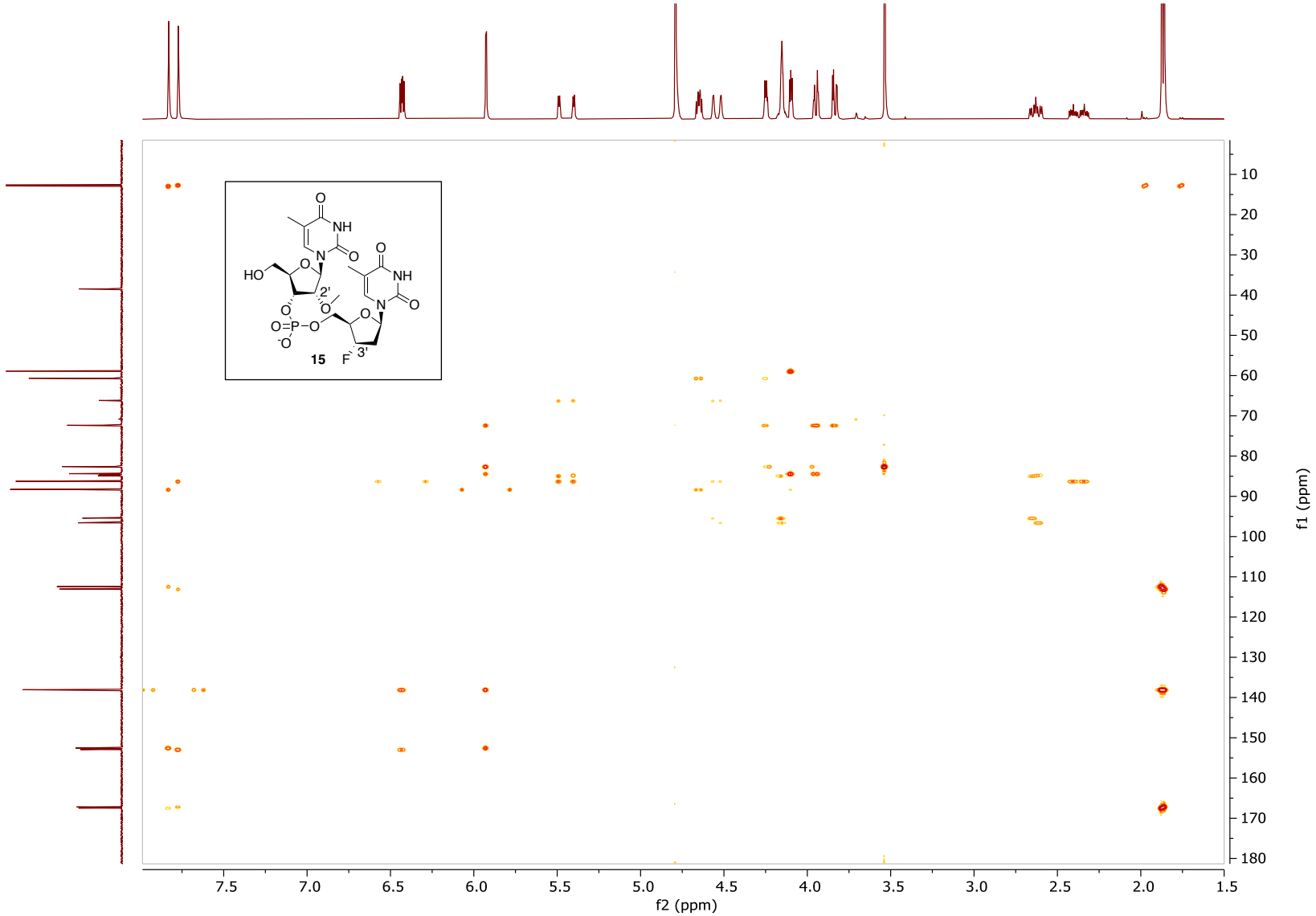

Figure S31: ^{1}H NMR spectrum of **16** (600 MHz, D_2O).

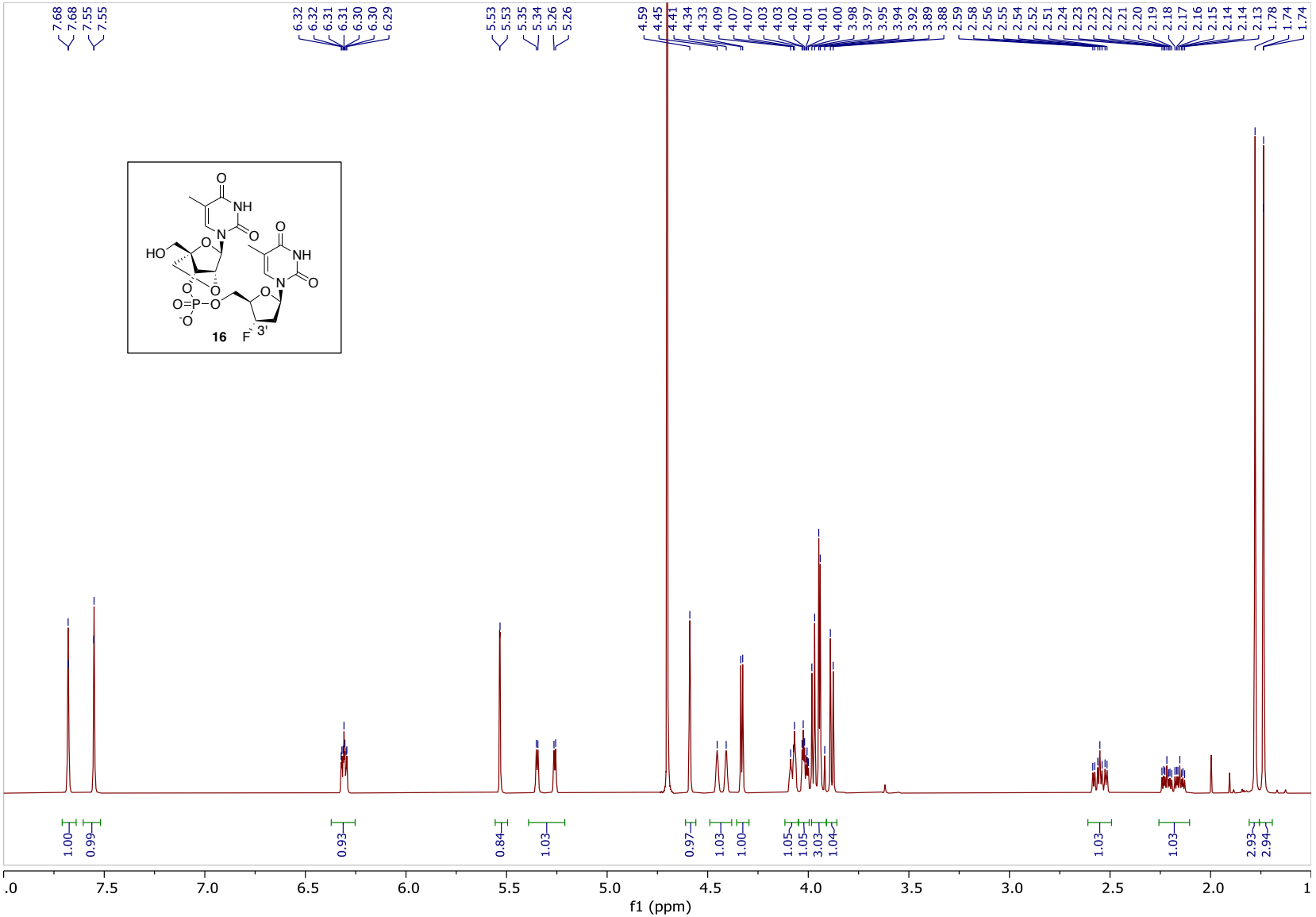

Figure S32: ^{13}C NMR spectrum of **16** (150 MHz, D_2O).

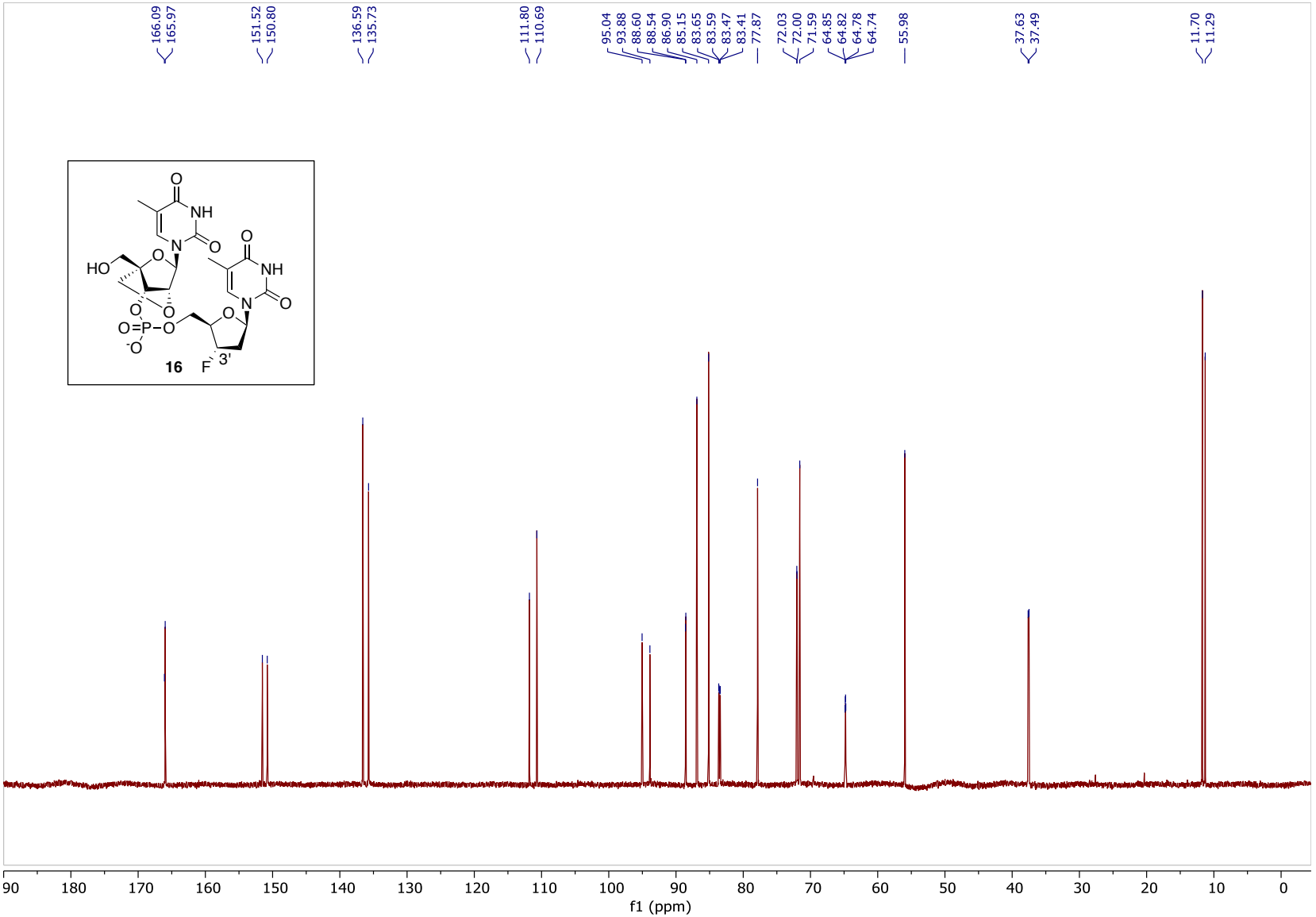

Figure S33: COSY spectrum of **16** (600 MHz, D_2O).

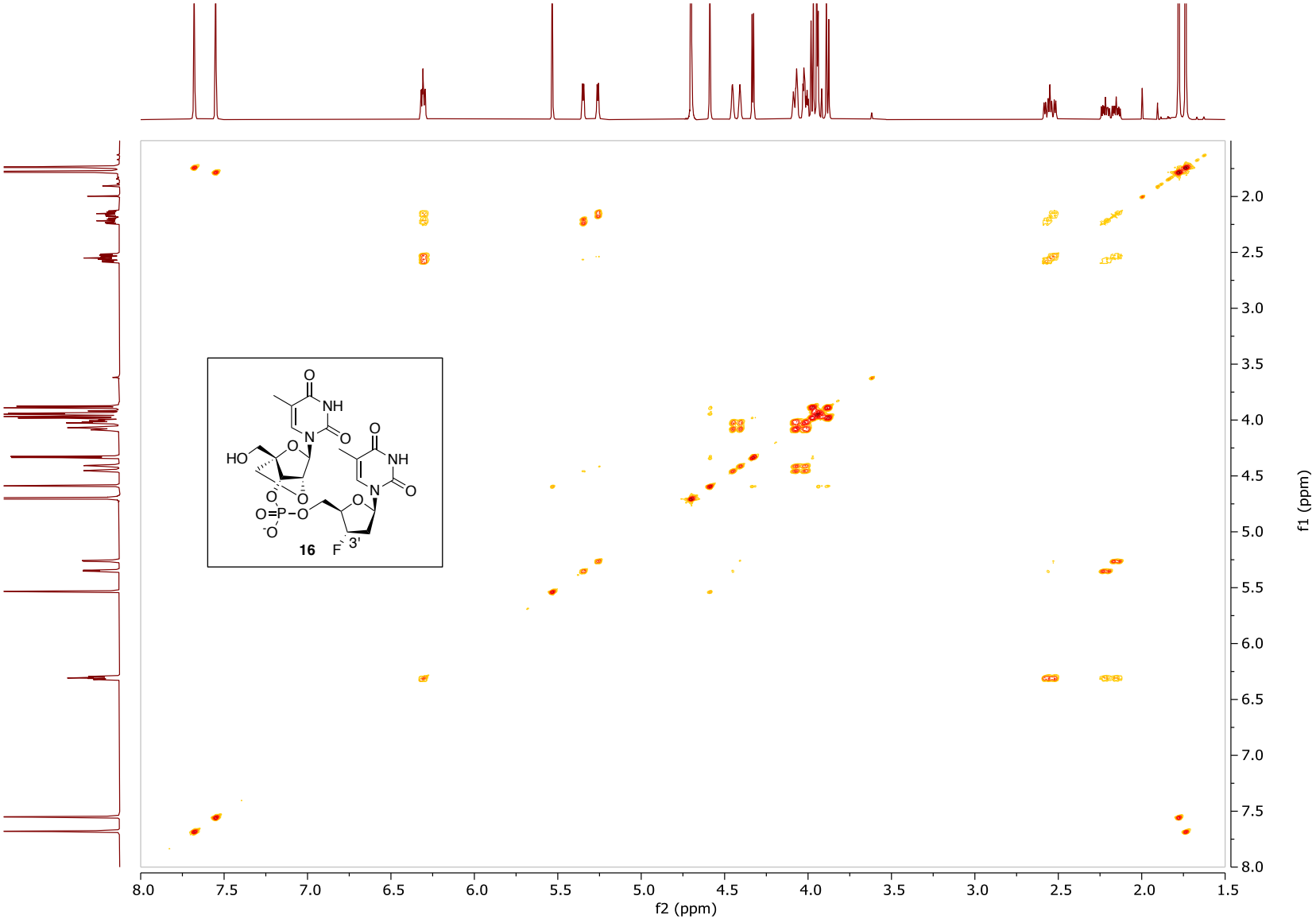

Figure S34: HSQC spectrum of **16** (600 MHz, D_2O).

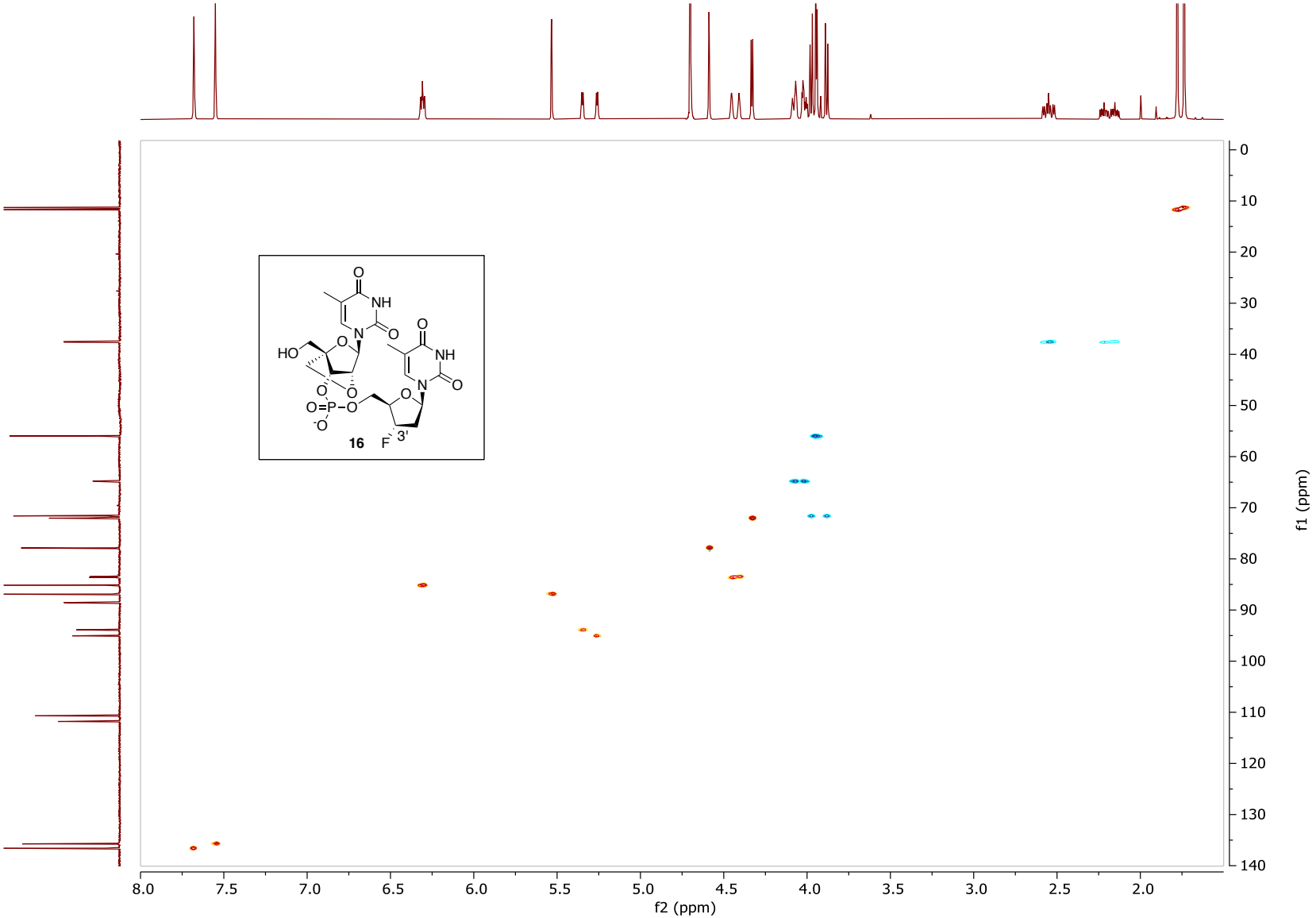

Figure S35: HMBC spectrum of **16** (600 MHz, D_2O).

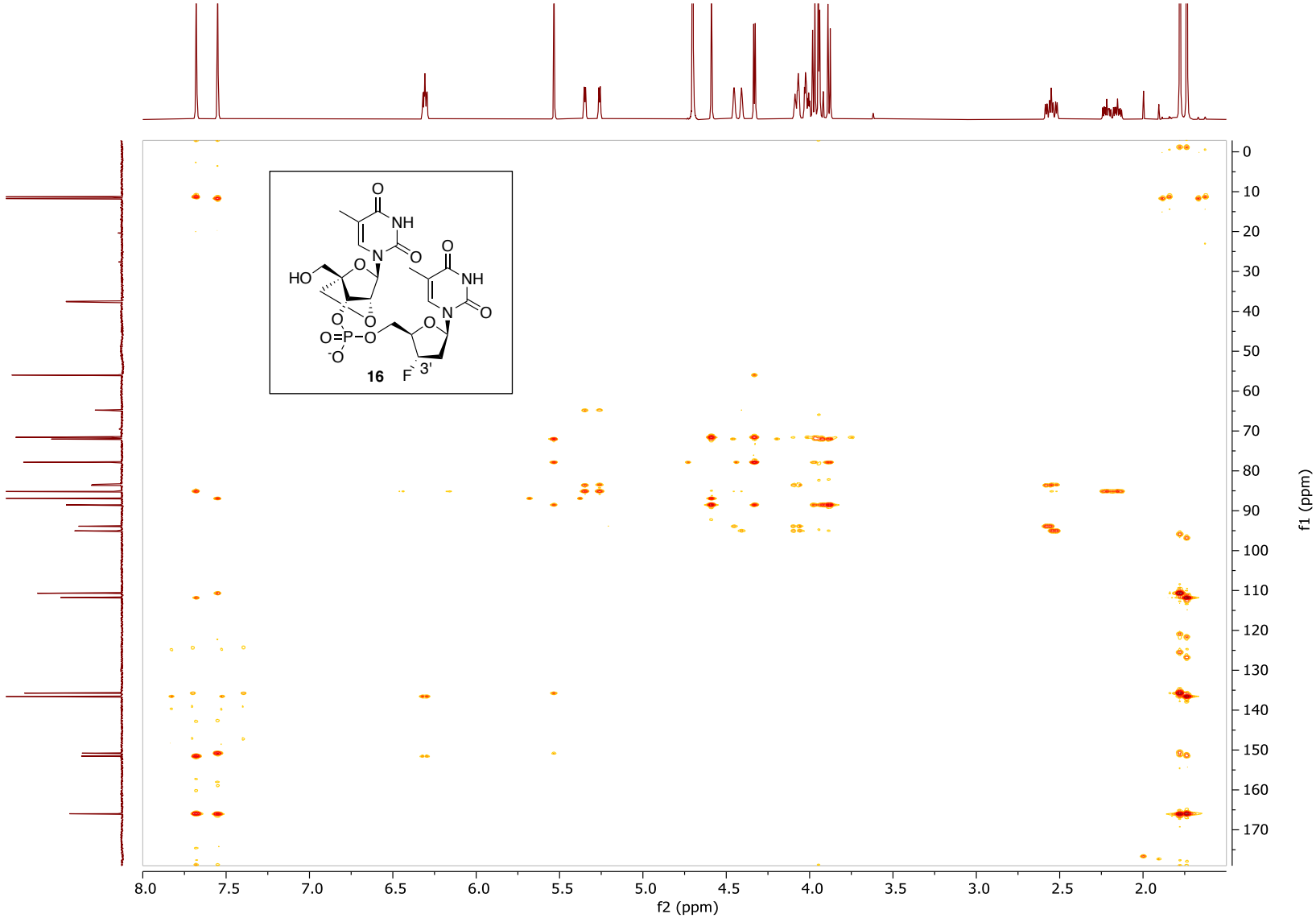

Figure S36: ^{1}H NMR spectrum of **17** (600 MHz, D_2O).

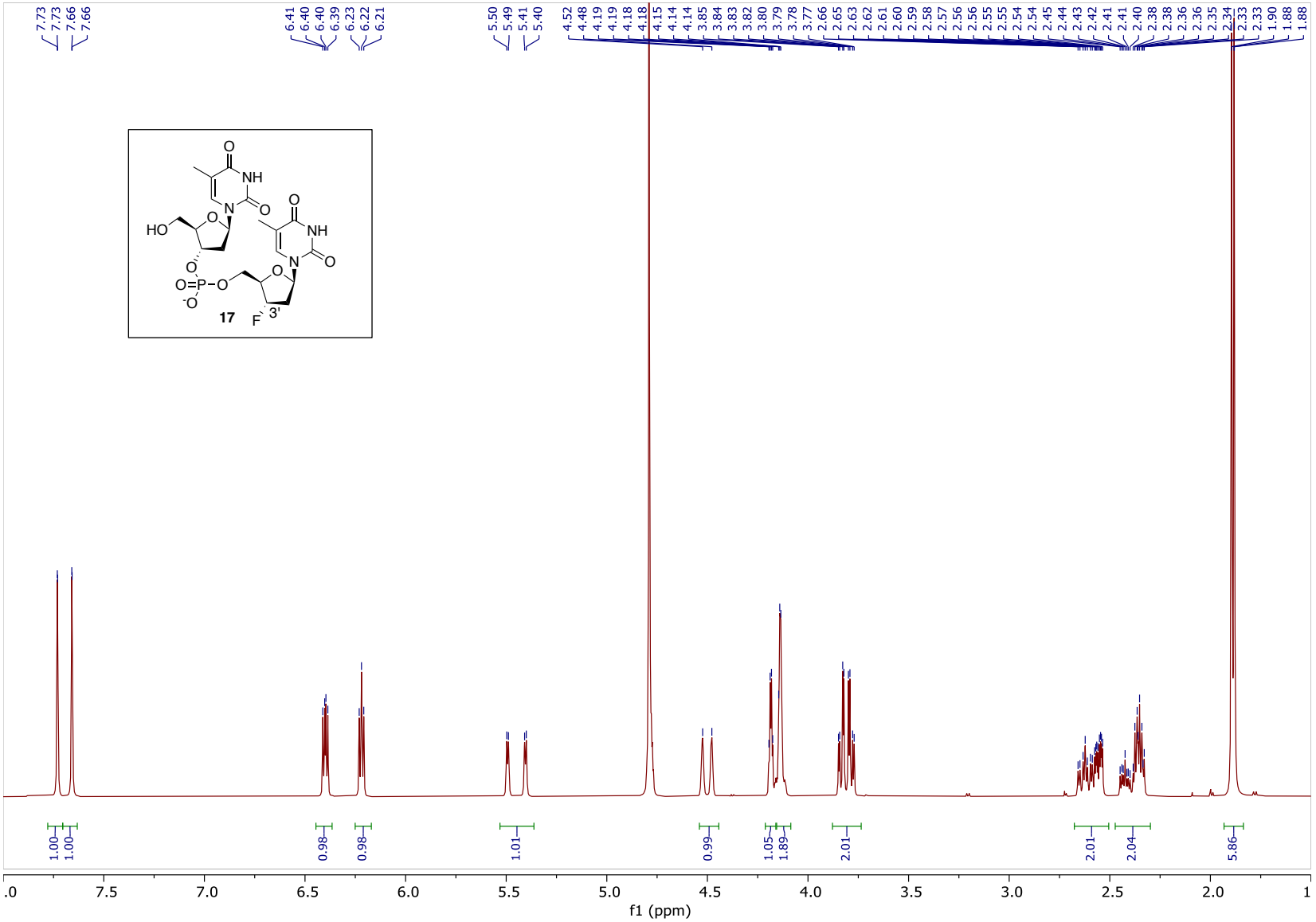

Figure S37: ^{13}C NMR spectrum of **17** (150 MHz, D_2O).

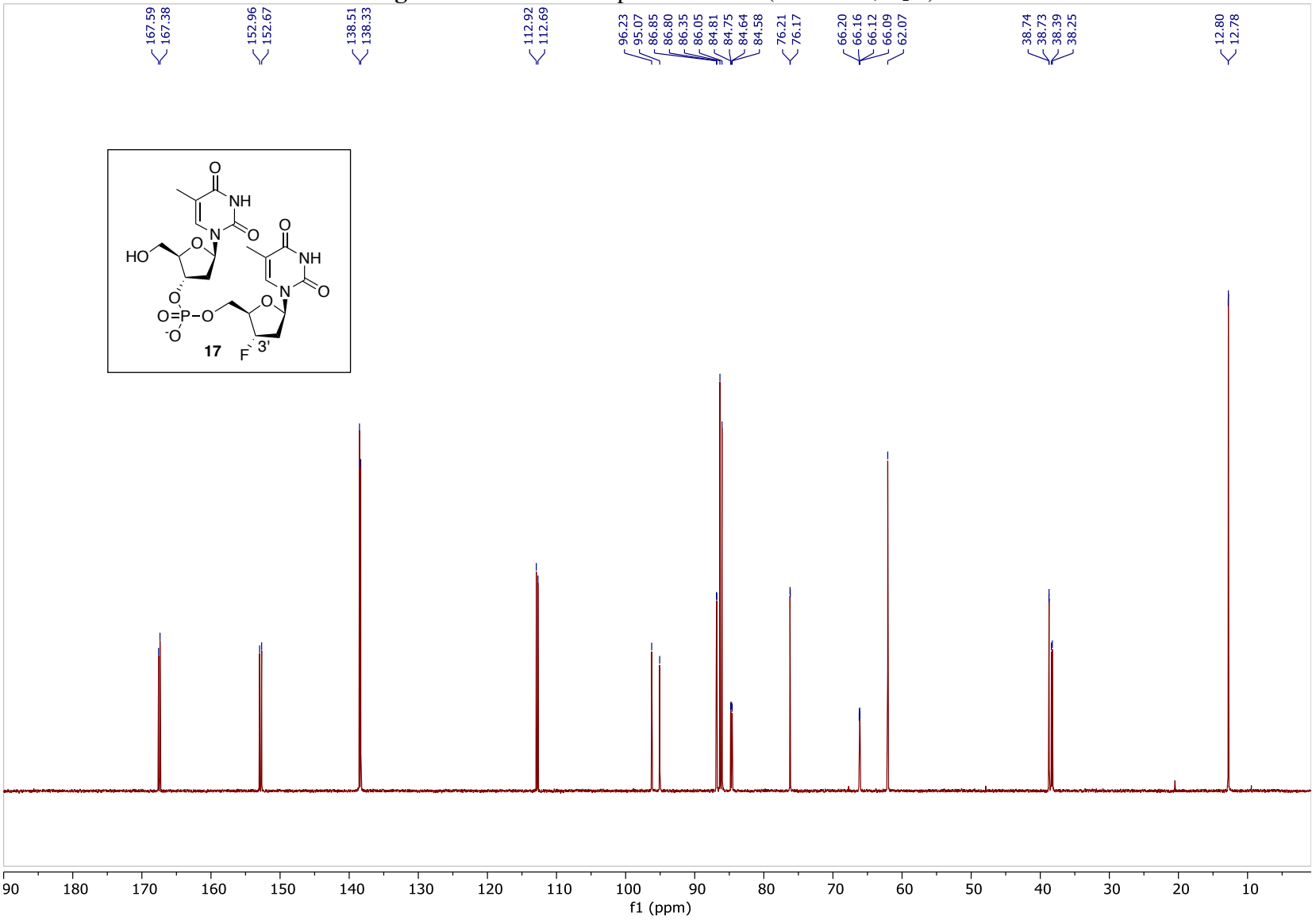

Figure S38: COSY spectrum of **17** (600 MHz, D_2O).

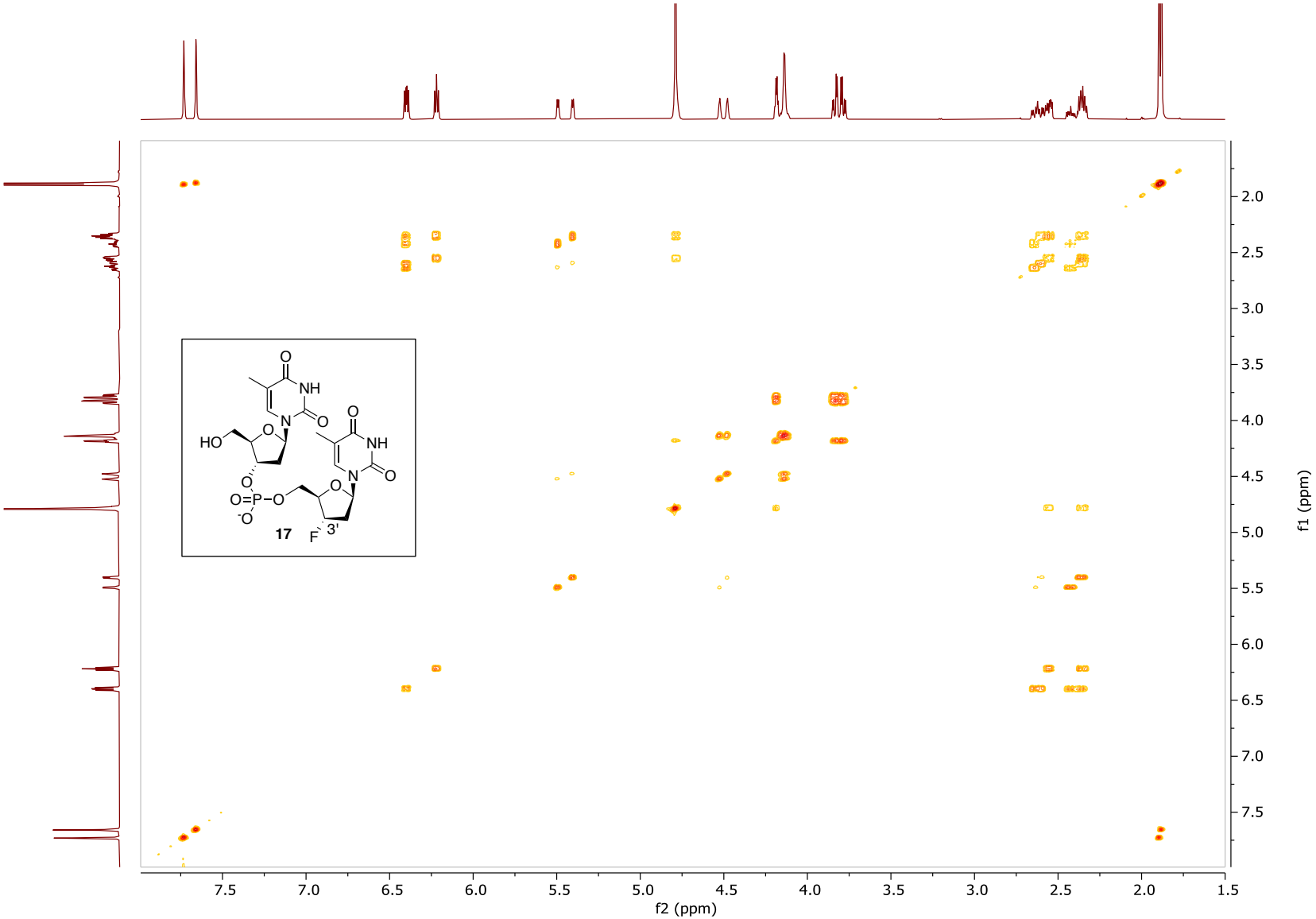

Figure S39: HSQC spectrum of **17** (600 MHz, D_2O).

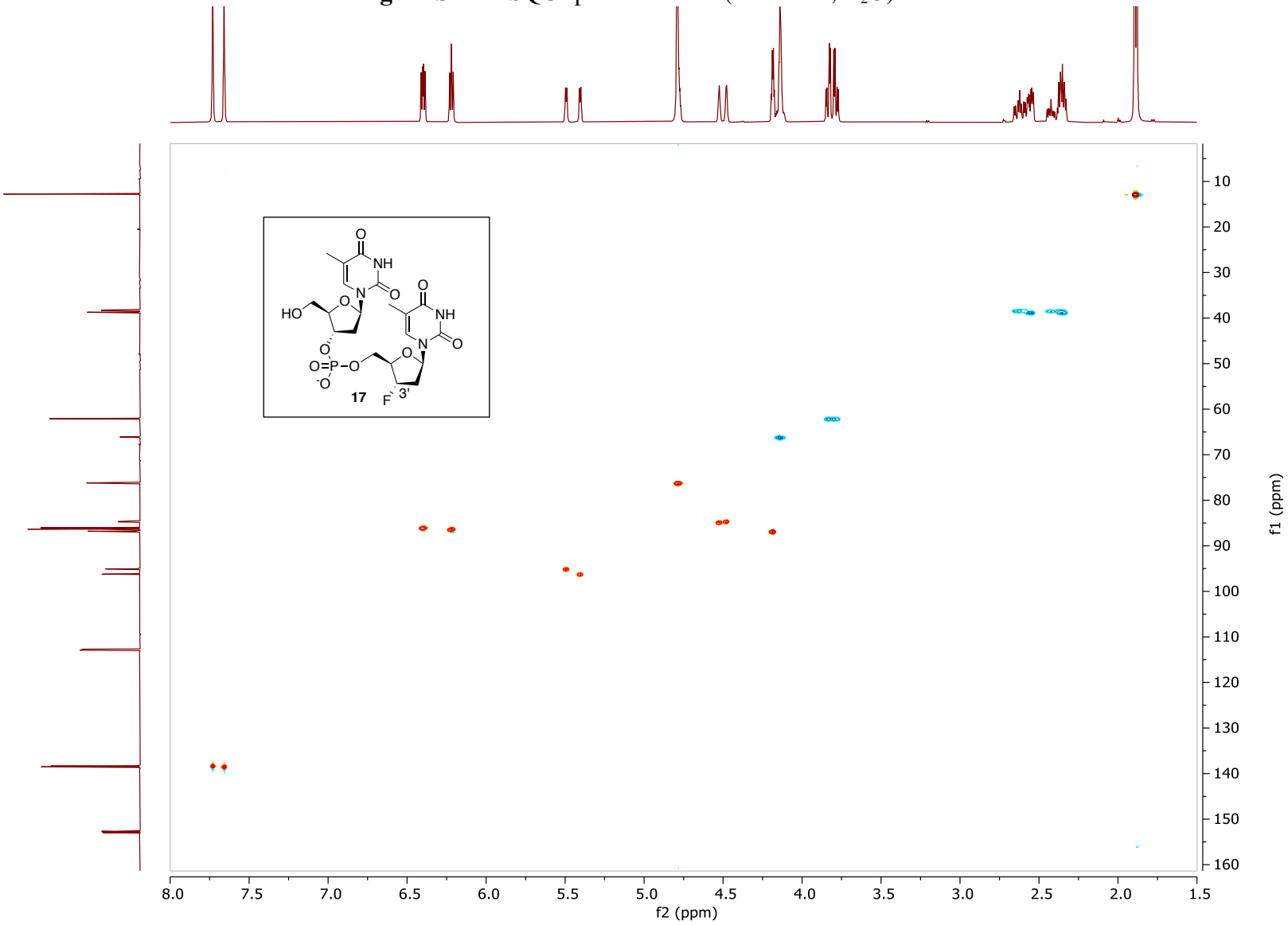

Figure S40: HMBC spectrum of **17** (600 MHz, D_2O).

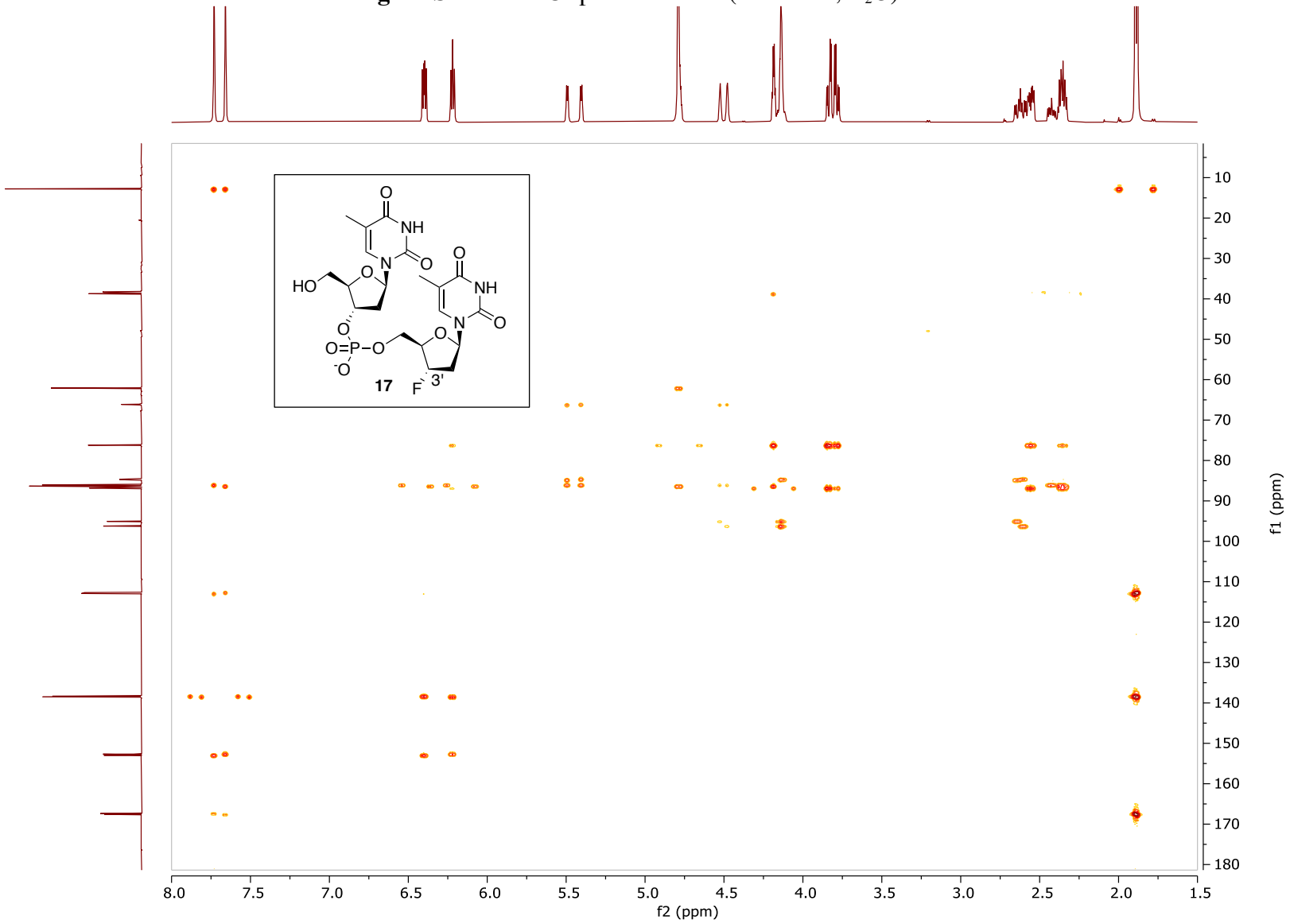

3. NMR Conformational analysis S41

3. 1. Variable temperature NMR coupling constants S41

Vicinal ^{1}H ^{1}H coupling constants of **12-17** at different temperatures were determined and refined as previously reported.[9]

Table S41. Refined vicinal *J*-coupling constants from melting ^{1}H NMR spectra of **12-17**.

		12 ($T_{2'}\alpha_F pT_{2'}\beta_F$)					**13** ($T_{2'}\alpha_F pT$)				
Temperature		**278**	**288**	**298**	**308**	**318**	**278**	**288**	**298**	**308**	**318**
5' moiety	$J_{1'2'}$	0.62	0.86	1.05	1.28	1.35	0.94	1.09	1.23	1.42	1.54
	$J_{2'3'}$	4.10	4.16	4.23	4.31	4.41	4.20	4.29	4.38	4.31	4.54
	$J_{3'4'}$	9.06	8.95	8.83	8.91	8.52	8.83	8.65	8.52	8.37	8.23
3' moiety	$J_{1'2'}$						5.8	5.99	6.22	6.44	6.60
	$J_{1'2''}$	5.24	5.18	5.06	4.97	4.86	6.6	6.67	6.64	6.59	6.56
	$J_{2'3'}$						6.63	6.70	6.63	6.65	6.64
	$J_{2''3'}$	4.95	4.85	4.56	4.33	4.12	5.51	5.20	4.97	4.72	4.56
	$J_{3'4'}$	6.62	6.42	6.19	6.13	5.97	4.70	4.49	4.35	4.23	4.15

		14 ($T_{2'}\alpha_F pT_{3'}\alpha_F$)					**15** ($T_{2'mo}pT_{3'}\alpha_F$)				
Temperature		**278**	**288**	**298**	**308**	**318**	**278**	**288**	**298**	**308**	**318**
5' moiety	$J_{1'2'}$	1.16	1.33	1.49	1.64	1.78	2.68	3.09	3.44	3.73	3.95
	$J_{2'3'}$	4.33	4.42	4.50	4.52	4.64	4.95	5.00	5.04	5.03	5.16
	$J_{3'4'}$	8.57	8.41	8.26	8.15	8.06	7.08	6.71	6.38	6.15	5.91
3' moiety	$J_{1'2'}$	9.24	9.2	9.18	9.17	9.13	9.17	9.16	9.14	9.12	9.09
	$J_{1'2''}$	5.76	5.76	5.75	5.75	5.76	5.78	5.77	5.77	5.77	5.78
	$J_{2'3'}$	4.95	5.00	5.04	5.10	5.13	4.96	4.99	5.03	5.08	5.11
	$J_{2''3'}$	1.10	1.19	1.14	1.16	1.27	1.24	1.22	1.18	1.21	1.28
	$J_{3'4'}$	1.23	1.29	1.24	1.24	1.16	1.22	1.24	1.24	1.25	1.32

		16 ($T_{2'4'L}pT_{3'}\alpha_F$)					**17** ($TpT_{3'}\alpha_F$)				
Temperature		**278**	**288**	**298**	**308**	**318**	**278**	**288**	**298**	**308**	**318**
5' moiety	$J_{1'2'}$	1.60	1.57	1.5	1.34	1.19	7.30	7.40	7.44	7.50	7.50
	$J_{1'2''}$						6.14	6.17	6.18	6.19	6.21
	$J_{2'3'}$	0.69	0.72	0.78	0.80	0.79	6.34	6.38	6.4	6.42	6.43
	$J_{2''3'}$						3.51	3.46	3.4	3.39	3.39
	$J_{3'4'}$						3.31	3.34	3.35	3.37	3.38
3' moiety	$J_{1'2'}$	8.99	8.99	8.94	8.89	8.90	9.44	9.4	9.34	9.28	9.22
	$J_{1'2''}$	5.77	5.82	5.79	5.78	5.81	5.59	5.62	5.64	5.67	5.69
	$J_{2'3'}$	4.98	5.07	5.04	5.09	5.18	5.11	5.15	5.12	5.24	5.26
	$J_{2''3'}$	1.50	1.33	1.42	1.46	1.41	1.08	1.12	1.16	1.11	1.26
	$J_{3'4'}$	1.26	1.3	1.31	1.29	1.30	1.10	1.19	1.32	1.32	1.35

3. 2. Matlab Pseudorotation GUI analysis of the sugar conformation S42

Refined variable temperature $^{3}J_{HH}$ of **12-17** were used as inputs in the Matlab Pseudorotation GUI program (version 1.01)[10] installed on Matlab software (version R.2022.a) assuming a two-state sugar conformational equilibrium as described previously.[9] The Matlab pseudorotation GUI was parametrized with integrated electronegativity editor and Aj and Bj parameters determined by DFT with the Gaussian program package (version 16 revision B.01).[11] No constraint was applied during the Matlab pseudorotation fitting process.

Table S42A. Injected parameters for $T_{2'}\alpha_{F}p$ moiety.

Vicinal coupling constant	***A***	***B***	***Electronegativities***			
$J_{1'2'}$	1.122	115.050	1.37	0.62	0.56	1.26
$J_{2'3'}$	1.020	4.013	1.26	0.62	0.68	1.37
$J_{3'4'}$	1.168	-122.400	1.27	0.68	0.72	1.26

Table S42B. Injected parameters for $T_{2'mo}p$ moiety.

Vicinal coupling constant	***A***	***B***	***Electronegativities***			
$J_{1'2'}$	1.195	123.600	1.40	0.62	0.56	1.26
$J_{2'3'}$	1.218	0.962	1.26	0.62	0.68	1.40
$J_{3'4'}$	1.062	-127.640	1.27	0.68	0.72	1.26

Table S42C. Injected parameters for Tp moiety.

Vicinal coupling constant	***A***	***B***	***Electronegativities***			
$J_{1'2'}$	1.109	119.330	0.00	0.62	0.56	1.26
$J_{1'2''}$	1.125	-1.144	0.62	0.00	0.56	1.26
$J_{2'3'}$	1.148	2.059	1.40	0.62	0.56	0.00
$J_{2''3'}$	1.174	1.22.740	1.40	0.62	0.00	0.56
$J_{3'4'}$	1.043	-124.880	1.27	0.68	0.72	1.40

Table S43A. Injected parameters for $pT_{3'}\alpha_{F}$ moiety.

Vicinal coupling constant	*A*	*B*	*Electronegativities*			
$J_{1'2'}$	1.226	116.090	0.00	0.62	0.56	1.26
$J_{1'2''}$	1.189	-4.615	0.62	0.00	0.56	1.26
$J_{2'3'}$	1.195	-1.849	1.37	0.62	0.68	0.00
$J_{2''3'}$	1.186	118.550	1.37	0.62	0.00	0.68
$J_{3'4'}$	1.108	-117.580	1.27	0.68	0.72	1.37

Table S43B. Injected parameters for $pT_{2'}\beta_F$ moiety.

Vicinal coupling constant	*A*	*B*	*Electronegativities*			
$J_{1'2'}$						
$J_{1'2''}$	1.129	-1.921	0.62	1.37	0.56	1.26
$J_{2'3'}$						
$J_{2''3'}$	1.165	121.570	1.33	0.62	1.37	1.00
$J_{3'4'}$	1.138	-124.180	1.27	0.68	0.68	1.33

Table S43C. Injected parameters for pT moiety.

Vicinal coupling constant	*A*	*B*	*Electronegativities*			
$J_{1'2'}$	1.205	116.120	0.00	0.62	0.56	1.26
$J_{1'2''}$	1.184	-4.312	0.62	0.00	0.56	1.26
$J_{2'3'}$	1.176	1.900	1.33	0.62	0.68	0.00
$J_{2''3'}$	1.161	122.760	1.33	0.62	0.00	0.68
$J_{3'4'}$	1.085	-122.210	1.27	0.68	0.72	1.33

Table S44. Matlab pseudorotation GUI puckering analysis yielded from experimental data of compound **12** ($T_{2'}\alpha_F pT_{2'}\beta_F$).

5' moiety ($T_{2'}\alpha_F p$)

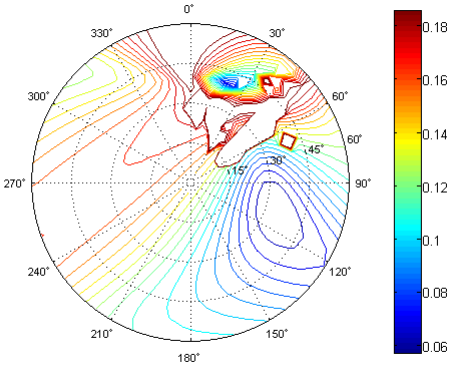

3' moiety ($pT_{2'}\beta_F$)

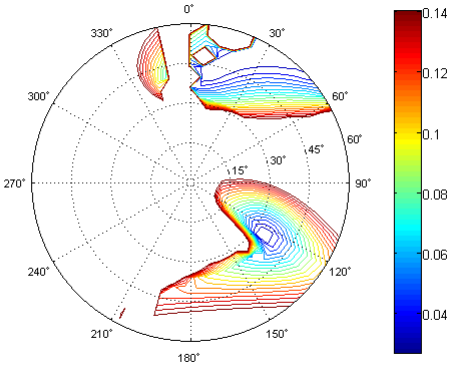

$T_{2'}\alpha_F p$ moiety

Conformation 1		*Temperature*	*% Conf 1*	*% Conf 2*
P	-46.77	278	4.2	95.8
Phi	60.00	288	8.0	92.0
Conformation 2		***298***	***11.5***	***88.5***
P	32.86	308	12.5	87.5
Phi	40.46	318	18.6	81.4

RMSD : 0.12 Hz

$pT_{2'}\beta_F$ moiety

Conformation 1		*Temperature*	*% Conf 1*	*% Conf 2*
P	8.39	278	60.0	40.0
Phi	41.46	288	58.0	42.0
Conformation 2		***298***	***54.3***	***45.7***
P	125.75	308	52.0	48.0
Phi	34.22	318	49.3	50.7

RMSD : 0.03 Hz

Table S45. Matlab pseudorotation GUI puckering analysis yielded from experimental data of compound **13** ($T_{2'}\alpha_F pT$).

5' moiety ($T_{2'}\alpha_F p$)

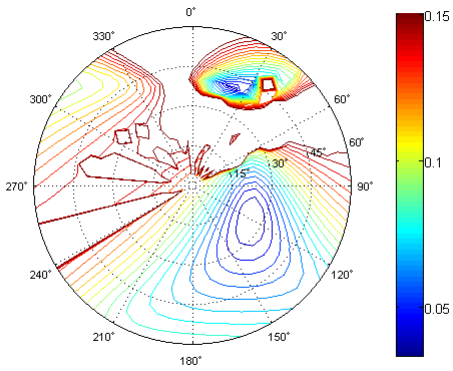

3' moiety (pT)

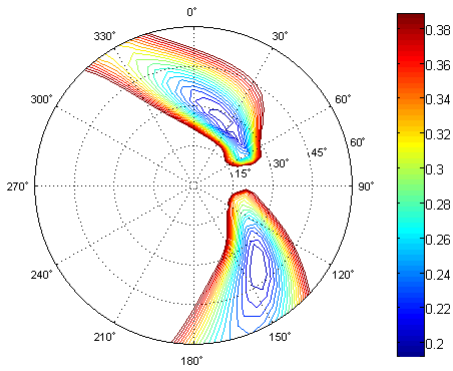

$T_{2'}\alpha_F p$ moiety

Conformation 1		*Temperature*	*% Conf 1*	*% Conf 2*
P	119.22	278	6.65	93.4
Phi	25.32	288	9.95	90.1
Conformation 2		***298***	***12.73***	***87.3***
P	19.90	308	15.46	84.5
Phi	39.075	318	18.73	81.3
			RMSD	**: 0.03 Hz**

pT moiety

Conformation 1		*Temperature*	*% Conf 1*	*% Conf 2*
P	27.46	278	58.97	41.0
Phi	26.56	288	56.41	43.6
Conformation 2		***298***	***53.89***	***46.1***
P	141.23	308	51.49	48.5
Phi	39.07	318	49.89	50.1
			RMSD	**: 0.19 Hz**

Table S46. Matlab pseudorotation GUI puckering analysis yielded from experimental data of compound **14** ($T_{2'}\alpha_F pT_{3'}\alpha_F$).

5' moiety ($T_{2'}\alpha_F p$)

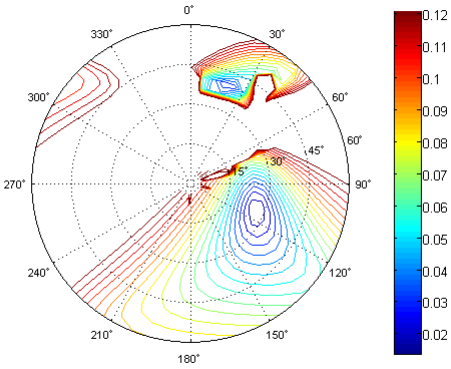

3' moiety ($pT_{3'}\alpha_F$)

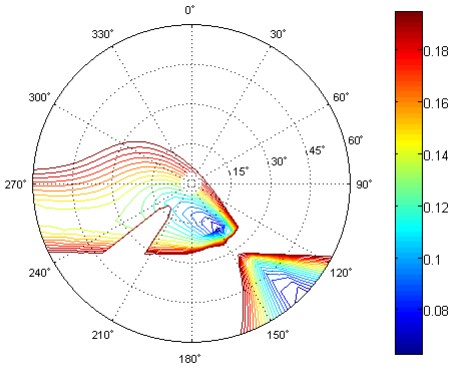

$T_{2'}\alpha_F p$ moiety

Conformation 1		*Temperature*	*% Conf 1*	*% Conf 2*
P	112.39	278	10.6	89.4
Phi	27.07	288	14.1	85.9
Conformation 2		***298***	***17.4***	***82.6***
P	16.77	308	20.0	80.0
Phi	38.024	318	22.7	77.3
			RMSD	**: 0.01 Hz**

$pT_{3'}\alpha_F$ moiety

Conformation 1		*Temperature*	*% Conf 1*	*% Conf 2*
P	146.80	278	72.8	27.2
Phi	22.19	288	73.0	27.0
Conformation 2		***298***	***73.4***	***26.6***
P	136.06	308	73.8	26.2
Phi	60.00	318	73.9	26.1
			RMSD	**: 0.06 Hz**

Table S47. Matlab pseudorotation GUI puckering analysis yielded from experimental data of compound **15** ($T_{2'mo}pT_{3'}\alpha_F$).

5' moiety ($T_{2'mo}p$)

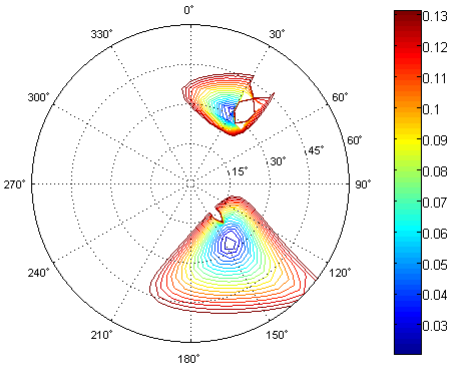

3' moiety ($pT_{3'}\alpha_F$)

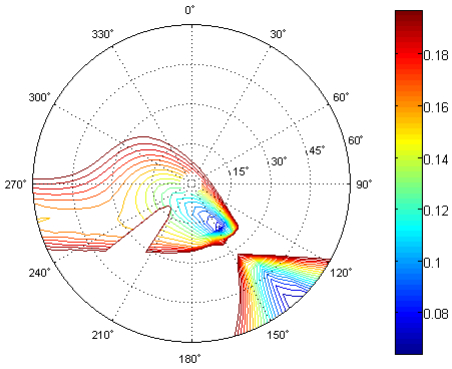

$T_{2'mo}p$ moiety

Conformation 1		*Temperature*	*% Conf 1*	*% Conf 2*
P	146.11	278	22.1	77.9
Phi	26.69	288	28.2	71.8
Conformation 2		***298***	***33.5***	***66.5***
P	29.65	308	37.5	62.5
Phi	30.42	318	41.2	58.8
			RMSD	**: 0.02 Hz**

$pT_{3'}\alpha_F$ moiety

Conformation 1		*Temperature*	*% Conf 1*	*% Conf 2*
P	144.88	278	72.7	27.3
Phi	21.96	288	73.0	27.0
Conformation 2		***298***	***73.5***	***26.5***
P	138.29	308	73.8	26.2
Phi	60	318	74.0	26.0
			RMSD	**: 0.06 Hz**

Table S48. Matlab pseudorotation GUI puckering analysis yielded from experimental data of compound **16** ($T_{2'4'L}pT_{3'}\alpha_F$).

5' moiety ($T_{2'4'L}p$)

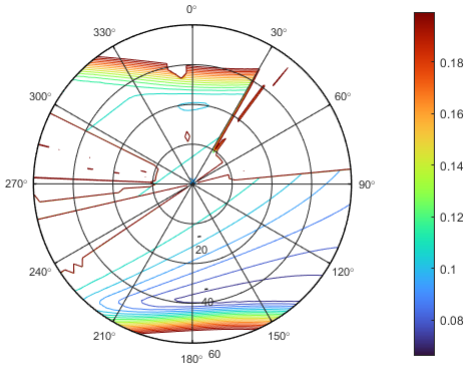

3' moiety ($pT_{3'}\alpha_F$)

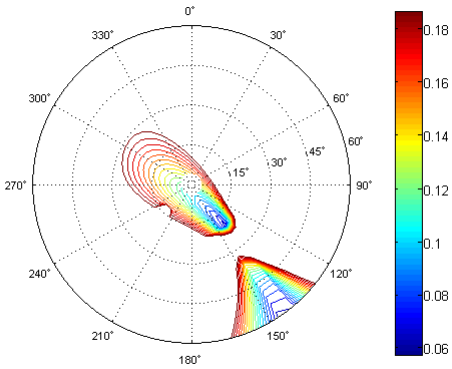

$T_{2'4'L}p$ moiety

Conformation 1		*Temperature*[a]	*% Conf 1*	*% Conf 2*
P	367.12	278	-	-
Phi	60.00	288	-	-
Conformation 2		***298***	***6.8***	***93.2***
P	11.56	308	-	-
Phi	60.00	318	-	-
			RMSD	**: 0.37 Hz**

$pT_{3'}\alpha_F$ moiety

Conformation 1		*Temperature*	*% Conf 1*	*% Conf 2*
P	140.58	278	70.9	29.1
Phi	20.72	288	72.7	27.3
Conformation 2		***298***	***72.1***	***27.9***
P	143.71	308	72.3	27.7
Phi	60.00	318	73.4	26.6
			RMSD	**: 0.06 Hz**

[a]Matlab GUI analysis was performed at 298 K since no significative thermal variation of *J*-coupling occurred for the $T_{2'4'L}p$ sugar residue.

Table S49. Matlab pseudorotation GUI puckering analysis yielded from experimental data of compound **17** ($TpT_{3'}\alpha_F$).

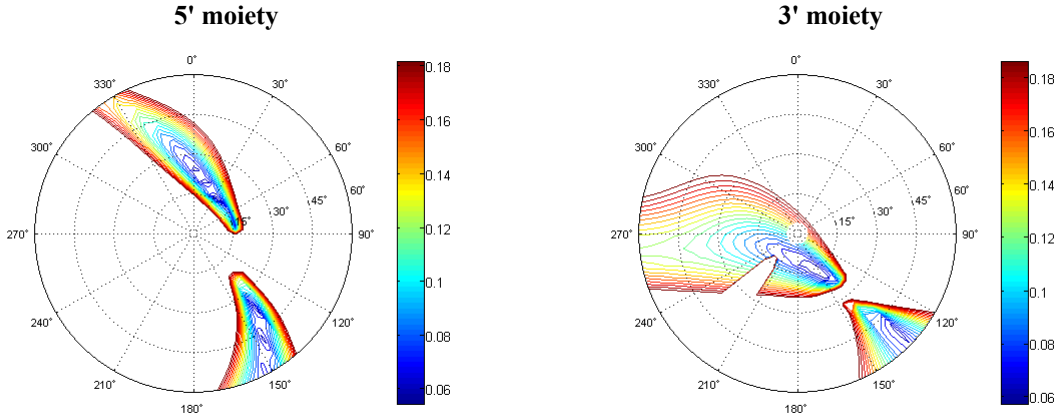

Tp moiety

Conformation 1		*Temperature*	*% Conf 1*	*% Conf 2*
P	15.64	278	42.6	57.3
Phi	19.17	288	42.3	57.7
Conformation 2		***298***	***41.9***	***58.1***
P	141.84	308	41.6	58.3
Phi	39.41	318	41.7	58.2
			RMSD	**: 0.05 Hz**

$pT_{3'\alpha F}$ moiety

Conformation 1		*Temperature*	*% Conf 1*	*% Conf 2*
P	152.25	278	49.6	50.4
Phi	15.85	288	50.4	49.6
Conformation 2		***298***	***50.9***	***49.1***
P	136.13	308	52.4	47.6
Phi	48.41	318	53.0	47.0
			RMSD	**: 0.06 Hz**

4. CD Experiments

CD spectra were recorded on a spectropolarimeter equipped with a Peltier temperature controller. Spectra were recorded between 10 to 80°C (10°C increment) in a 0.01 M Na phosphate, 0.1 M NaCl, pH 7.0 buffer as previously reported.[12] CD data are expressed in molar ellipticity per residue [θ] ($deg.cm^2.decimol^{-1}$). The molar extinction coefficient at 267 nm of **1** (TpT) and of its nucleoside constituent thymidine (T)[13] ($2 \times 9.65\ M^{-1}cm^{-1} \times 10^3$ and $9.65 \times 10^3\ M^{-1}cm^{-1}$, respectively) were used for **12-17**, and for their nucleosides constituent.[12] Experimental CD parameters were identical as those reported.[12]

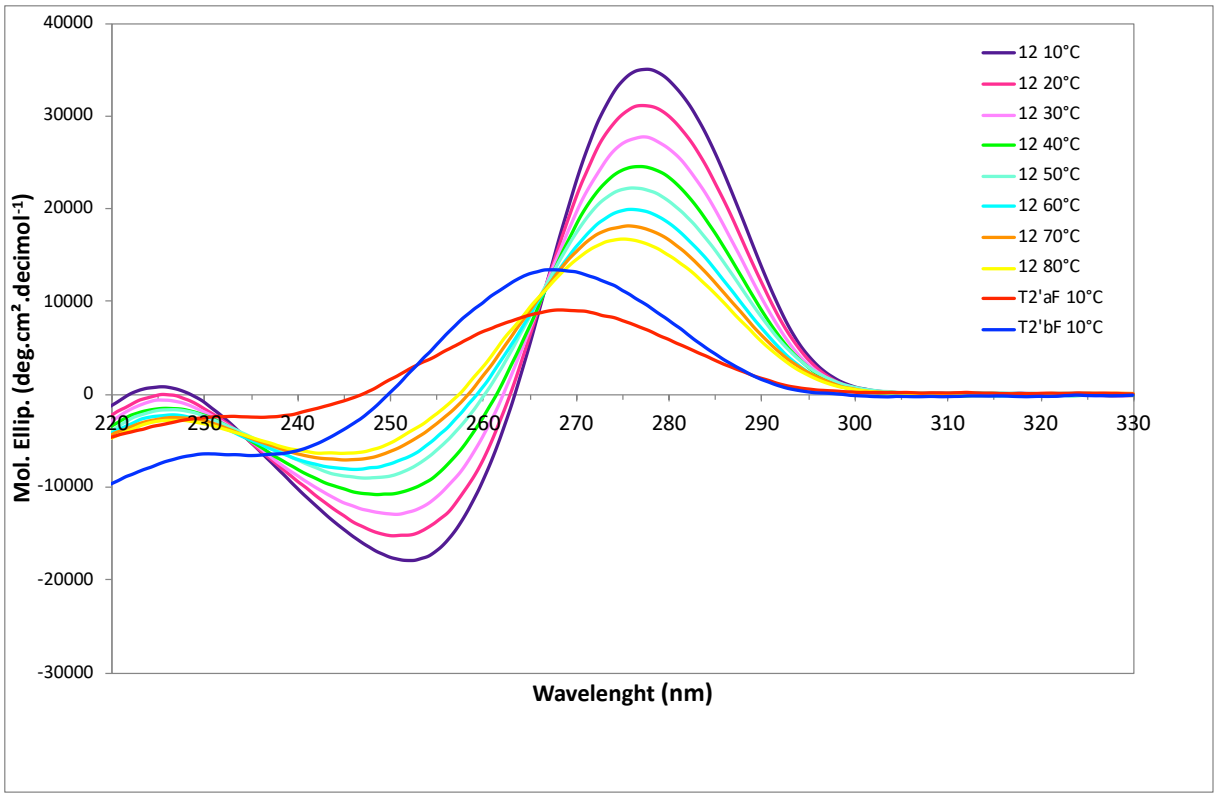

Figure S51A. CD spectra of **12** ($T_{2'}\alpha_F pT_{2'}\beta_F$) between 10 to 80°C and CD spectra at 10°C of 2'-α-fluorothymidine ($T_{2'}\alpha_F$) and 2'-β-fluorothymidine ($T_{2'}\beta_F$).

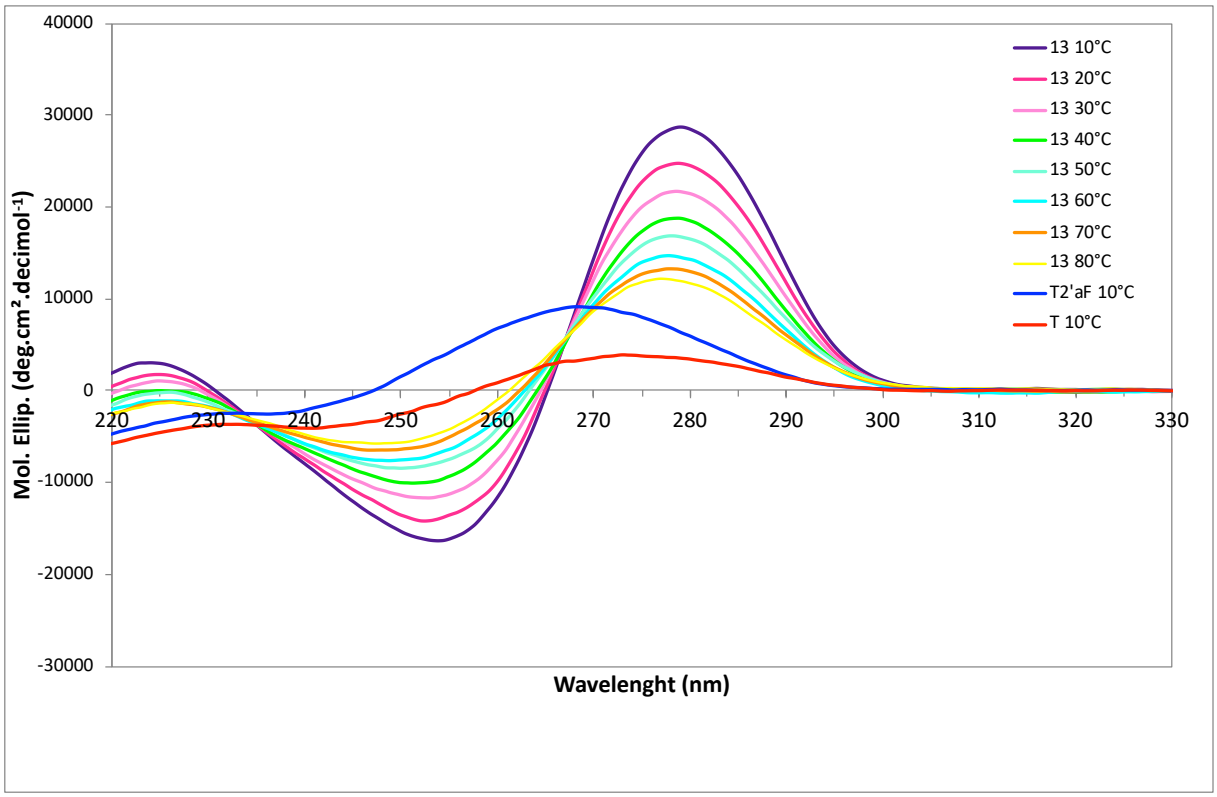

Figure S51B. CD spectra of **13** ($T_{2'}\alpha_F pT$) between 10 to 80°C and CD spectra at 10°C of 2'-α-fluorothymidine ($T_{2'}\alpha_F$) and thymidine (T).

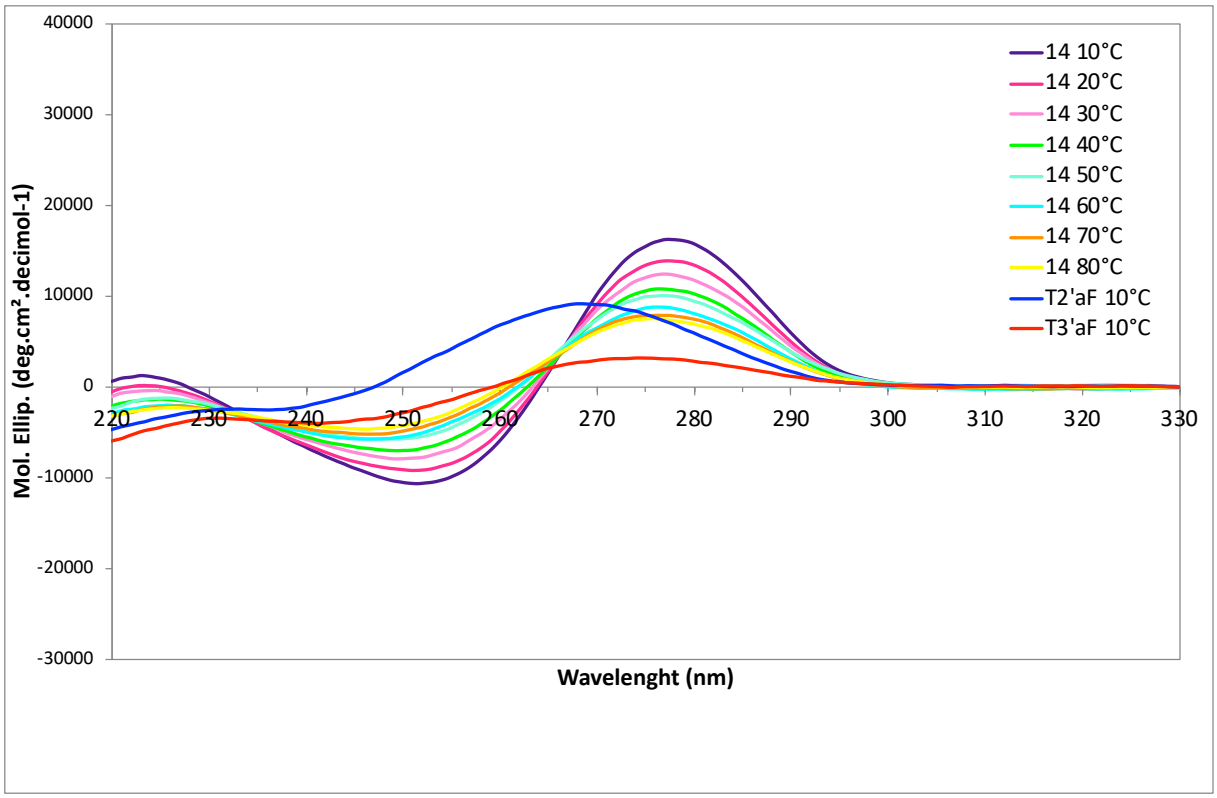

Figure S52A. CD spectra of **14** ($T_{2'}\alpha_F pT_{3'}\alpha_F$) between 10 to 80°C and CD spectra at 10°C of 2'-α-fluorothymidine ($T_{2'}\alpha_F$) and 3'-deoxy-3'-α-fluorothymidine ($T_{3'}\alpha_F$).

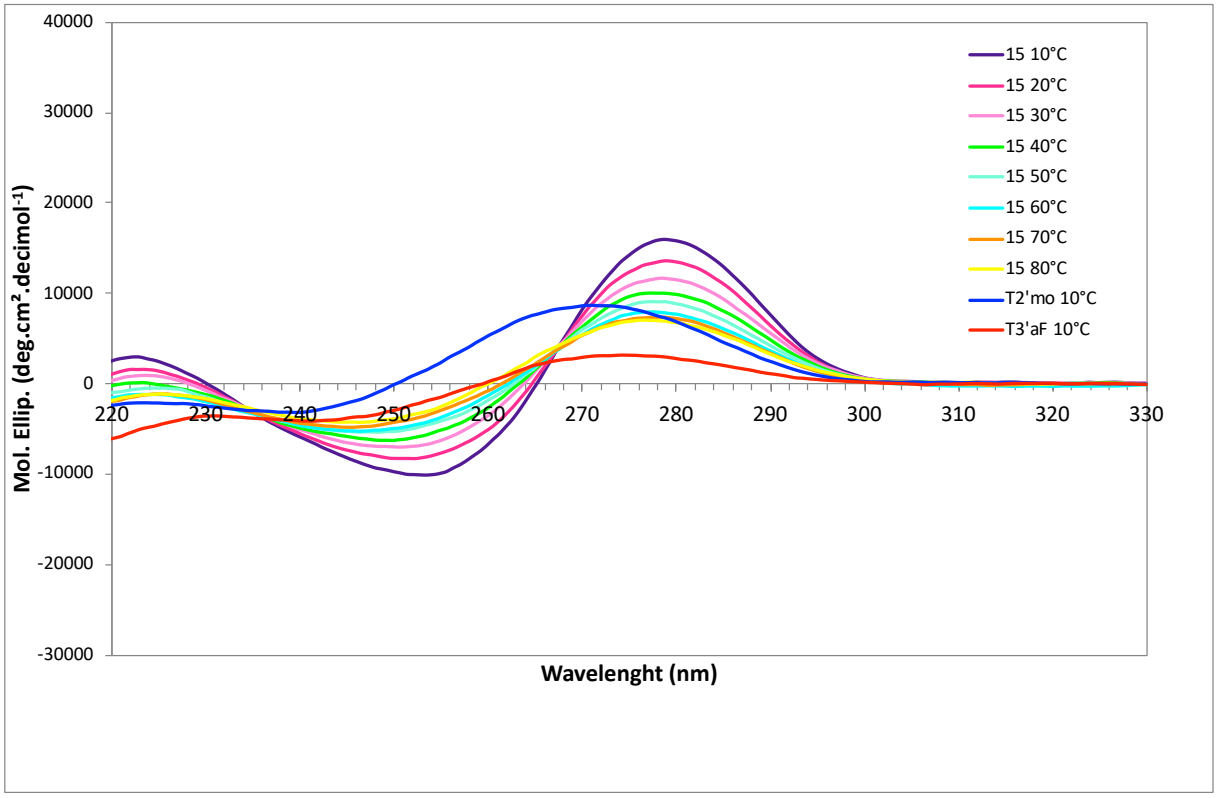

Figure S52B. CD spectra of **15** ($T_{2'ome}pT_{3'}\alpha_F$) between 10 to 80°C and CD spectra at 10°C of 2',5-dimethyluridine ($T_{2'mo}$) and 3'-deoxy-3'-α-fluorothymidine ($T_{3'}\alpha_F$).

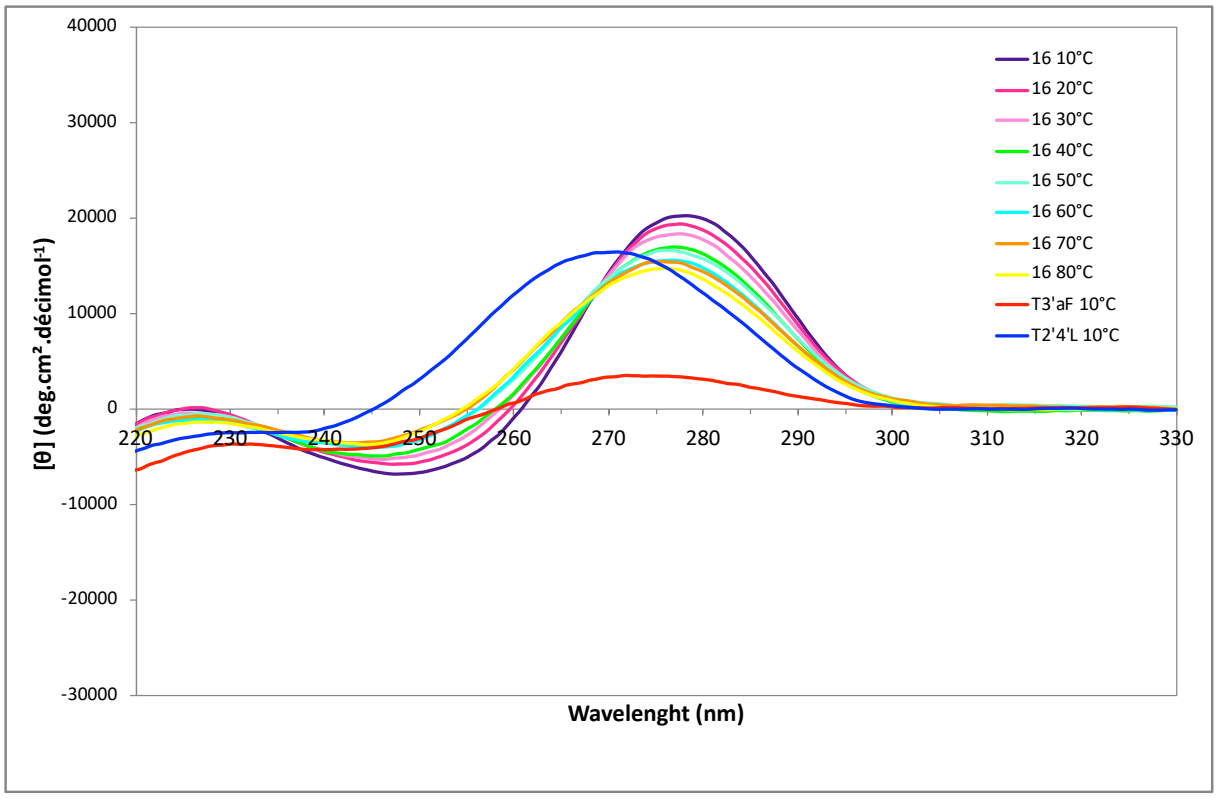

Figure S53A. CD spectra of **16** ($T_{2'4'L}pT_{3'}\alpha_F$) between 10 to 80°C and CD spectra at 10°C of 2′-*O*-4′-*C*-methylene-5-methyluridine ($T_{2'4'L}$) and 3'-deoxy-3'-α-fluorothymidine ($T_{3'}\alpha_F$).

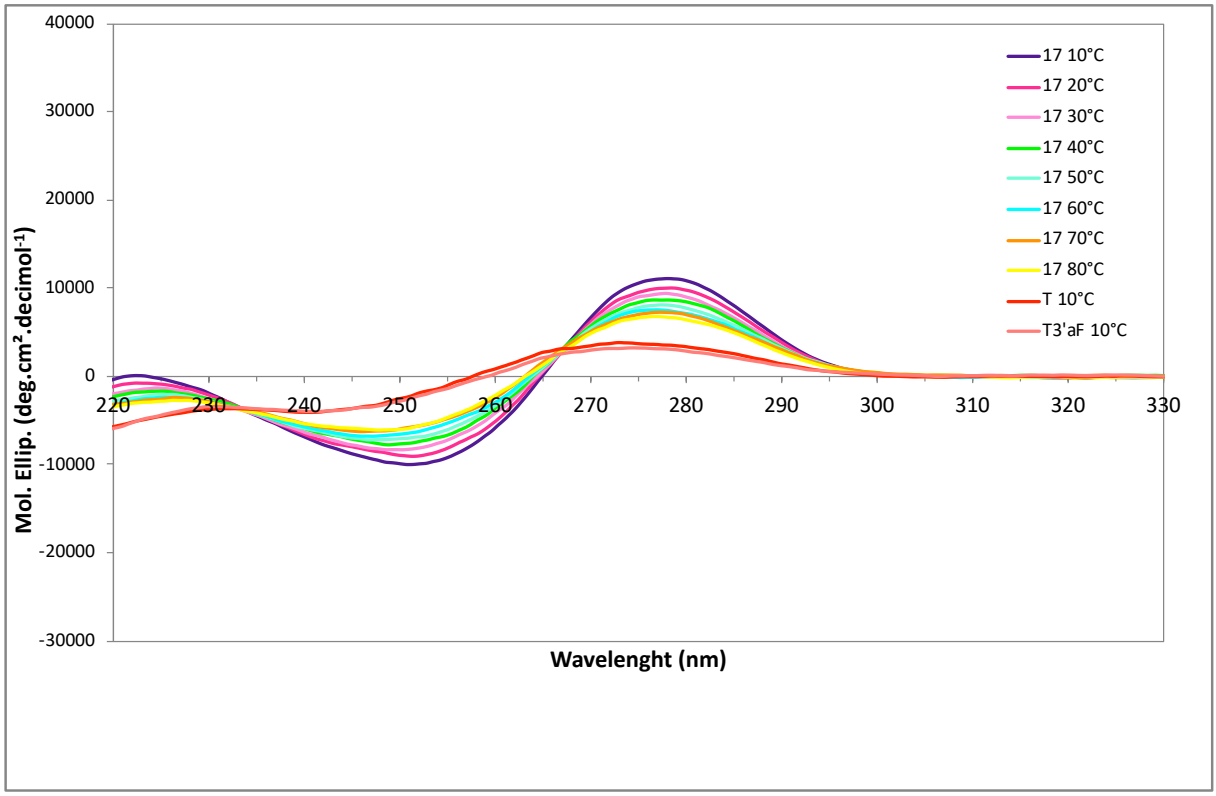

Figure S53B. CD spectra of **17** ($TpT_{3'}\alpha_F$) between 10 to 80°C and CD spectra at 10°C of thymidine (T) and 3'-deoxy-3'-α-fluorothymidine ($T_{3'}\alpha_F$).

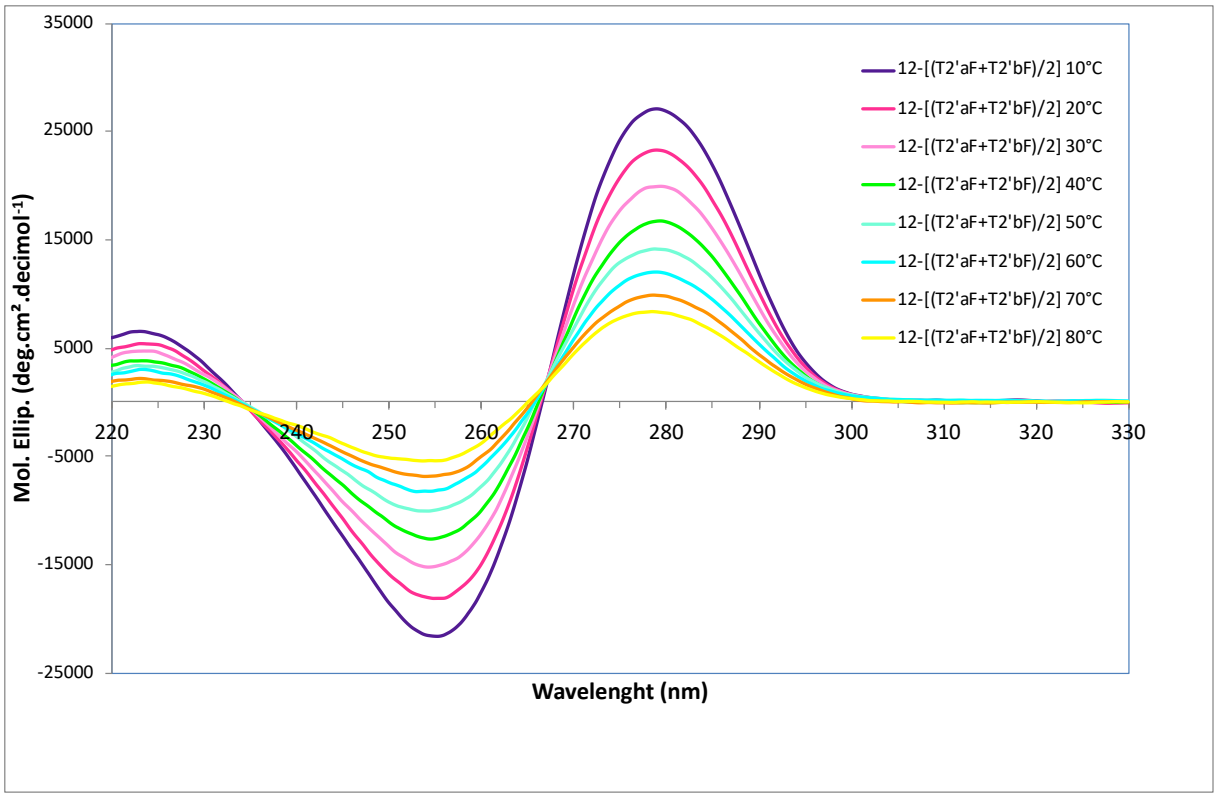

Figure S54A. CD differential spectra of **12** ($T_{2'}\alpha_F pT_{2'}\beta_F$) between 10 to 80°C.

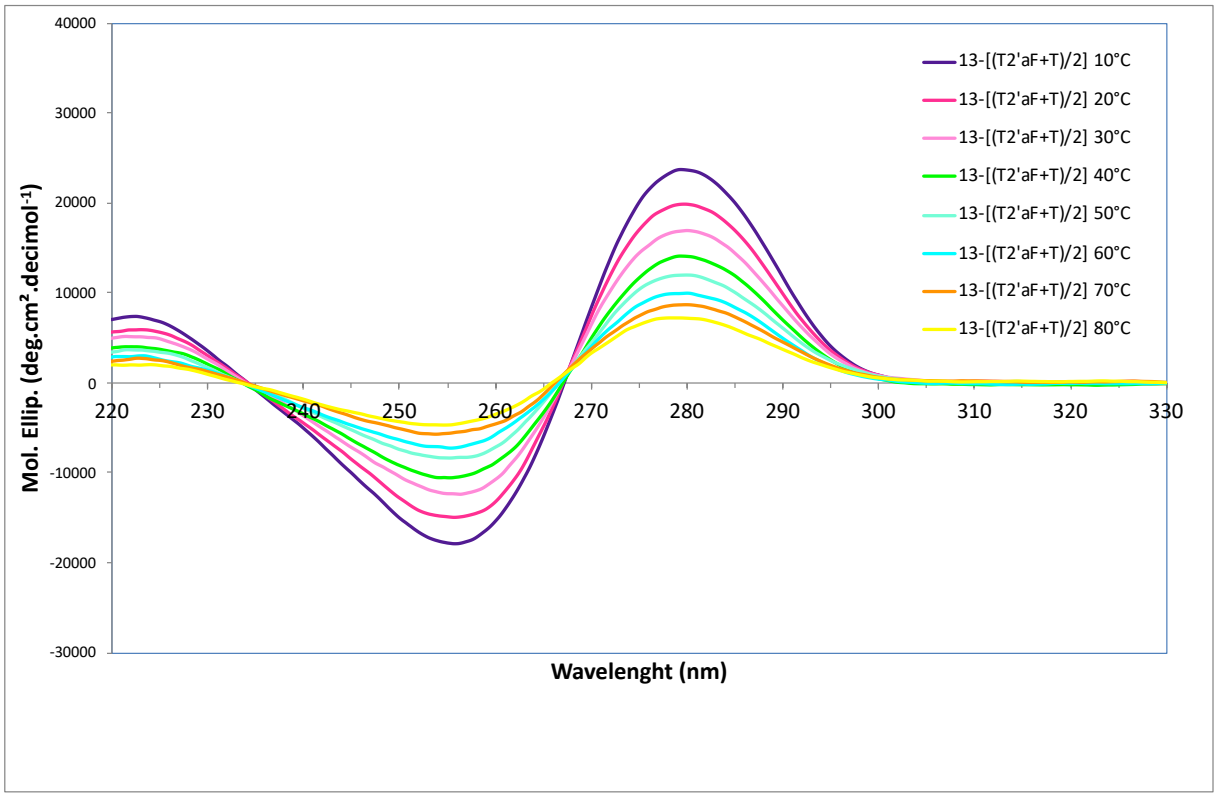

Figure S54B. CD differential spectra of **13** ($T_{2'}\alpha_F pT$) between 10 to 80°C.

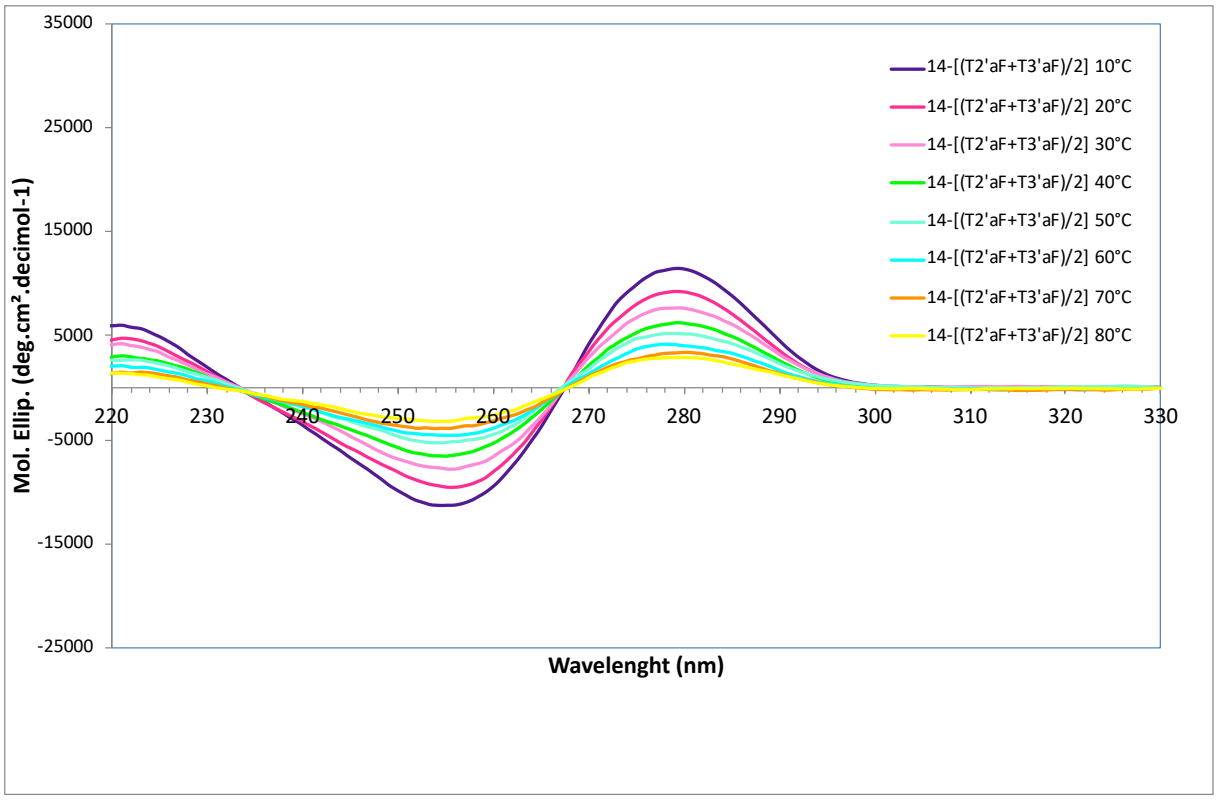

Figure S55A. CD differential spectra of **14** ($T_{2'}\alpha_F pT_{3'}\alpha_F$) between 10 to 80°C.

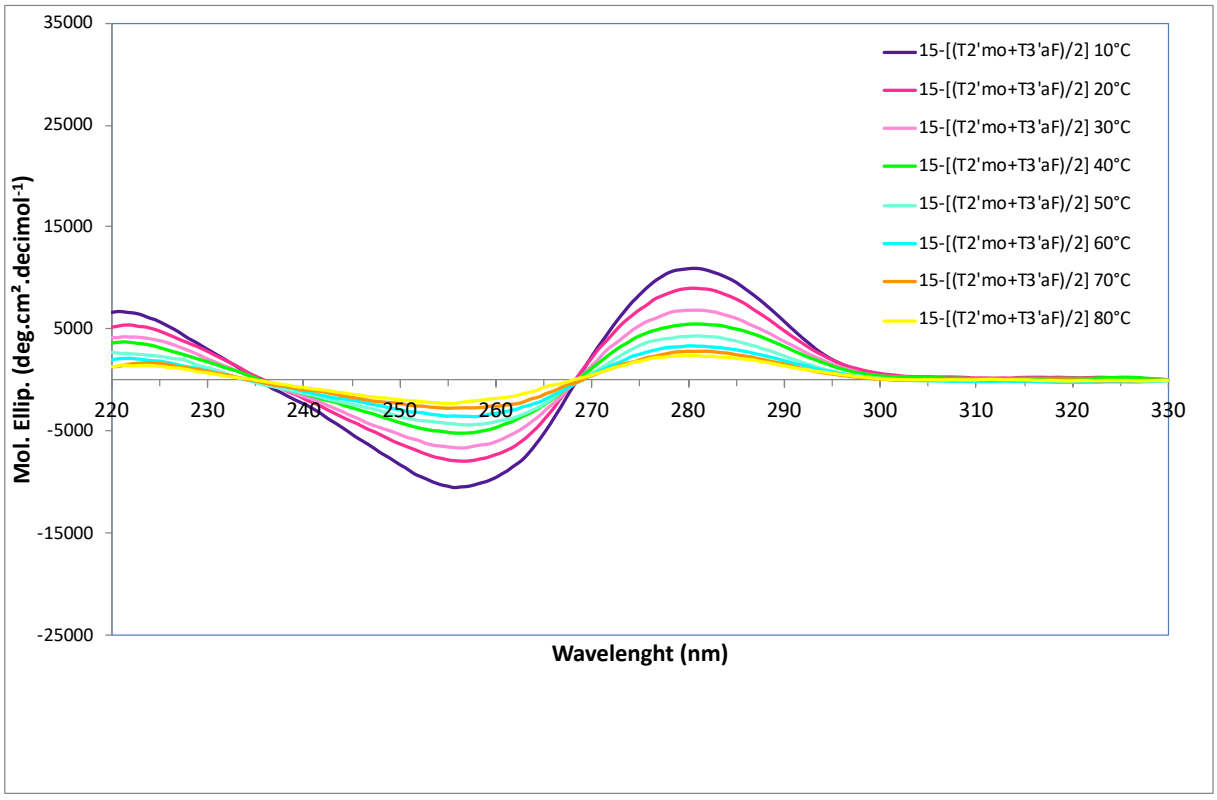

Figure S55B. CD differential spectra of **15** ($T_{2'mo}pT_{3'}\alpha_F$) between 10 to 80°C.

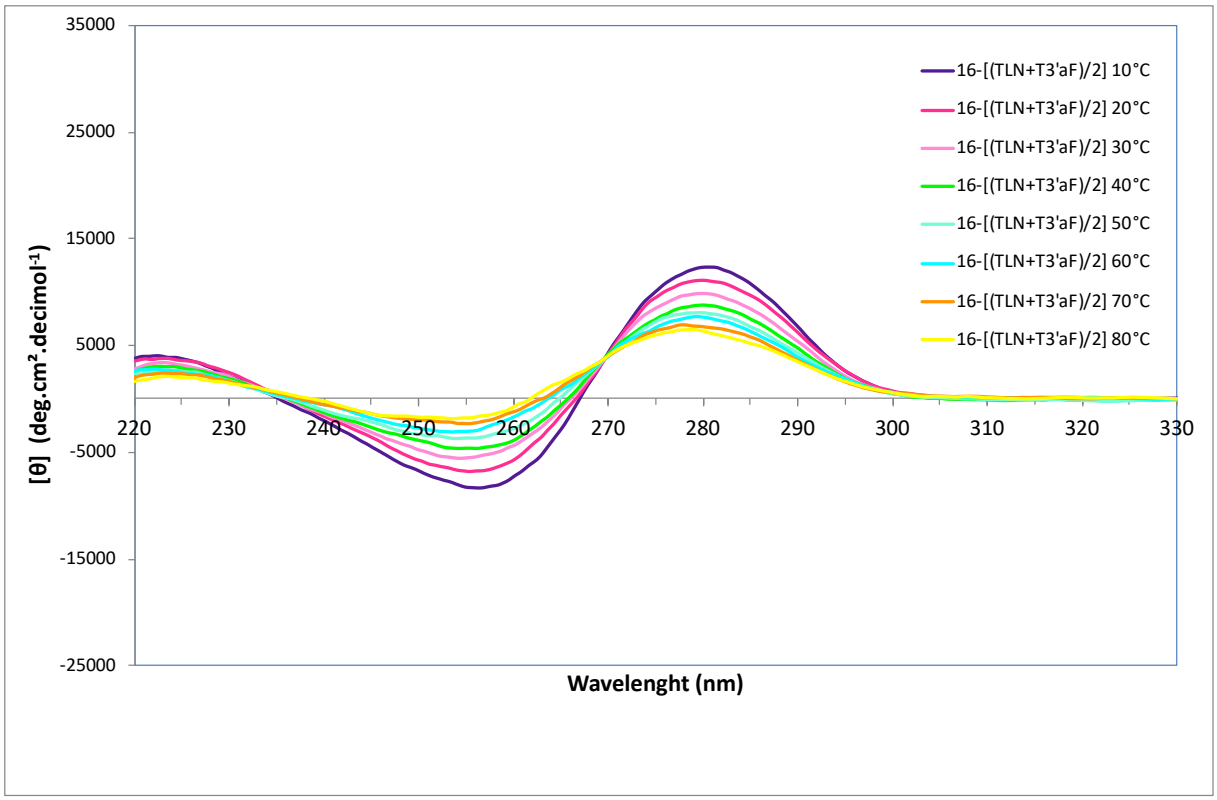

Figure S56A. CD differential spectra of **16** ($T_{2'4'L}pT_{3'}\alpha_F$) between 10 to 80°C.

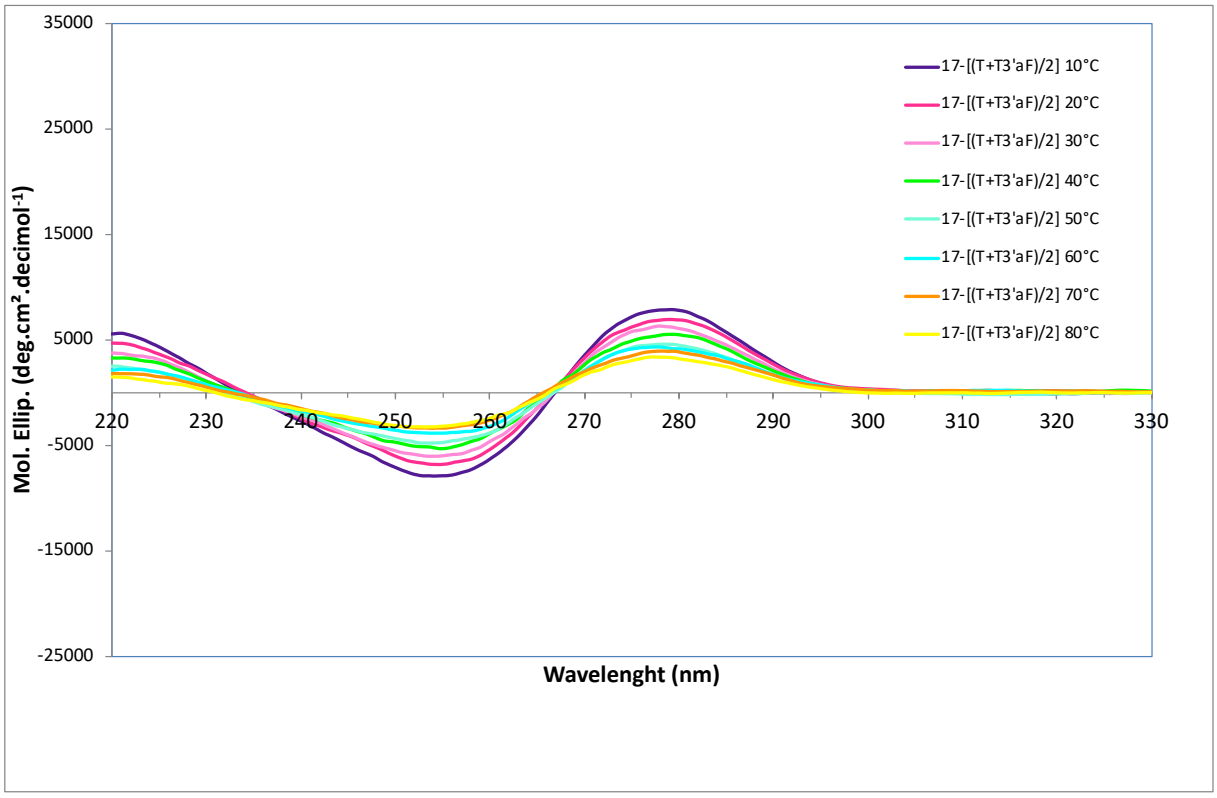

Figure S56B. CD differential spectra of **17** ($TpT_{3'}\alpha_F$) between 10 to 80°C.

5. CD Data Analysis by SVD and dinucleotide CD stacking level S57

Singular value decomposition (SVD) analysis of the CD differential melting spectra of **12**-**17** and dinucleotide CD stacking level calculation were performed as reported[12] except that the Matlab software (version R.2022.a) was used instead of the R software (version 3.1.1).

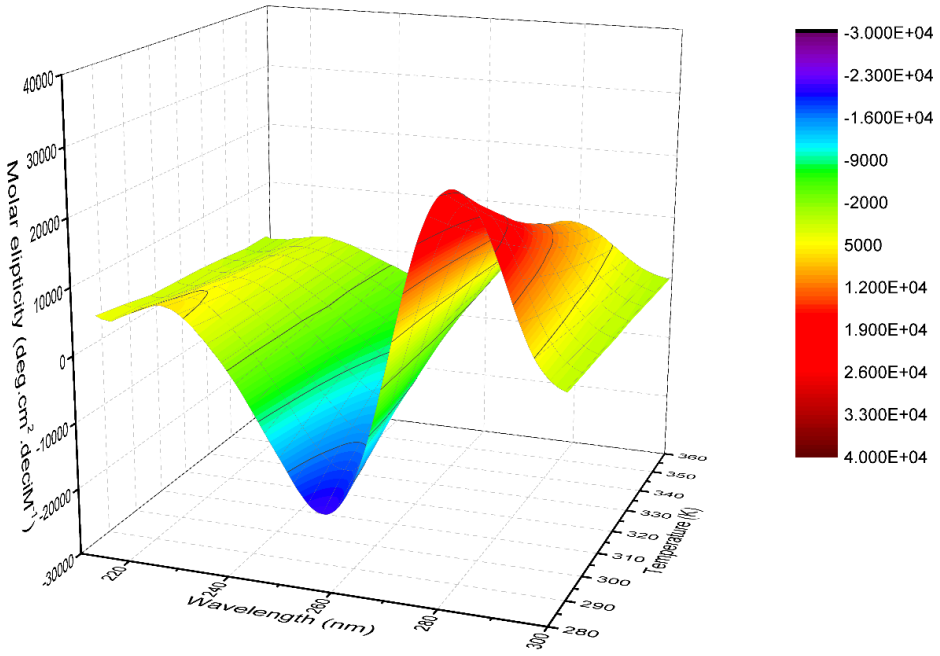

Figure S57. Tridimensional representation of matrix D generated from CD differential melting spectra of compound **12** ($T_{2'}\alpha_F pT_{2'}\beta_F$).

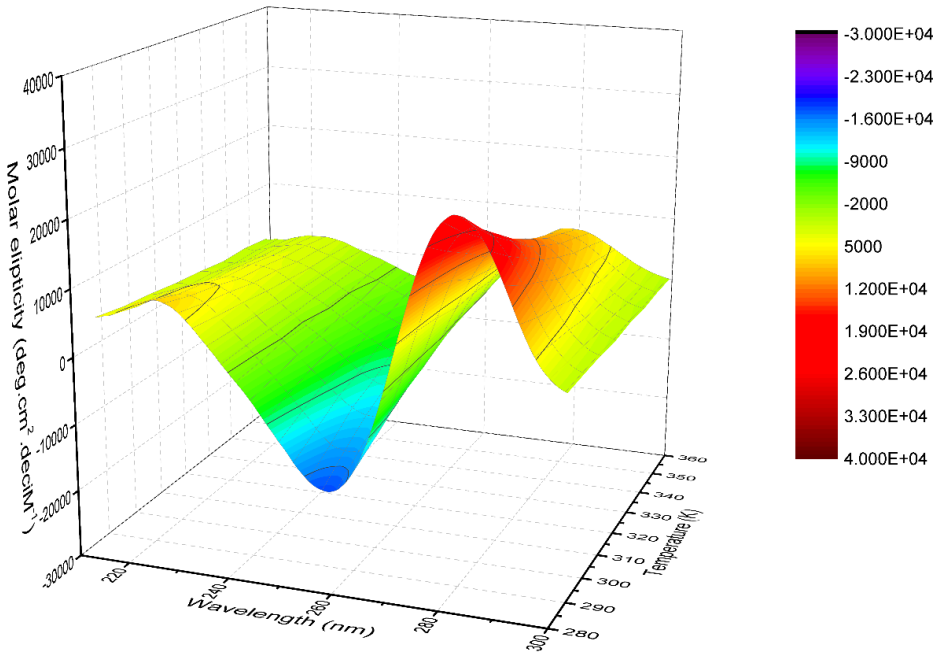

Figure S58A. Tridimensional representation of matrix D generated from CD differential melting spectra of compound **13** ($T_{2'}\alpha_F pT$).

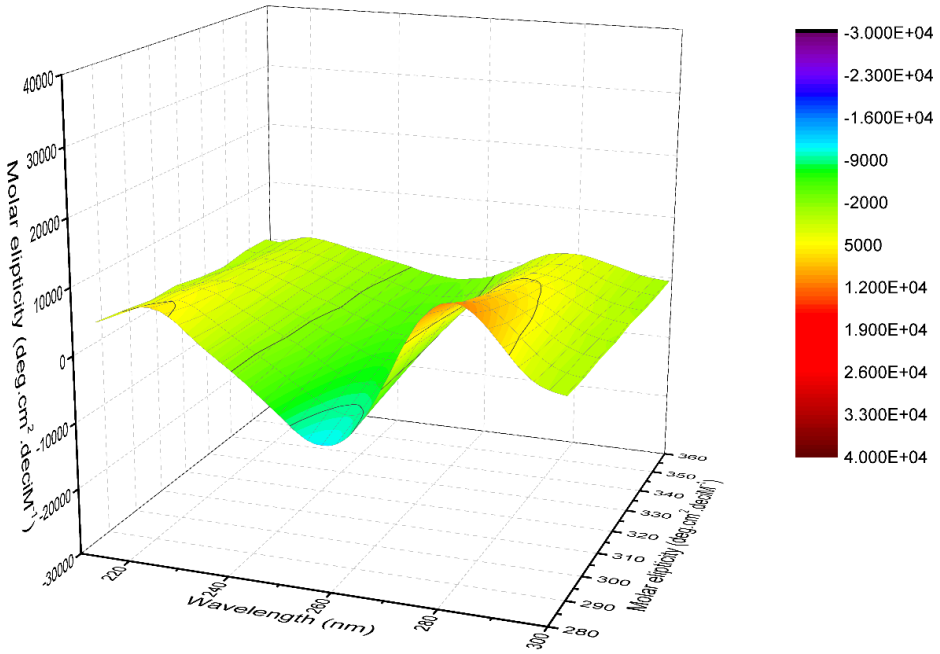

Figure S58B. Tridimensional representation of matrix D generated from CD differential melting spectra of compound **14** ($T_{2'}\alpha_F pT_{3'}\alpha_F$).

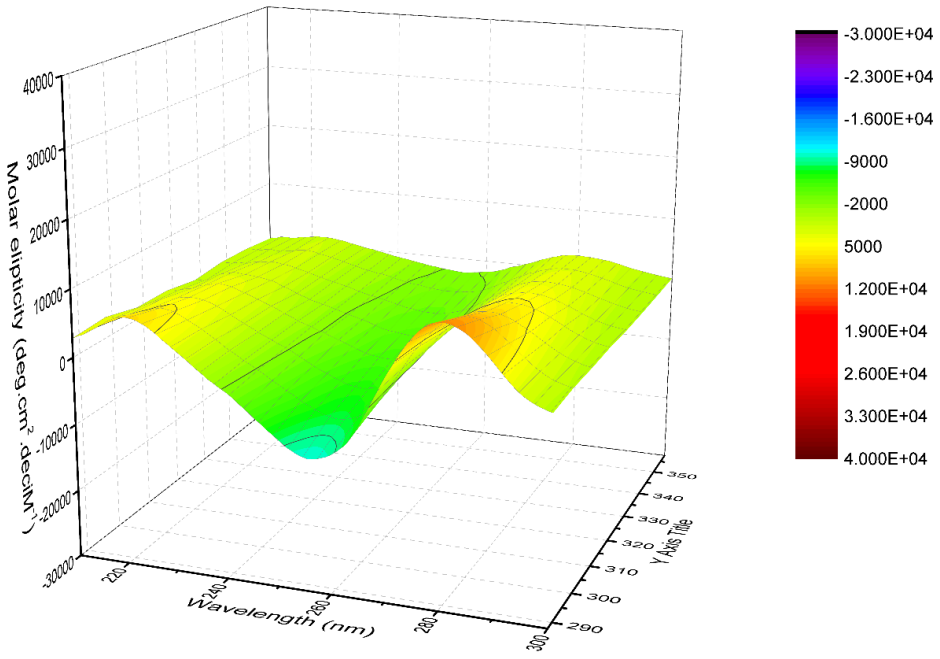

Figure S59A. Tridimensional representation of matrix D generated from CD differential melting spectra of compound **15** ($T_{2'mo}pT_{3'}\alpha_F$).

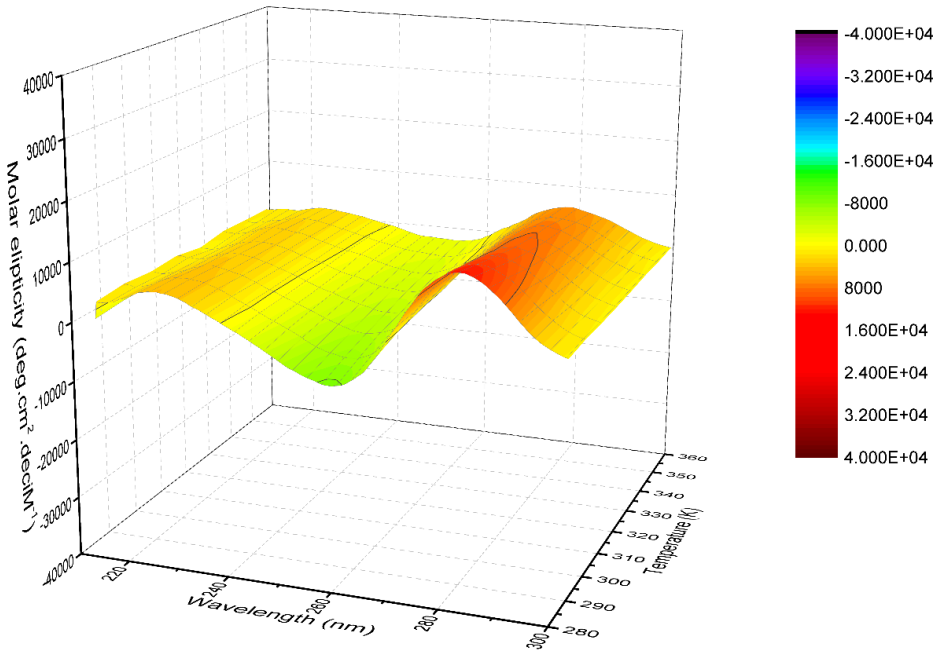

Figure S59B. Tridimensional representation of matrix D generated from CD differential melting spectra of compound **16** ($T_{2'4'L}pT_{3'}\alpha_F$).

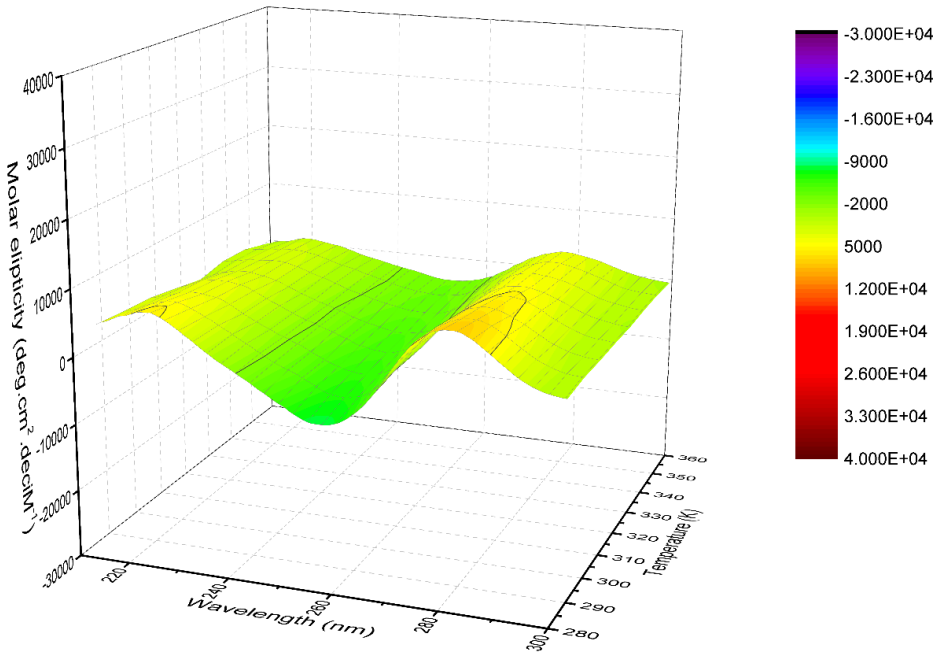

Figure S60. Tridimensional representation of matrix D generated from CD differential melting spectra of compound **17** ($TpT_{3'}\alpha_F$).

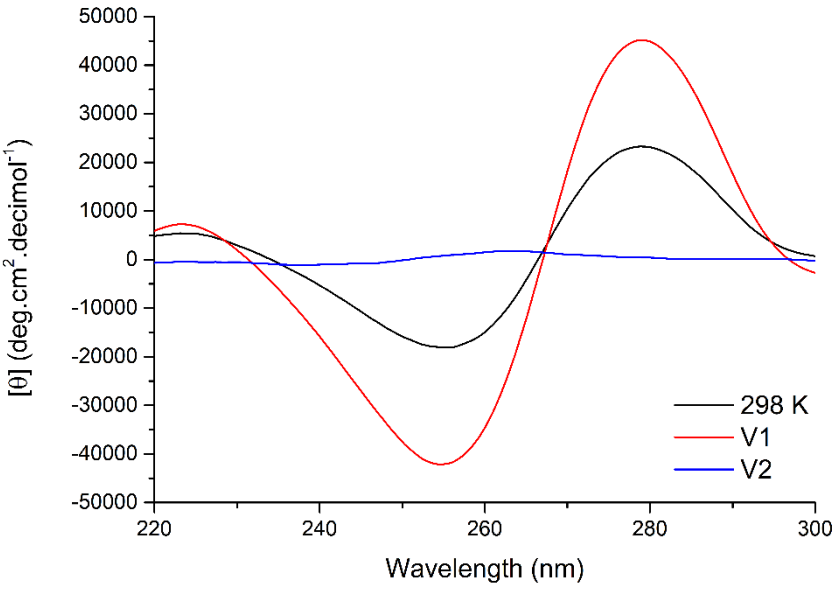

Figure S61A. Representation of the first (V1), second (V2) wavelength basis vectors determined from SVD and 298 K CD spectrum of CD differential melting spectra of compound **12** ($T_{2'}\alpha_F pT_{2'}\beta_F$).

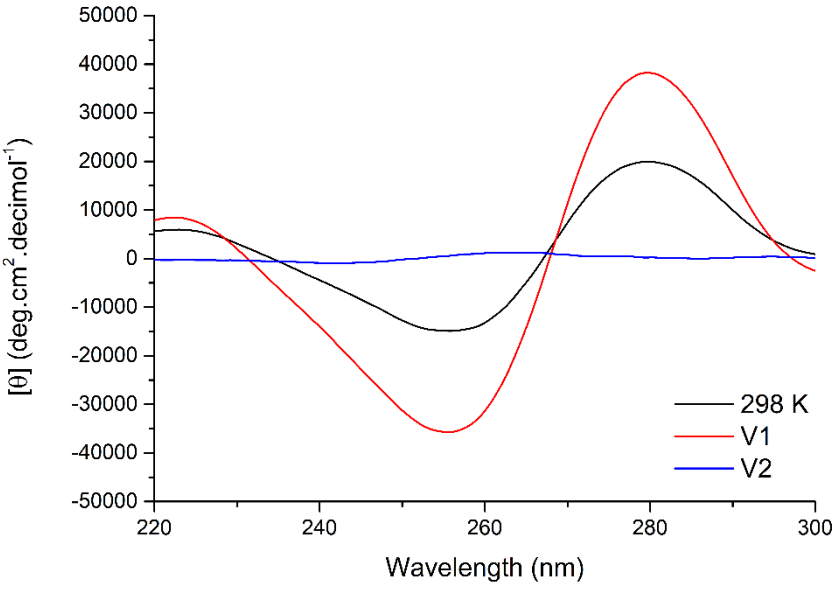

Figure S61B. Representation of the first (V1), second (V2) wavelength basis vectors determined from SVD and 298 K CD spectrum of CD differential melting spectra of compound **13** ($T_{2'}\alpha_F pT$).

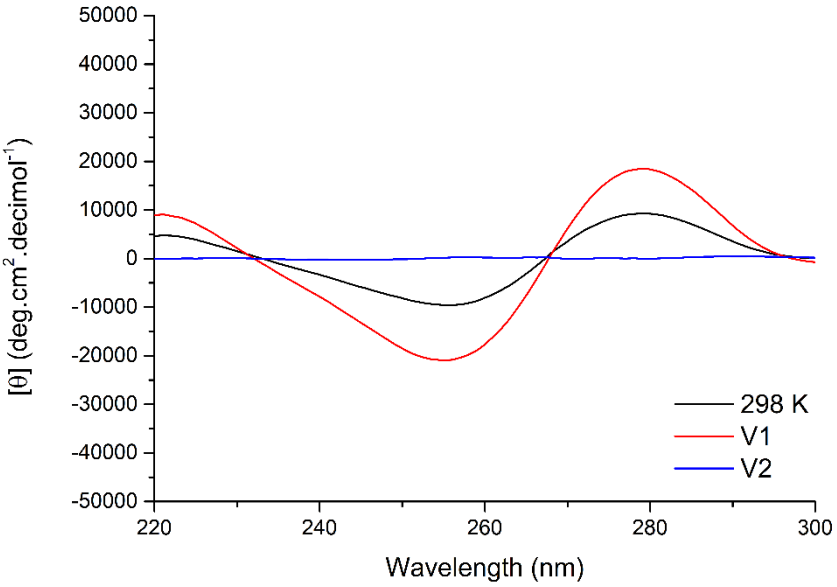

Figure S62A. Representation of the first (V1), second (V2) wavelength basis vectors determined from SVD and 298 K CD spectrum of CD differential melting spectra of compound **14** ($T_{2'}\alpha_F pT_{3'}\alpha_F$).

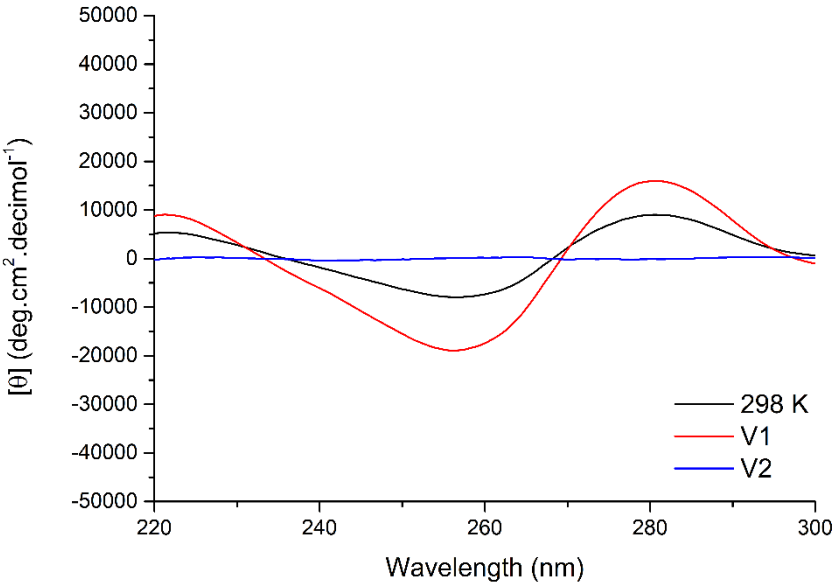

Figure S62B. Representation of the first (V1), second (V2) wavelength basis vectors determined from SVD and 298 K CD spectrum of CD differential melting spectra of compound **15** ($T_{2'mo}pT_{3'}\alpha_F$).

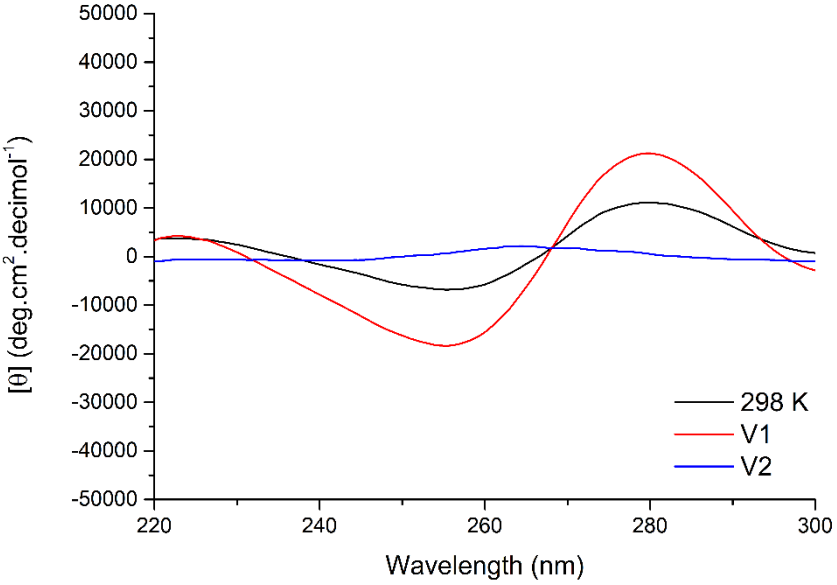

Figure S63A. Representation of the first (V1), second (V2) wavelength basis vectors determined from SVD and 298 K CD spectrum of CD differential melting spectra of compound **16** ($T_{2'4'L}pT_{3'}\alpha_F$).

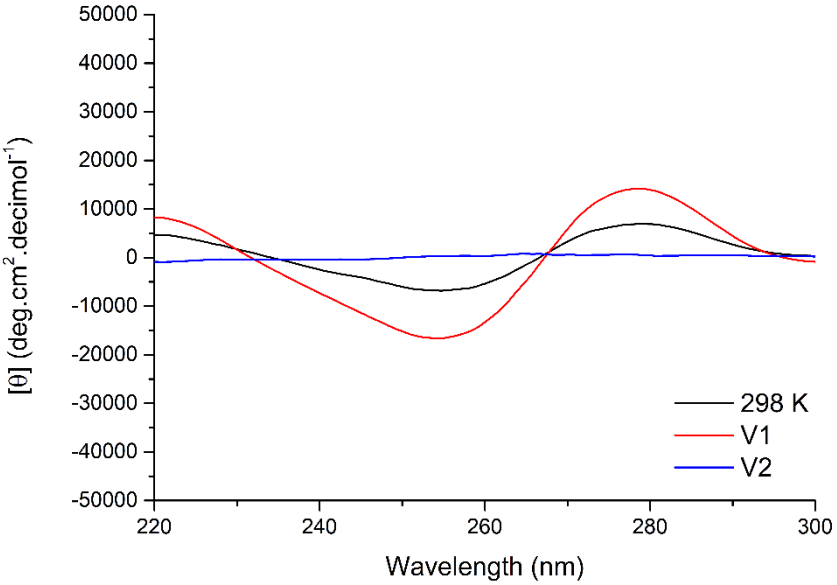

Figure S63B. Representation of the first (V1), second (V2) wavelength basis vectors determined from SVD and 298 K CD spectrum of CD differential melting spectra of compound **17** ($TpT_{3'}\alpha_F$).

Table S64. Thermodynamic parameters of stacking extracted from CD melting experiment of dinucleotides **12**-**17**.

	12 ($T_{2'}\alpha_F pT_{2'}\beta_F$)		**13** ($T_{2'}\alpha_F pT$)	
	Value	Standard error	Value	Standard error
ΔH° (kJ/mol)	-22.28	0.21	-23.54	0.57
ΔS° (J/mol.K)	-76.14	0.58	-82.04	1.50
ΔG° (kJ/mol)	0.43	0.06	0.93	0.18
% stacking @ RT	45.7	0.40	40.8	1.21

	14 ($T_{2'}\alpha_F pT_{3'}\alpha_F$)		**15** ($T_{2'mo}pT_{3'}\alpha_F$)	
	Value	Standard error	Value	Standard error
ΔH° (kJ/mol)	-20.71	1.31	-26.82	0.94
ΔS° (J/mol.K)	-76.45	3.02	-95.86	2.29
ΔG° (kJ/mol)	2.08	0.58	1.76	0.36
% stacking @ RT	30.1	3.48	32.9	2.27

	16 ($T_{2'4'L}pT_{3'}\alpha_F$)		**17** ($TpT_{3'}\alpha_F$)	
	Value	Standard error	Value	Standard error
ΔH° (kJ/mol)	-15.57	0.98	-13.43	2.93
ΔS° (J/mol.K)	-59.43	2.15	-55.55	4.74
ΔG° (kJ/mol)	2.15	0.49	3.13	2.15
% stacking @ RT	29.6	2.88	22.0	10.55

6. Photochemical studies

6. 1. UV irradiation and HPLC conditions

Studies were conducted as previously described[9] except that a 50 min, 1 mL/min gradient of 0-15% CH_3CN in 0.05 M aqueous ammonium acetate was used for the HPLC analysis of all the irradiation mixtures and that all peak areas were measured at 230 nm.

Retention times (min):

TpT (**1**, ●): 30.5, TpT CPD (■): 9.2, TpT (6-4) (◆): 13.0

$T_{2'}\alpha_F pT_{2'}\beta_F$ (**12**, ●): 38.3, $T_{2'}\alpha_F pT_{2'}\beta_F$ CPD (■): 23.3, $T_{2'}\alpha_F pT_{2'}\beta_F$ (6-4) (◆): 20.7

$T_{2'}\alpha_F pT$ (**13**, ●): 36.3, $T_{2'}\alpha_F pT$ CPD (■): 16.5, $T_{2'}\alpha_F pT$ (6-4) (◆): 18.9

$T_{2'}\alpha_F pT_{3'}\alpha_F$ (**14**, ●): 44.0, $T_{2'}\alpha_F pT_{3'}\alpha_F$ CPD (■): 20.9, $T_{2'}\alpha_F pT_{3'}\alpha_F$ (6-4) (◆): 19.6

$T_{2'mo}pT_{3'}\alpha_F$ (**15**, ●): 41.2, $T_{2'mo}pT_{3'}\alpha_F$ CPD (■): 21.9, $T_{2'mo}pT_{3'}\alpha_F$ (6-4) (◆): 19.3

$T_{2'4'L}pT_{3'}\alpha_F$ (**16**, ●): 37.3, $T_{2'4'L}pT_{3'}\alpha_F$ CPD (■): 19.7, $T_{2'4'L}pT_{3'}\alpha_F$ (6-4) (◆): 18.3

$TpT_{3'}\alpha_F$ (**17**, ●): 38.2, $TpT_{3'}\alpha_F$ CPD (■): 17.0, $TpT_{3'}\alpha_F$ (6-4) (◆): 13.7

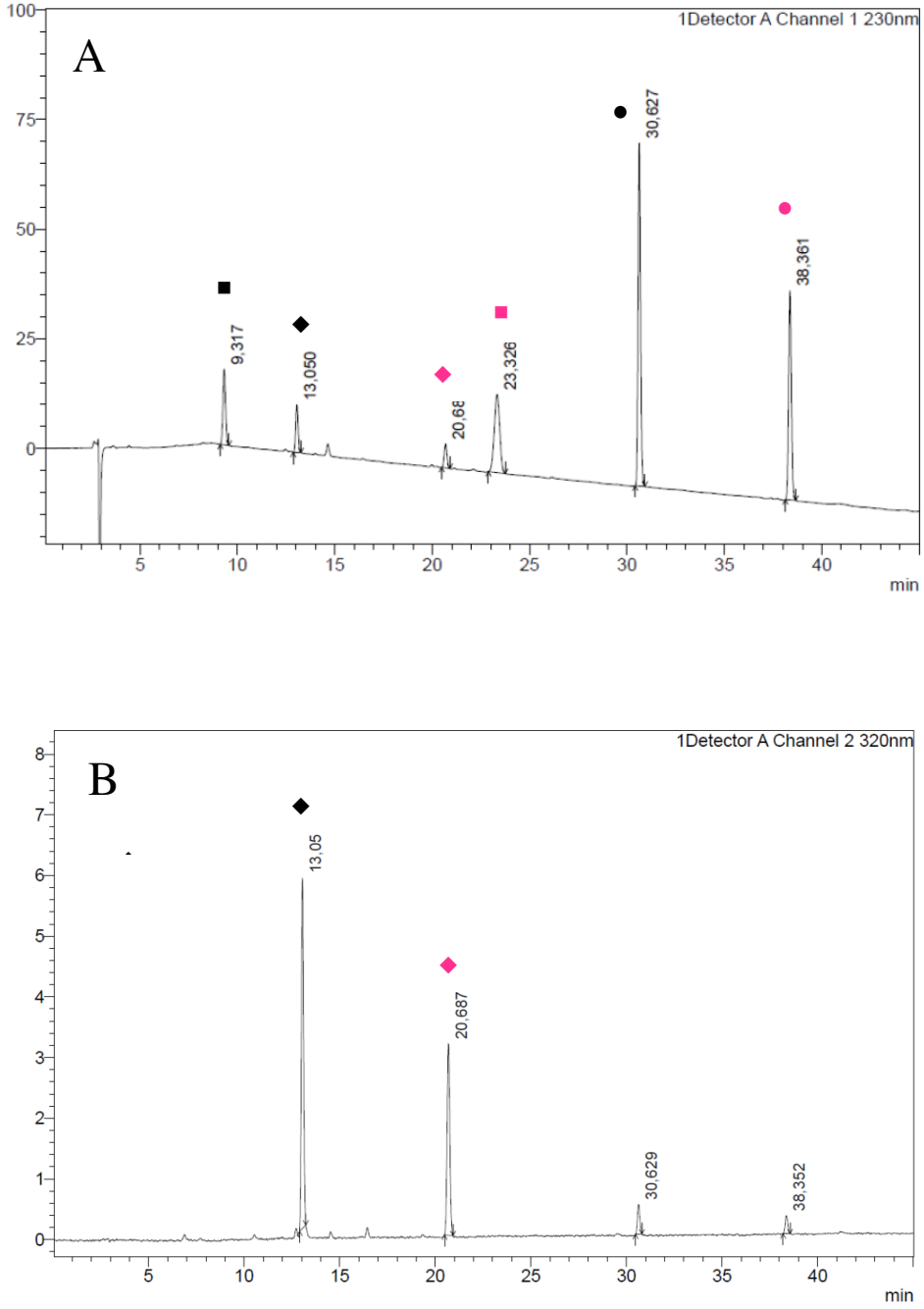

Figure S66. HPLC chromatogram of the 8 min irradiation mixture of **12** and **1** at 230 nm (A) and 320 nm (B): TpT **1** (●), TpT CPD (■), TpT (6-4) (◆), $T_{2'}\alpha_F pT_{2'}\beta_F$ **12** (●), $T_{2'}\alpha_F pT_{2'}\beta_F$ CPD (■), $T_{2'}\alpha_F pT_{2'}\beta_F$ (6-4) (◆).

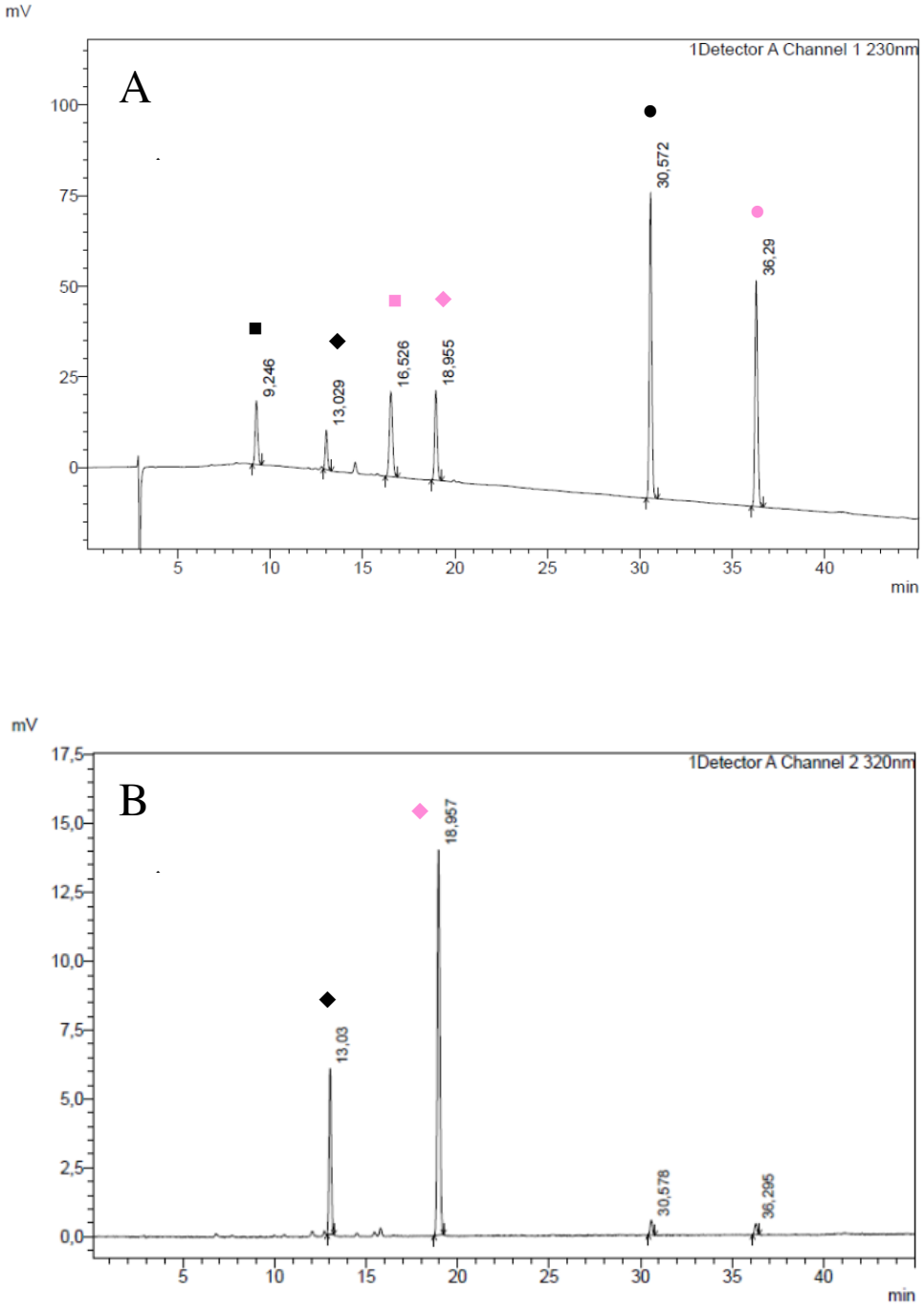

Figure S67. HPLC chromatogram of the 8 min irradiation mixture of **13** and **1** at 230 nm (A) and 320 nm (B): TpT **1** (●), TpT CPD (■), TpT (6-4) (◆), $T_{2'}\alpha_F pT$ **13** (●), $T_{2'}\alpha_F pT$ CPD (■), $T_{2'}\alpha_F pT$ (6-4) (◆).

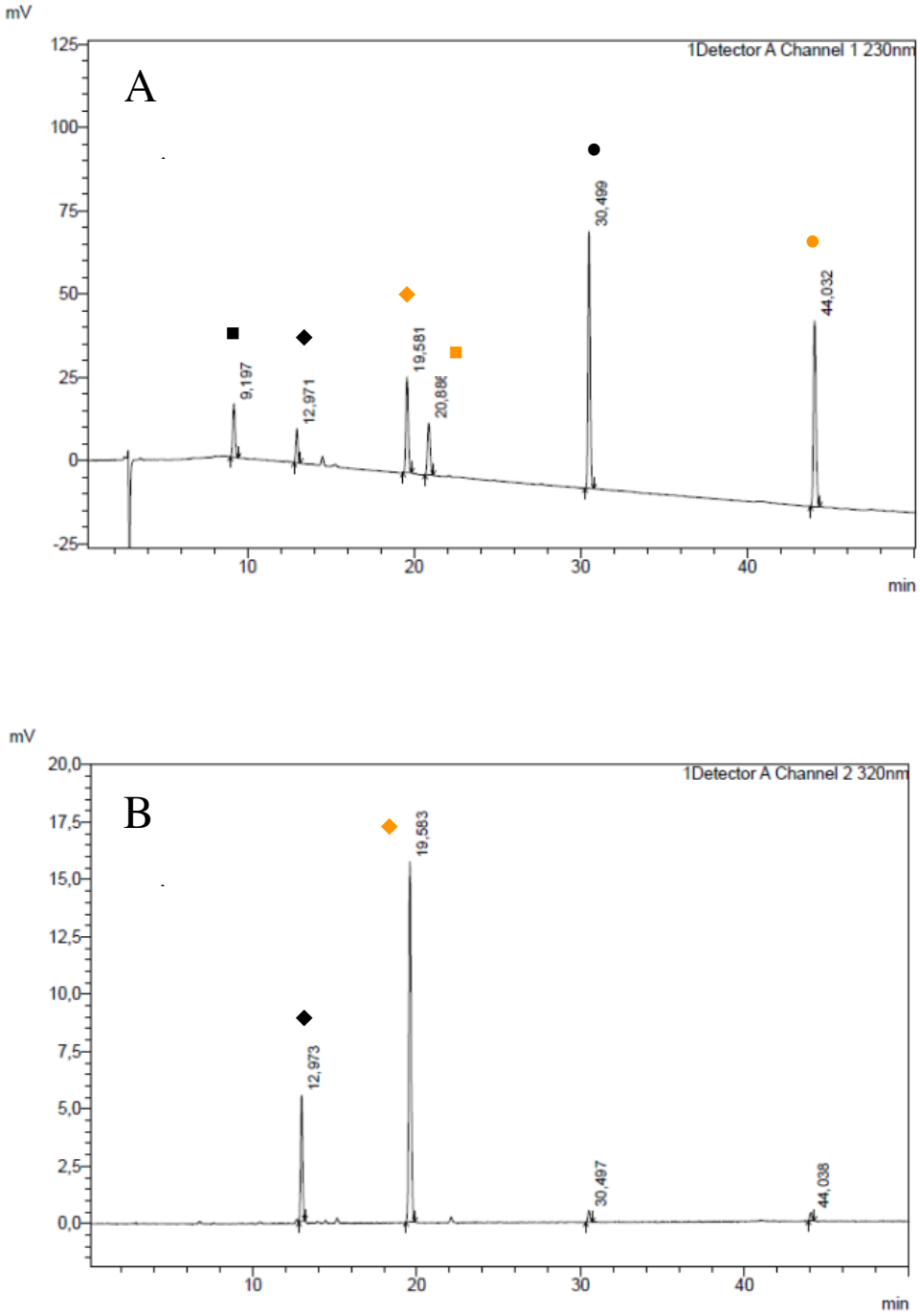

Figure S68. HPLC chromatogram of the 8 min irradiation mixture of **14** and **1** at 230 nm (A) and 320 nm (B): TpT **1** (●), TpT CPD (■), TpT (6-4) (◆), $T_{2'}\alpha_F pT_{3'}\alpha_F$ (**14**, ●), $T_{2'}\alpha_F pT_{3'}\alpha_F$ CPD (■), $T_{2'}\alpha_F pT_{3'}\alpha_F$ (6-4) (◆).

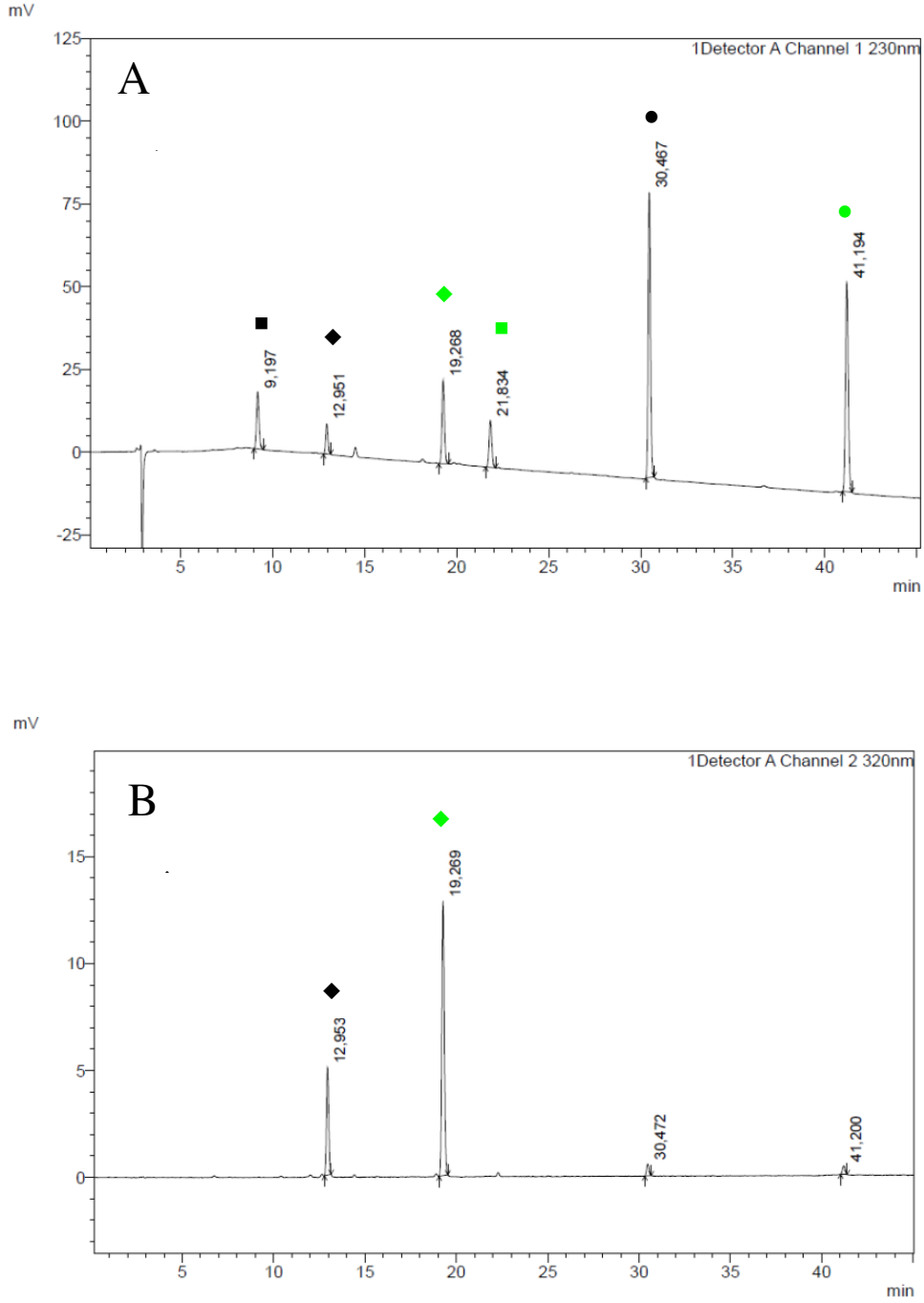

Figure S69. HPLC chromatogram of the 8 min irradiation mixture of **15** and **1** at 230 nm (A) and 320 nm (B): TpT **1** (●), TpT CPD (■), TpT (6-4) (◆), $T_{2'mo}pT_{3'}\alpha_F$ **15** (●),$T_{2'mo}pT_{3'}\alpha_F$ CPD (■), $T_{2'mo}pT_{3'}\alpha_F$ (6-4) (◆).

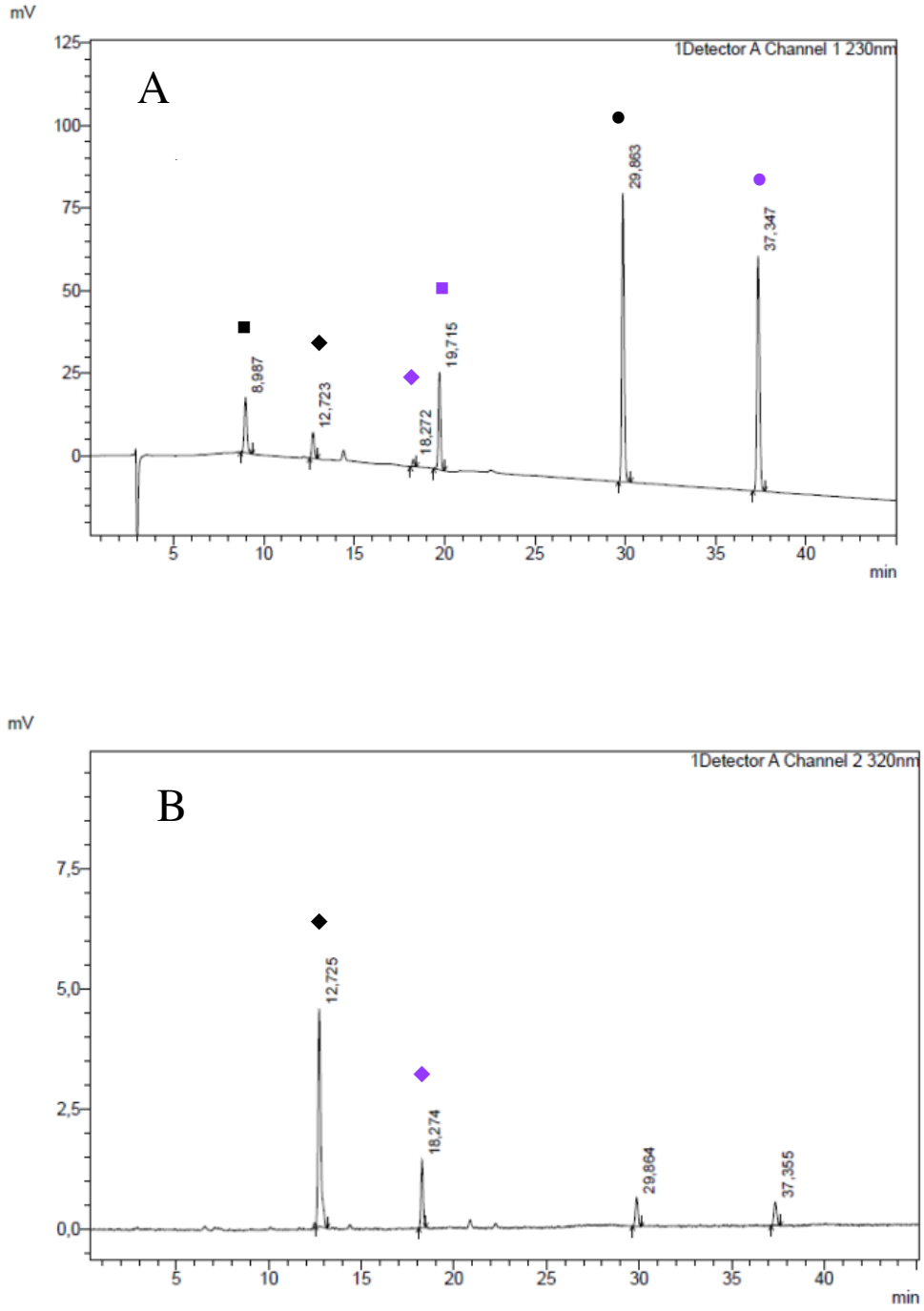

Figure S70. HPLC chromatogram of the 8 min irradiation mixture of **16** and **1** at 230 nm (A) and 320 nm (B): TpT **1** (●), TpT CPD (■), TpT (6-4) (◆), $T_{2'4'L}pT_{3'}\alpha_F$ **16** (●), $T_{2'4'L}pT_{3'}\alpha_F$ CPD (■), $T_{2'4'L}pT_{3'}\alpha_F$ (6-4) (◆).

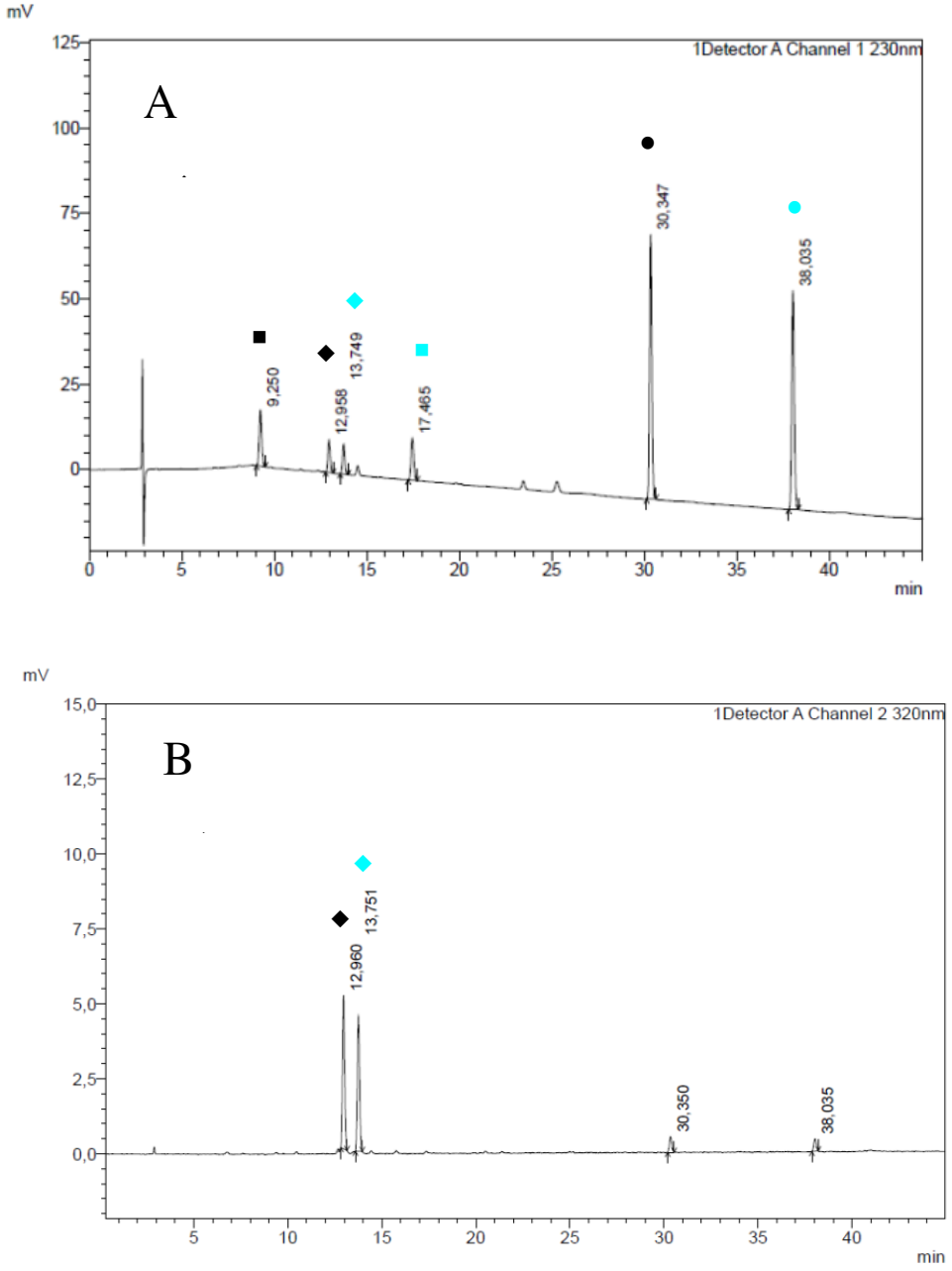

Figure S71. HPLC chromatogram of the 8 min irradiation mixture of **17** and **1** at 230 nm (A) and 320 nm (B): TpT **1** (●), TpT CPD (■), TpT (6-4) (◆), $TpT_{3'}\alpha_F$ **17** (●), $TpT_{3'}\alpha_F$ CPD (■), $TpT_{3'}\alpha_F$ (6-4) (◆).

6. 2. Photoproduct identification by HPLC-ES-MS/MS

UV irradiation of each dinucleotide **12**-**17** and HPLC conditions for ES-MS/MS analysis were identical to those previously reported.[9]

Retention times:

$T_{2'}\alpha_F pT_{2'}\beta_F$ (**12**): 27.5 min, $T_{2'}\alpha_F pT_{2'}\beta_F$ CPD: 18.9 min, $T_{2'}\alpha_F pT_{2'}\beta_F$(6-4): 17.3 min

$T_{2'}\alpha_F pT$ (**13**): 28.1 min, $T_{2'}\alpha_F pT$ CPD: 14.3 min, $T_{2'}\alpha_F pT$ (6-4): 16.2 min

$T_{2'}\alpha_F pT_{3'}\alpha_F$ (**14**): 31.5 min, $T_{2'}\alpha_F pT_{3'}\alpha_F$ CPD: 17.3 min, $T_{2'}\alpha_F pT_{3'}\alpha_F$ (6-4): 16.7 min

$T_{2'mo}pT_{3'}\alpha_F$ (**15**): 31.1 min, $T_{2'mo}pT_{3'}\alpha_F$ CPD: 18.3 min, $T_{2'mo}pT_{3'}\alpha_F$ (6-4): 16.8 min

$T_{2'4'L}pT_{3'}\alpha_F$ (**16**): 28.6 min, $T_{2'4'L}pT_{3'}\alpha_F$ CPD: 17.8 min, $T_{2'4'L}pT_{3'}\alpha_F$ (6-4): 17.3 min

$TpT_{3'}\alpha_F$ (**17**): 29.0 min, $TpT_{3'}\alpha_F$ CPD: 14.5 min, $TpT_{3'}\alpha_F$ (6-4): 12.5 min.

Electrospray MS/MS spectra were recorded on a API 3000 triple quadrupolar spectrometer (SCIEX, Framingham MA) as previously reported.[9] Pseudomolecular and specific fragment ions are reported Table S72.

Table S72: Pseudomolecular ion and specific fragment ions for (6-4) PP and CPD from **12**-**17**

Fragments (*m/z*)	$T_{2'}\alpha_F pT_{2'}\beta_F$ (**12**)	$T_{2'}\alpha_F pT$ (**13**)	$T_{2'}\alpha_F pT_{3'}\alpha_F$ (**14**)	$T_{2'mo}pT_{3'}\alpha_F$ (**15**)	$T_{2'4'L}pT_{3'}\alpha_F$ (**16**)	$TpT_{3'}\alpha_F$ (**17**)
$[M-H]^-$	581	563	565	577	574	547
(6-4) PP						
$[M-H-113]^-$	468	450	452	464	461	434
CPD						
$[M-H-98]^-$		465				449
$[M-H-100]^-$			465	477	474	
$[M-H-116]^-$	465					

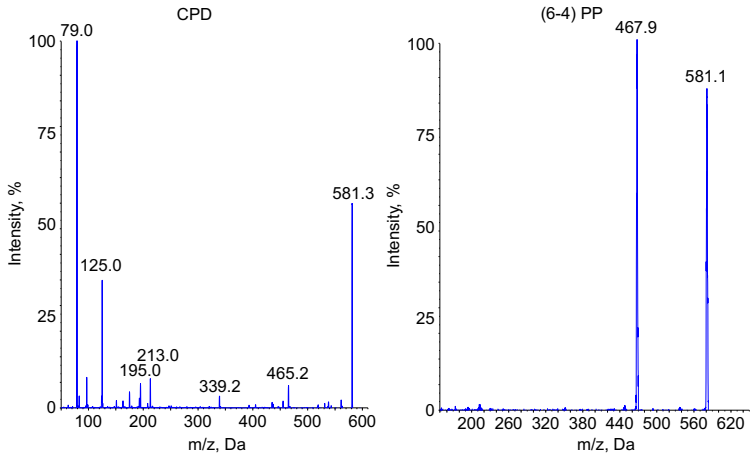

Figure S73A. ES/MS–MS spectra (negative mode) of the CPD (left panel) and the (6–4) PP (right panel) of $T_{2'}\alpha_F pT_{2'}\beta_F$ (**12**).

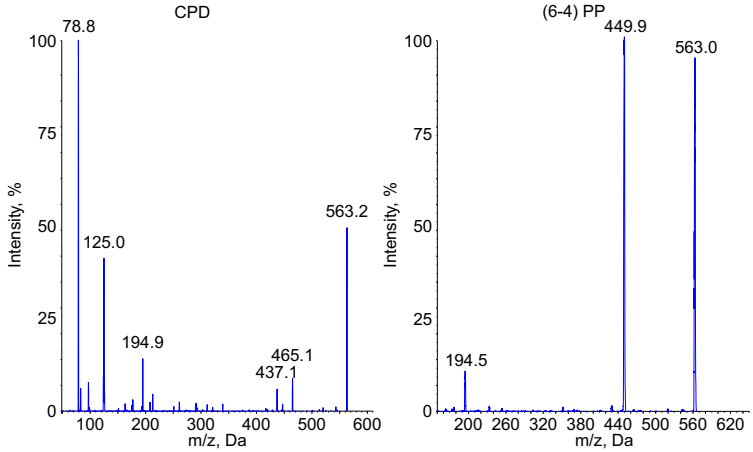

Figure S73B. ES/MS–MS spectra (negative mode) of the CPD (left panel) and the (6–4) PP (right panel) of $T_{2'}\alpha_F pT$ (**13**).

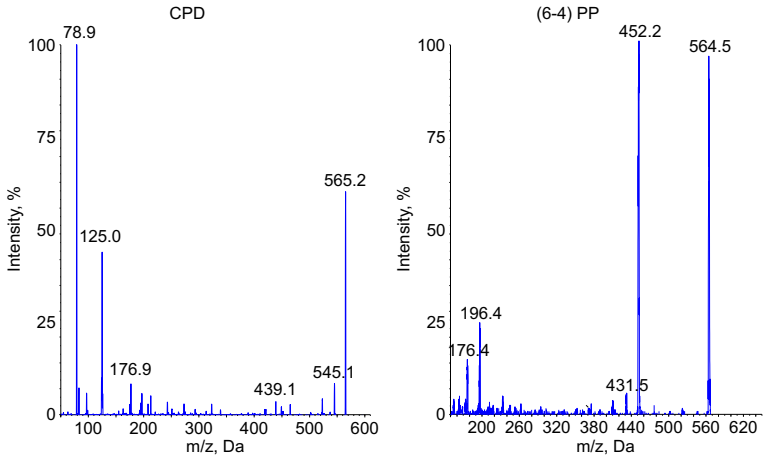

Figure S73C. ES/MS–MS spectra (negative mode) of the CPD (left panel) and the (6–4) PP (right panel) of $T_{2'}\alpha_F pT_{3'}\alpha_F$ (**14**).

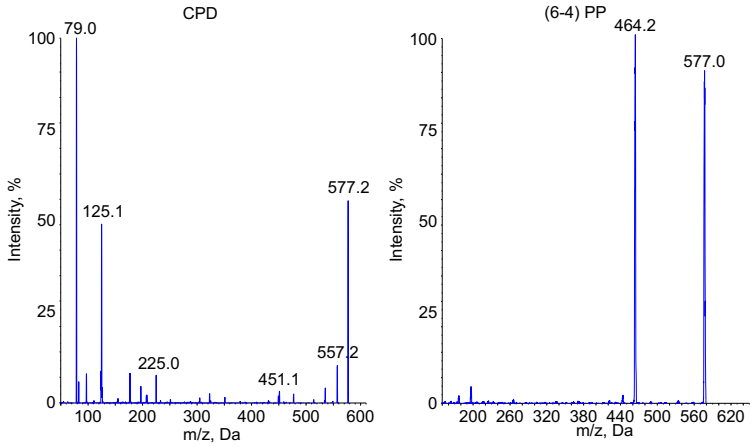

Figure S74A. ES/MS–MS spectra (negative mode) of the CPD (left panel) and the (6–4) PP (right panel) of $T_{2'mo}pT_{3'}\alpha_F$ (**15**).

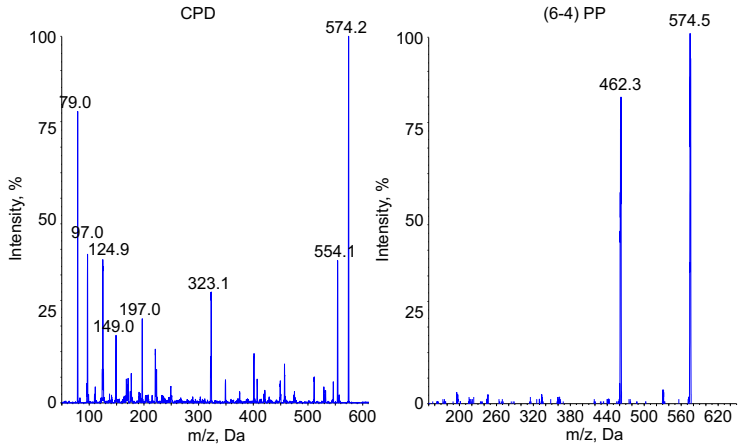

Figure S74B. ES/MS–MS spectra (negative mode) of the CPD (left panel) and the (6–4) PP (right panel) of $T_{2'4'L}pT_{3'}\alpha_F$ (**16**).

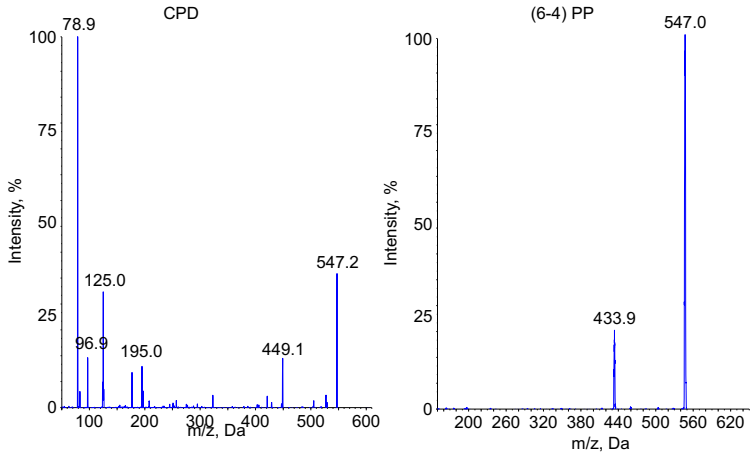

Figure S74C. ES/MS–MS spectra (negative mode) of the CPD (left panel) and the (6–4) PP (right panel) of $TpT_{3'}\alpha_F$ (**17**).

Scheme S75A. Proposed fragmentation pathway for the [M-H-116]$^-$ product ion observed on the LC-MS/MS spectrum of the CPD of $T_{2'}\alpha_F pT_{2'}\beta_F$ (12)

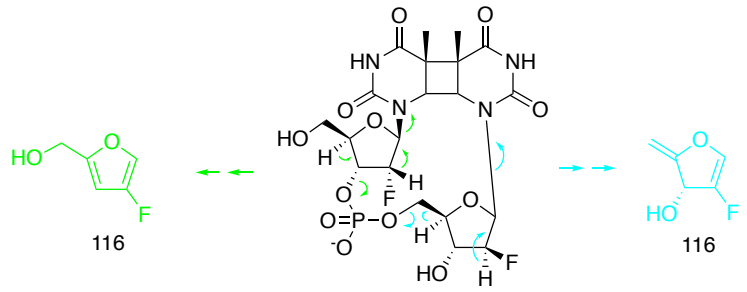

$T_{2'\alpha F}pT_{2'\beta F}$ CPD

Scheme S75B. Proposed fragmentation pathway for the [M-H-98]$^-$ product ions observed on the LC-MS/MS spectra of the CPD of $T_{2'}\alpha_F pT$ (13) and $TpT_{3'}\alpha_F$ (17)

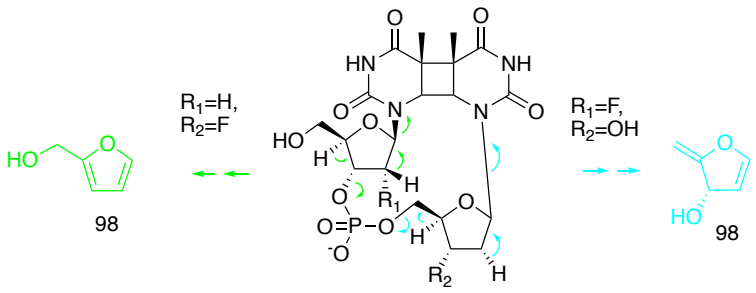

$T_{2'\alpha F}pT$ (13) CPD

$TpT_{3'\alpha F}$ (17) CPD

Scheme S75C. Proposed fragmentation pathway for the [M-H-100]$^-$ product ion observed on the LC-MS/MS spectra of the CPD of $T_{2'}\alpha_F pT_{3'}\alpha_F$ (14), $T_{2'mo}pT_{3'}\alpha_F$ (15), $T_{2'4'L}pT_{3'}\alpha_F$ (16)

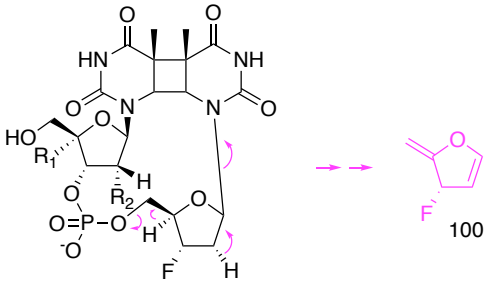

$T_{2'\alpha F}pT_{3'\alpha F}$ (R_1 = H, R_2 = F, 14) CPD

$TpT_{3'\alpha F}$ (R_1 = H, R_2 = OMe, 15) CPD

$TpT_{3'\alpha F}$ (R_1, R_2 = OCH_2 16) CPD

6. 3. Kinetic of the 254 nm photoreaction of 12-17 and of PP formation

The kinetic studies were performed and analyzed as previously described.[9,13] Briefly, the HPLC peak of each compound was integrated at 230 nm at sampled irradiation times. The fractional amount of each compound at time t of the reaction was calculated as the peak area of this compound at time t divided by the peak area of the reactant at t = 0 and taking into account of their respective molar extinction coefficient at 230 nm. It was assumed that ε at 230 nm of **12-17** and of their corresponding PPs are identical.[13]

Fractional amount of **12-17** and **1** and of their respective PPs as a function of irradiation time are reported Figures S77A-C, S78A-C.

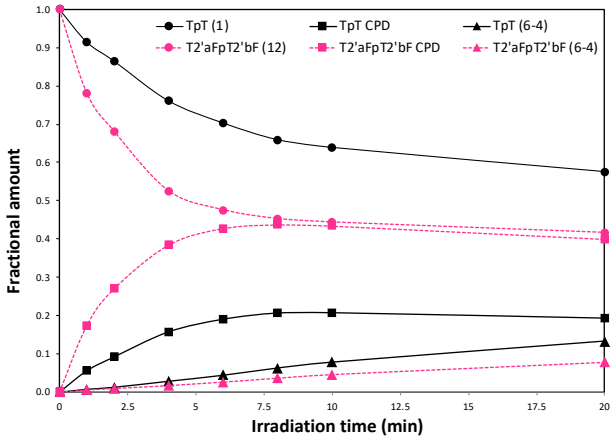

Figure S77A. Fractional amount of **12** ($T_{2'}\alpha_F pT_{2'}\beta_F$), **1** (TpT) and of their respective photoproducts as a function of irradiation time at 254 nm (monitored at 230 nm).

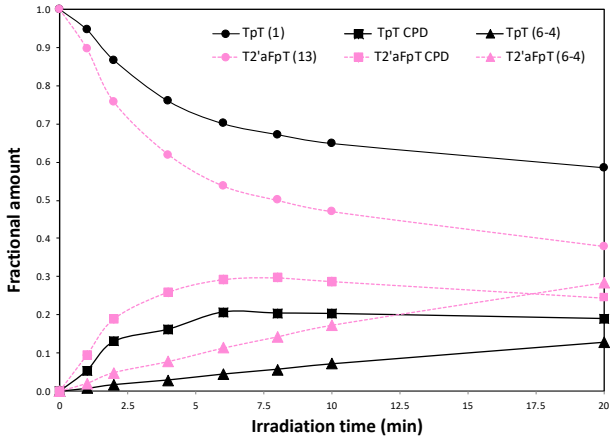

Figure S77B. Fractional amount of **13** ($T_{2'}\alpha_F pT$), **1** (TpT) and of their respective photoproducts as a function of irradiation time at 254 nm (monitored at 230 nm).

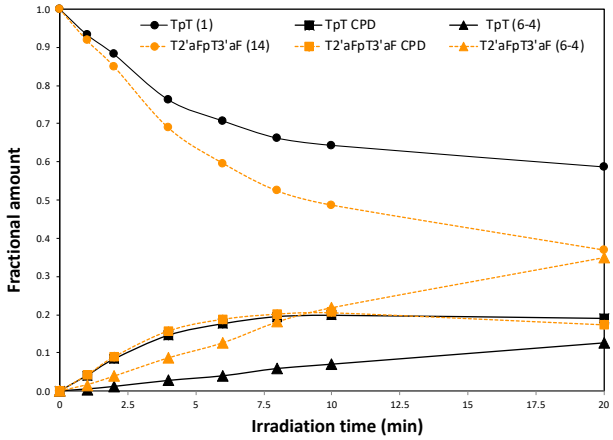

Figure S77C. Fractional amount of **14** ($T_{2'}\alpha_F pT_{3'}\alpha_F$), **1** (TpT) and of their respective photoproducts as a function of irradiation time at 254 nm (monitored at 230 nm).

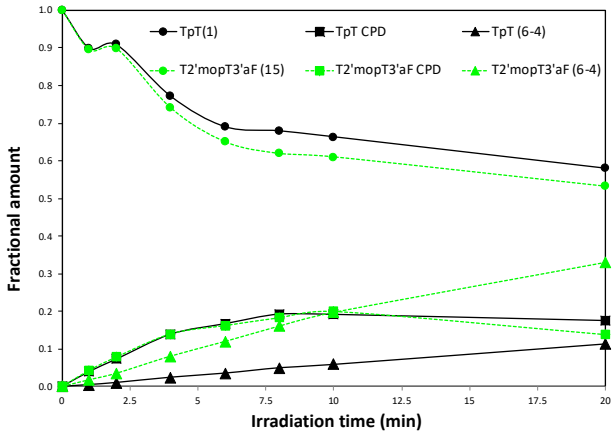

Figure S78A. Fractional amount of **15** ($T_{2'mo}pT_{3'}\alpha_F$), **1** (TpT) and of their respective photoproducts as a function of irradiation time at 254 nm (monitored at 230 nm).

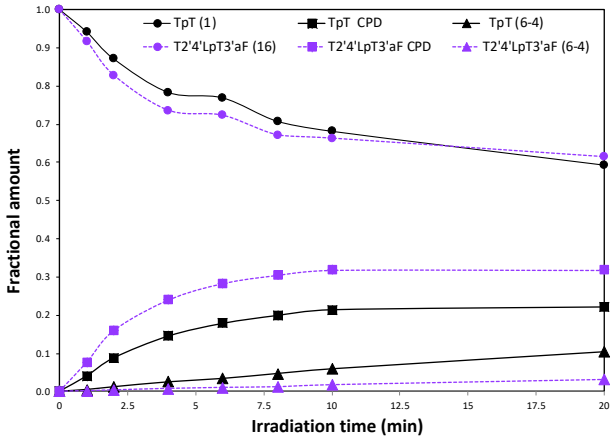

Figure S78B. Fractional amount of **16** ($T_{2'4'L}pT_{3'}\alpha_F$), **1** (TpT) and of their respective photoproducts as a function of irradiation time at 254 nm (monitored at 230 nm).

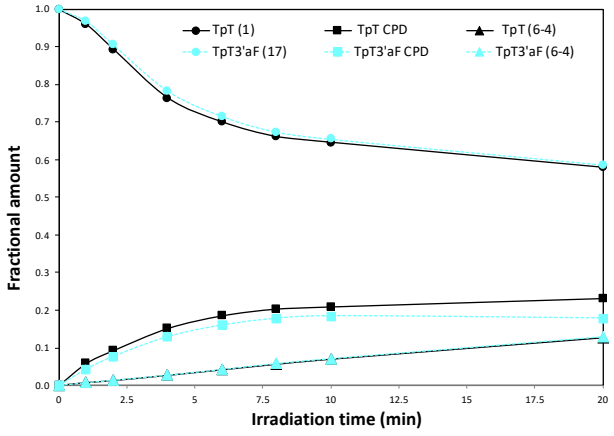

Figure S78C. Fractional amount of **17** ($TpT_{3'}\alpha_F$), **1** (TpT) and of their respective photoproducts as a function of irradiation time at 254 nm (monitored at 230 nm).

6. 4. Quantum yield determination

Quantum yields of PP formation were determined relative to those of the TpT photoproducts[14] as previously described.[9,13]

References

(1) H. Ikeda, R. Fernandez, A. Wilk, J. J. Barchi, X. Huang and V. E. Marquez, *Nucleic Acids Res*., 1998, **26**, 2237-2244.

(2) D. M. Williams, F. Benseler and F. Eckstein, *Biochemistry*, 1991, **30**, 4001-4009.

(3) L. Chanteloup and N. T. Thuong, *Tetrahedron Lett.*, 1994, **35**, 877-880.

(4) A. F. Lewis, G. R. Revankar and M. E. Hogan, *J. Heterocyclic Chem.*, **1993**, *30*, 1309-1315.

(5) A. A. Koshkin, S. K. Singh, P. Nielsen, V. K. Rajwanshi, R. Kumar, M. Meldgaard, C. E. Olsen and J. Wengel, *Tetrahedron*, **1998**, *54*, 3607-3630.

(6) C. Moriou, A. D. Da Silva, M. J. Vianelli Prado, C. Denhez, O. Plashkevych, J. Chattopadhyaya, D. Guillaume and P. Clivio, *J. Org. Chem.*, 2018, **83**, 2473-2478.

(7) A. Marchand, D. Marchand, R. Busson, P. Marliere and P. Herdewijn, *Chem. Biodivers.*, **2007**, *4*, 1450-1465.

(8) M. Yun, S. J. Oh, H. J. Ha, J.S. Ryu and D. H. Moon, *Nucl. Med. Biol*., **2003**, *30*, 151-157.

(9) J. Jakhlal, C. Denhez, S. Coantic-Castex, A. Martinez, D. Harakat, T. Douki, D. Guillaume and P. Clivio, *Org. Biomol. Chem*., 2022, **20**, 2300-2307.

(10) P. Hendrickx and J. C. Martins, *Chem. Cent. J.*, **2008**, *2*, 20.

(11) Gaussian16, Revision B.01

M. J. Frisch, G. W. Trucks, H. B. Schlegel, G. E. Scuseria, M. A. Robb, J. R. Cheeseman, G. Scalmani, V. Barone, G. A. Petersson, H. Nakatsuji, X. Li, M. Caricato, A. V. Marenich, J. Bloino, B. G. Janesko, R. Gomperts, B. Mennucci, H. P. Hratchian, J. V. Ortiz, A. F. Izmaylov, J. L. Sonnenberg, D. Williams-Young, F. Ding, F. Lipparini, F. Egidi, J. Goings, B. Peng, A. Petrone, T. Henderson, D. Ranasinghe, V. G. Zakrzewski, J. Gao, N. Rega, G. Zheng, W. Liang, M. Hada, M. Ehara, K. Toyota, R. Fukuda, J. Hasegawa, M. Ishida, T. Nakajima, Y. Honda, O. Kitao, H. Nakai, T. Vreven, K. Throssell, J. A. Jr. Montgomery, J. E. Peralta, F. Ogliaro, M. J. Bearpark, J. J. Heyd, E. N. Brothers, K. N. Kudin, V. N. Staroverov, T. A. Keith, R. Kobayashi, J. Normand, K. Raghavachari, A. P. Rendell, J. C. Burant, S. S. Iyengar, J. Tomasi, M. Cossi,

J. M. Millam, M. Klene, C. Adamo, R. Cammi, J. W. Ochterski, R. L. Martin, K. Morokuma, O. Farkas, J. B. Foresman and D. J. Fox, Gaussian, Inc., Wallingford CT, 2016.

(12) J. Jakhlal, S. Coantic-Castex, C. Denhez, C. Pertermann, A. Martinez, D. Harakat, D. Guillaume and P. Clivio, *Chem. Commun.*, 2015, **51**, 12381-12383.

(13) C. Moriou, M. Thomas, M.-T. Adeline, M.-T. Martin, A. Chiaroni, S. Pochet, J.-L. Fourrey, A. Favre and P. Clivio, *J. Org. Chem.*, 2007, **72**, 43-50.

(14) H. E. Johns, M. L. Pearson, J. C. LeBlanc and C. W. Helleiner, *J. Mol. Biol.*, 1964, **9**, 503-524.